Improved Solar Thermal Technology For Decarbonising Residential Heating

Trinity College Dublin
Coláiste na Tríonóide, Baile Átha Cliath
The University of Dublin

Cian Fogarty

Master of Science in Physics

Supervisor: Prof. David McCloskey

2023

Abstract

The field of solar energy harvesting has emerged over the last number of years as one with considerable scope to provide clean and renewable electricity and heat. Solar Thermal (ST) technology is vital to tackle the pressing issue of CO_2-induced global warming. The objective of this project was to investigate if solar thermal collector efficiency could be increased, without increasing the overall cost of the system. This thesis presents a comparison of the energy performance of a market available flat plate solar collector (MFPC) and a novel flat plate solar collector (NFPC) containing a hexadic transparent insulating material (TIM). The energy performance of the two systems was compared experimentally, through FEM analysis, and by transient simulation software in the Irish climate. Results obtained showed that for a range of incident solar insolation of 100 – 1000 W/m^2, the NFPC system showed a relative efficiency increase of up to 20.84% over the MFPC. Over a yearlong simulation, the total useful energy gained was 1022.22 kWh and 1237.36 kWh for the $6m^2$ MFPC and $6m^2$ NFPC systems respectively. The MFPC required 2465.62 kWh and the NFPC required 2409.37 kWh of additional auxiliary energy to reach the residential required load as per the EN 12976/6 standards. This equated to an average annual solar fraction of 28% for the MFPC and 32% for the NFPC. The annual average collector efficiencies were 40.93% and 49.46% for the MFPC and NFPC respectively. The maximum efficiencies were found to be 65.73% for the MFPC and 79.86% for the NFPC. The efficiency curves were verified experimentally on a lab scale. The inclusion of the hexadic TIM reduced the air circulation speed within the solar collector cavity by 79.16%, producing near stagnant air. An economic analysis of both systems for an average household in Ireland showed that the NFPC system can save a homeowner up to €337.50 more than the current MFPC. This reduces the simple payback period (SPP) from 13.04 years (MFPC) to 10.81 years (NFPC). The inclusion of the hexadic polymer structure also contributed to a 54.54% decrease in the overall weight of the solar thermal collector. The net present value of the NFPC was found to be €764.77 greater than the MFPC making it a more economically attractive system for the public.

Keywords: Decarbonisation, Solar Thermal, Transparent Insulator, Renewable Energy

Declaration

I declare that this thesis has not been submitted as an exercise for a degree at this or any other university and it is entirely my own work.

I agree to deposit this thesis in the University's open access institutional repository or allow the library to do so on my behalf, subject to Irish Copyright Legislation and Trinity College Library conditions of use and acknowledgement.

I consent to the examiner retaining a copy of the thesis beyond the examining period, should they so wish (EU GDPR May 2018).

Signed:

Acknowledgements

Firstly, I would like to thank my principal investigator, Professor David McCloskey. His guidance and assistance throughout the duration of my project was invaluable. Professor McCloskey was the person who first inspired me to explore the world of solar energy physics and for that I can only thank him. The impact of his recommendations on the investigations performed throughout this project cannot be overstated. His leadership, creativity, and guidance over the course of the last two years was admirable and ever appreciated.

I would also like to immensely thank my colleagues in the McCloskey research group, namely Eoin Cotter and Erik Soderholm. For their knowledgeable and patience assistance throughout my project, to being there as friends inside and outside of work I can only thank them.

Secondly, I would like to thank the staff at the Sami Nasr Institute of Advanced Materials in Trinity College Dublin. Your polite assistance never went unnoticed. I would particularly like to thank Patrick Murphy for his unfaltering help with machining and production in this project, and Karl Gogan who help facilitate numerous orders.

To my parent, family and friends. I can't begin to thank you enough for everything you do. Just know my gratitude is eternal and I am proud every single day to represent you.

Finally, I would like to show my appreciation to the Government of Ireland, Irish Research Council who kindly funding this research.

Dedication

This thesis and all the work that went into it is dedicated to my late grandparents, Liam O' Hanlon and Mary Fogarty. The lessons you taught me since I was a child moulded me into the person I am today.

You will never know the extent of the impact that you have had on me.

Love always.

Contents

List of Tables

List of Figures

List of Abbreviations

CAD – Computer Aided Design

CFD – Computational Fluid Dynamics

DHWS – Domestic Hot Water System

DSC – Differential Scanning Calorimetry

ETC – Evacuated Tube Collector

FEA – Finite Element Analysis

FEM – Finite Element Method

FEP - Fluorinated ethylene propylene

FPC - Flat plate collectors

h – Hour

Hz - Hertz

IAM – Incident Angle Modifier

IR – Infrared

ISO – International Organization for Standardisation

k – Kilo

K – Kelvin

ktoe - kilo tonne per oil equivalent

L - Litre

m – Metre

MFPC – Market Flat Plate Collector

mtoe - mega-ton of oil equivalent

N – North

NFPC – Novel Flat Plate Collector

NIR – Near Infrared

NPV – Net Present Value

NSAI - National Standards Authority of Ireland

PC - Polycarbonate

PLA - Polylactic Acid

PV - Photovoltaic

PW – Petawatt

SF – Solar Fraction

SPP – Simple Payback Period

ST – Solar Thermal

TIM – Transparent Insulating Material

TMY - Typical meteorological year

TW – Terawatt

UV – Ultraviolet

VIS - Visible

W – Watts

W – West

Wh – Watt hour

Yr – Year

1. Introduction

Energy is the most basic of human needs and one which is common among all organisms on our planet. Many of the greatest accomplishments of human civilization have been achieved through the increasingly efficient and extensive harnessing of various forms of energy, from fire in the Palaeolithic era to electricity in modern times. This mastery of energy harnessing allowed humans to vastly extend their capabilities and ingenuity. To further improve the quality of human life across the globe, it is essential that we provide sustainable and affordable energy. Doing so will aid our populous to eradicate poverty, improve human welfare, and raise living standards worldwide [1].

As highlighted at the Conference of the Parties 26 at the end of 2020, the issue of sustainable and renewable energy has moved from a climate crisis to a children's rights crisis [2]. The decisions and technology implemented in the next number of years may decide the fate of all future generations.

Two thirds of residential energy demand is used for space and water heating, as shown in Figure 1 [3]. Although in recent years progress has been made in decarbonising our electricity supply, residential heating still relies heavily on oil, natural gas and solid fuels. 87% of all primary energy in Ireland in 2019 came from fossil fuels with almost half of all energy use from oil [3]. There are proposals to transition residential heating to electricity, taking advantage of renewable sources at generation [4]. However, this proposal would require a huge investment in both additional generation capacity and our electrical grid capacity. Technologies such as solar thermal provide a local low carbon, sustainable heat source, without increasing electrical demand. Although solar thermal technologies such as flat plate or tube collectors are at a high level of maturity, they are currently not cost competitive with fossil fuels, with payback periods in the range of 30 years. This project investigates techniques to improve the efficiency of solar thermal systems while reducing their costs to the consumer. This would make solar thermal a much more attractive option for residential customers and incentivise a natural decarbonisation of residential heating aiding Ireland to reach its ambitions targets in 2030, to increase national consumption of renewable energy to 16% of overall energy usage.

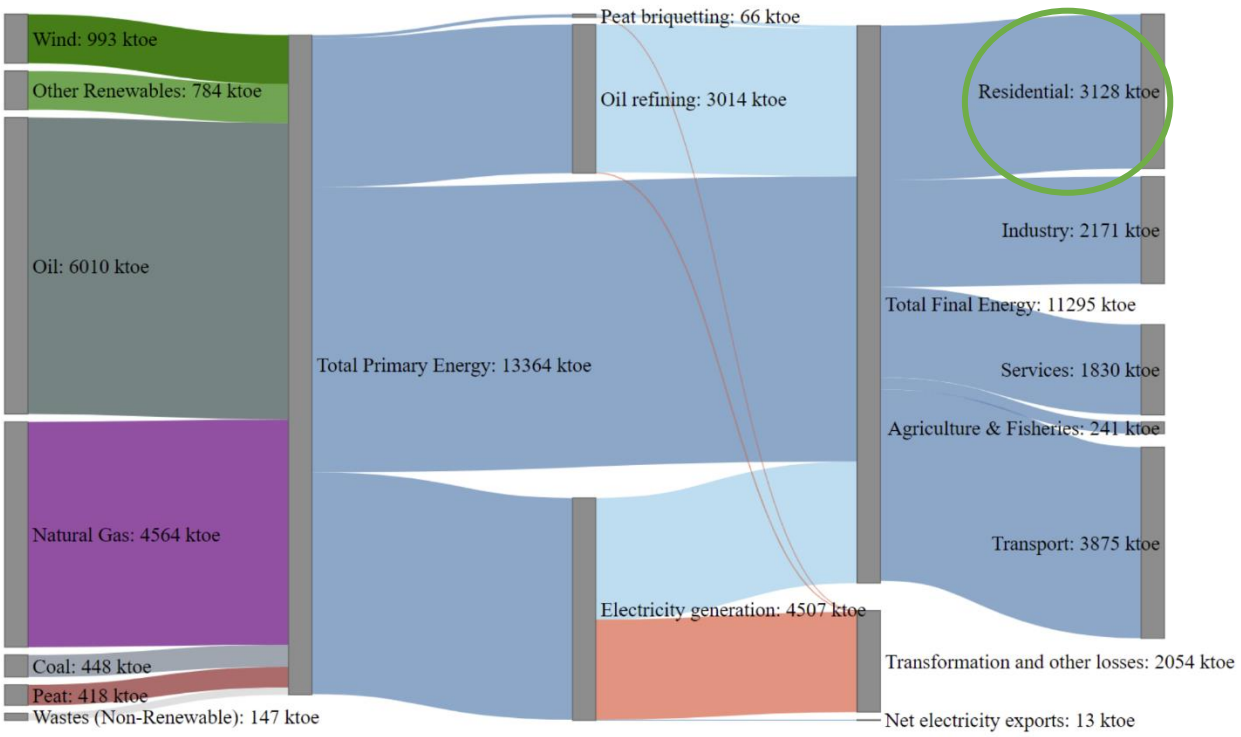

Figure 1. Overall energy flow from source to final consumption in Ireland in 2021 (kiloton of oil equivalent) [3]

1.1 Aim of Project

The goal of this project is to increase the efficiency of solar thermal technology to decarbonise residential heating. This will be achieved by three key objectives:

1. Identifying the limitations of current solar thermal technologies.
2. Examination of the potential of improving efficiencies and reducing costs using transparent insulating materials.
3. Development of a new solar thermal collector design with improved efficiency for market.

These objectives will then be subdivided into actionable and deliverable tasks:

1. A thorough critical analysis of the solar technology currently available on the market will be conducted. By examining the contribution to the costs of this technology and the technical limits of these devices, areas of improvement can be identified.

2. Finite Element Method (FEM) numerical simulations will be performed to optimise convective heat loss supressing designs. An indoor solar thermal testing rig will be produced to allow for accurate lab scale testing of new designs.
3. Using the most promising designs developed through Task 1 and 2, a novel solar thermal collector will be created with improved efficiency.
4. A system-level model will be simulated to examine the collector's overall performance within a domestic hot water system in Ireland.
5. The simulation results will be verified on the laboratory scale.

1.2 Sustainable Energy

Apart from humans, every other living organism's total energy demand is supplied in the form of food and derived directly or indirectly from sun's energy. [5] For humans, the energy requirements are not just for food and agriculture, but also for achieving a certain quality of life *i.e.,* for heating, cooling, transportation, and manufacture of goods. In its 1987 report, Our Common Future, the World Commission on Environment and Development defined sustainable energy development as development that "meets the needs of the present without compromising the ability of future generations to meet their own needs" [6]. This report describes sustainable development "as a process of change in which the exploitation of resources, the direction of investments, the orientation of technological development, and institutional change are all in harmony and enhance both current and future potentials to meet human needs and aspirations". The relationship of energy production and consumption with sustainable development has two important features. One is the importance of adequate energy services for satisfying basic human needs - energy as a source of prosperity. The other is that **the production and use of energy should not endanger the quality of life of current or future generations and should not exceed the carrying capacity of ecosystems [7].** Figure 2 shows the world's energy consumption per million tons of oil equivalent of all major energy sources.

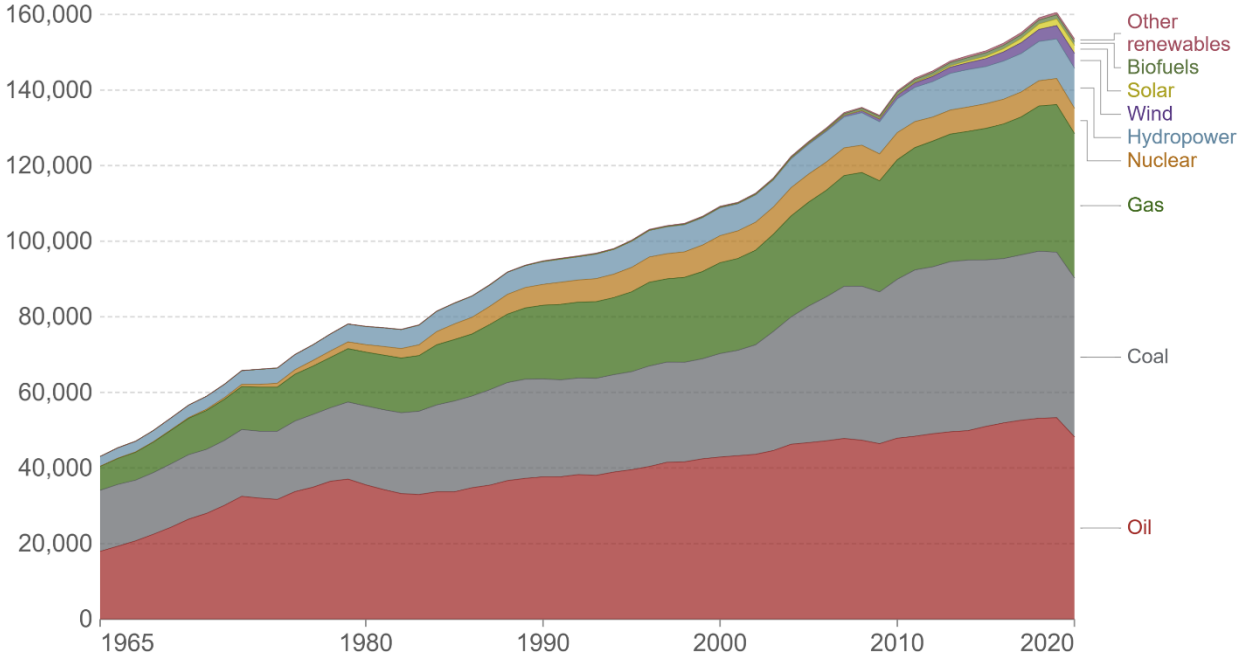

Figure 2. World energy consumption per million tons of oil equivalent by major energy sources [5]

1.3 Solar Energy

The Sun releases an enormous amount of radiation energy to its surroundings: The Earth receives an average of 1367 W/m^2 of solar radiation outside of its atmosphere [8]. This value is an average and fluctuates consistently throughout the year being 3.3% higher in January and 3.3% lower in July [9]. This due to the Earth having an elliptical orbit around the sun and thus it is closer in January and farther away in July. Due to the interaction of solar radiation within our atmosphere, the Earth's surface at the zenith receives a maximum of 1050W/m^2 of direct sunlight. Additionally, the indirect radiation, through processes such as scattering and reflection, results in an overall value of 1120 W/m^2. Therefore, the total illuminated surface of the Earth received a total of approximately 174 PW after being attenuated twice. Despite the attenuation, the total energy received annually from the sun is ≈ 23000TWyr which vastly outweighs all other energy sources on our planet [10], shown in Figure 3. Considering that the world's energy consumption is ≈ 16TWyr, nearly 1500% less than what we receive from the sun each year, solar energy seems like the logical choice if it can be collected and stored efficiently. Locally, Ireland receives 1241 kWh/m^2 of solar irradiation at the optimum angles annually [11].

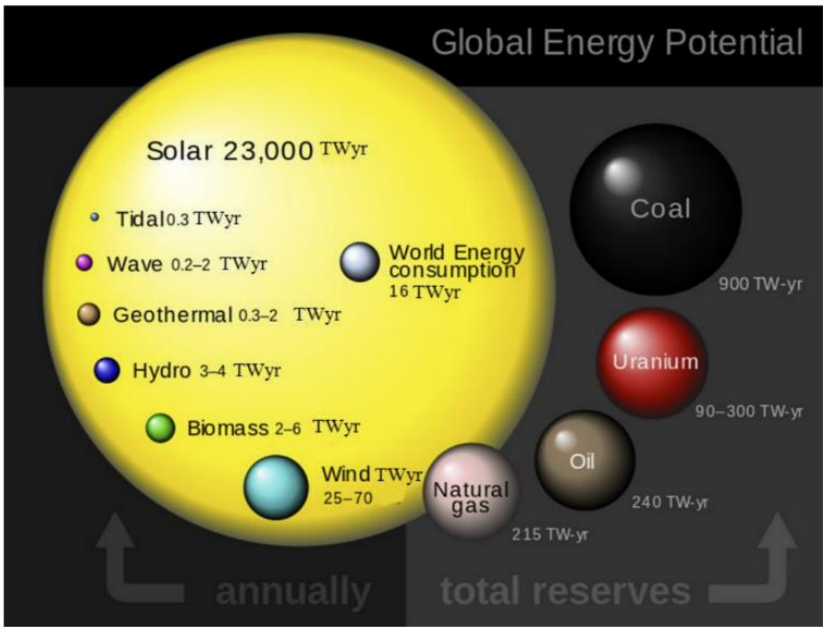

Figure 3. Global energy potential of both renewable and non-renewable energy sources [12]

1.4 Residential Heating

Residential energy demand in Ireland increased by 9% from 2520 kilo tonne per oil equivalent (ktoe) to 2749 ktoe in the period between 2014 and 2018, and accounts for around a quarter of Ireland's overall energy demand [3]. For 2018 it was estimated that 61% of all energy used in households was for space heating and 19% for water heating [3]. That is more than two-thirds of Ireland's energy being used for heating, an application which can be done using local renewable energy sources such as solar thermal panels aided with heat pumps or passive house designs which use solar gain as their only source of space heating. Figure 4 below shows the proportion of the residential energy demand by end use and by source in 2020.

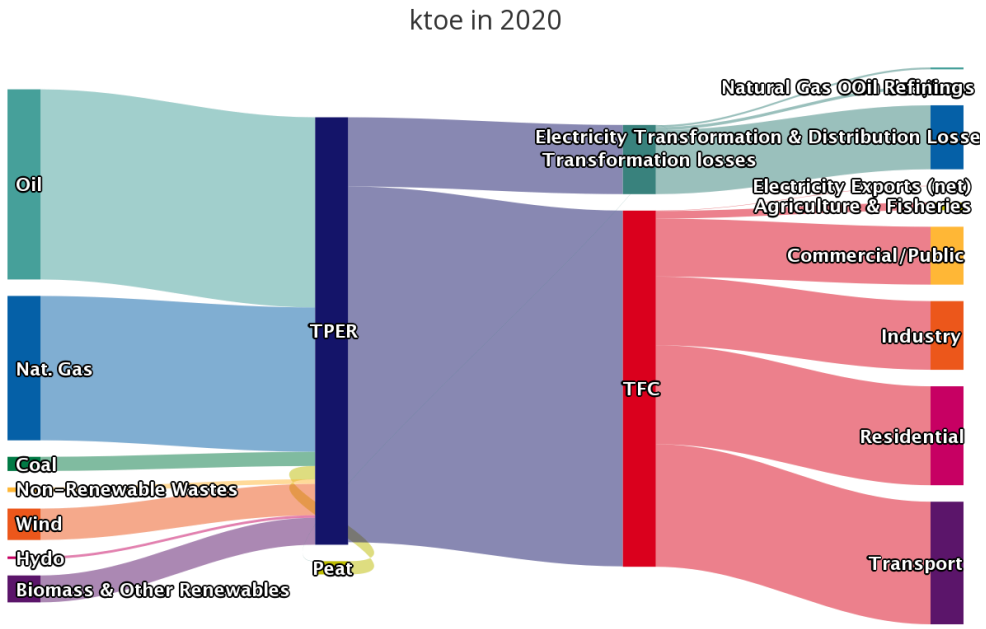

Figure 4. End use of residential energy demand by energy source in Ireland (kiloton of oil equivalent) [3]

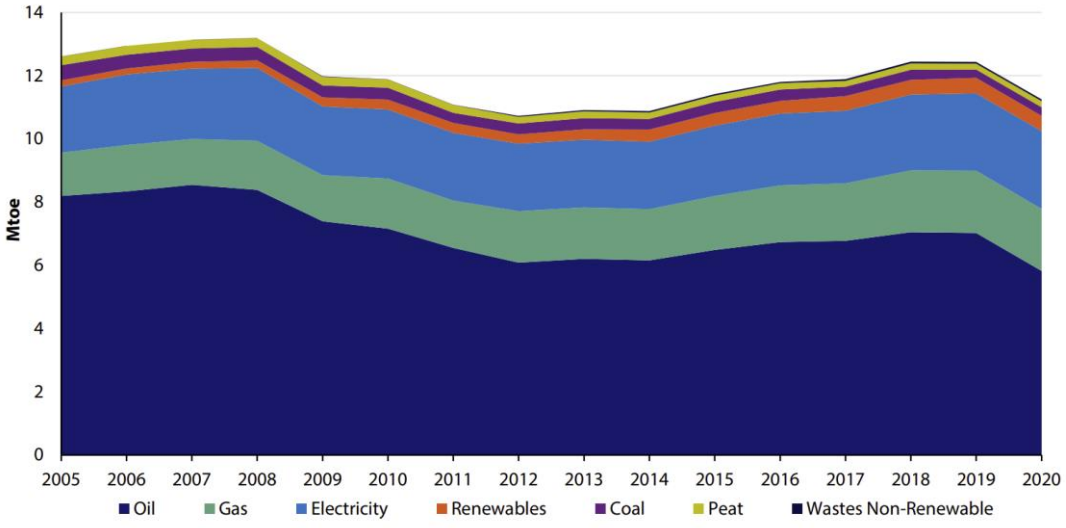

Figure 5. Residential final energy use by fuel type in Ireland (mega-ton of oil equivalent) [4]

The very small share of renewable energy use in Figures 4 and 5 is quite surprising, considering that there are market-ready renewable solutions to domestic water heating available on the market. Solar thermal collectors utilise the energy from the sun to heat domestic water with total energy collection efficiencies of up to 70% [13].

1.5 Solar Thermal Collectors

Solar thermal collectors, also known as solar collectors, produce heat in contrast to the increasingly more common solar photovoltaic (PV) which generates electricity. There are many different classifications of solar thermal collector. However, they can commonly be regarded as specialised heat exchangers, that absorb solar radiation from the sun, transferring that to thermal energy in a circulating fluid. This fluid is usually either air which is used to heat a living or other indoor space directly, or a liquid which is used to generate hot water stored in a tank [14]. In these types of solar thermal collectors, heat can be distributed along a network of tubing via a medium called solar fluid which usually is a mixture of water and a type of antifreeze in varying concentrations. There are two common types of solar collectors used in domestic hot water systems (DHWS) which are evacuated tube collectors (ETCs) and flat plate collectors (FPCs). Both types of collectors use the same physical concepts to convert solar energy to heat energy. The technology in FPCs has stagnated in the last number of years due to a greater efficiency achieved in ETCs, leading to more uptake by the public. However, ETCs cost an average of €385 more compared to FPCs [15]. Should new technology emerge that brings the efficiency of FPCs in line with ETCs, it could revolutionise the industry and make solar energy technology more accessible to the Irish public.

1.6 Flat Plate Collectors

Flat plate collectors (FPCs) are the most popular solar thermal collectors in Europe [16]. They were first produced in 1942 by Hottel and Woertz [17]. The collectors consist of a black solar absorber material connected to channels containing the heat transfer fluid. They are covered with a transparent screen (usually glass) and with thermal insulation covering the back surface of the plate to reduce both radiation and convection losses. The absorber consists of a thin sheet usually of aluminium or copper to which black or selective absorber paint is applied [18]. The working fluid absorbs heat from the absorber and is then circulated through a heat exchanger to an insulated water tank and therefore it is a closed loop system as shown in Figure 6 below.

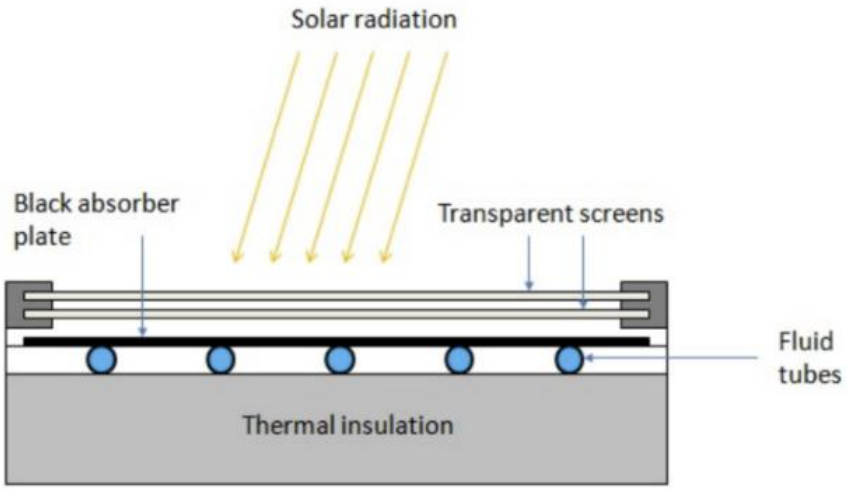

Figure 6. Simple schematic of a flat plate solar collector with liquid transport medium [19]

This simple structure makes FPCs cheap to manufacture and safe to operate, while also having a high optical efficiency of around 51% without a reflector screen [20]. These systems can collect both direct beam and diffused radiation. They are easily integrated onto most rooftops and are more visually appealing to consumers and architects than evacuated tube collectors. They are permanently fixed to the mount (*i.e.,* rooftop) meaning that they require no sophisticated solar tracking equipment and need little maintenance. Figure 7 shows a more in-depth graphically schematic of a solar thermal collector.

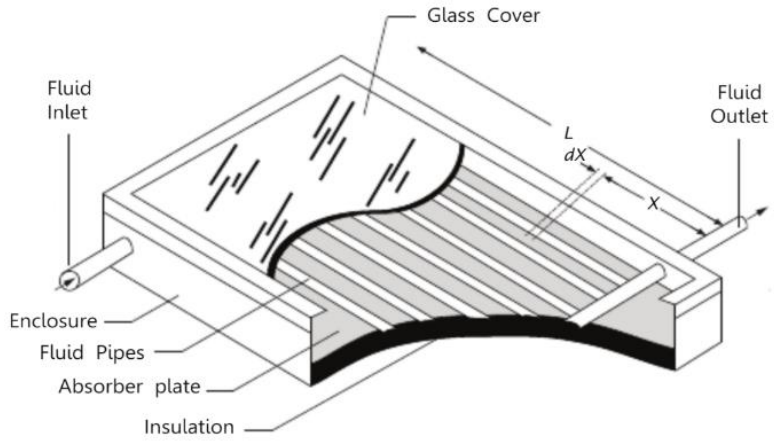

Figure 7. Complete schematic of the elements of a flat plate solar collector [20]

The energy balance equation is used to describe the performance of an FPC [21]:

$$Q_u = A_c[\mathrm{S} - U_L(T_{pm} - \mathrm{T}_a)]$$

Where Q_u is the useful energy output of the collector, A_c is the absorber area, S is the solar radiation per unit absorber area, U_L is the total heat transfer coefficient, and T_{pm} and T_a are the absorber plate and ambient temperatures respectively.

There have been many studies published researching the performance of FPCs in domestic hot water systems (DHWS) [22-25]. Ayompe *et al.* [26] performed a field comparison of FPCs and heat pipe ETCs in an Irish climate. Zambolin and Del Col analysed the thermal performance of FPC and ETC in Italy [27]. Allen *et al.* conducted an appraisal of a solar hot water system in the UK residential sector to assess its overall performance in terms of energy, environmental and economics [28]. Attempts to improve the performance of FPCs are generally focused on trying to reduce the losses of conduction, convection and infrared radiation (IR) while also maximising the absorbance of the absorber material. Convection losses have been identified as the dominant form of loss in FPCs [29]. Suppressing these losses in a cost effective way is paramount to improving performance and efficiency.

1.7 Critical Analysis of Existing Technology

The initial objective of this project was to complete a thorough investigation of the state-of-the-art technology in the solar thermal sector. This was done by examining the weight and cost contributions of the individual components of a solar thermal collector. The aim of this was to identify possible components of the collector which could be modified to reduce overall costs, overall weight, and areas where it may be possible to modify to increase the efficiency of the collector.

1.7.1 Cost Analysis

Using a SolidWorks model that was produced of a solar thermal collector, a cost analysis of a solar collector was carried out. The computer-aided design (CAD) model allowed the weight and cost contribution of each component to be analysed. Table 1 shows these results and Figure 8 shows a visual representation of the results.

Table 1. Cost overview of the components of a Joule Navita 2m^2 Solar Thermal Collector

Material	Weight (kg)	Cost Per Kg	Cost Contribution to Collector	% of Costs
Aluminium				
Sheet	1.8	1.8	3.24	5.34
Frame	3.5	1.8	6.3	10.39
Glass				
Glass cover	19	1.35	25.65	42.30
Copper				
Pipes	4.2	2.25	9.45	15.59
Fibre Glass				
Insulation	3.5	4.57	15.995	26.38
Total:	32		**60.635**	

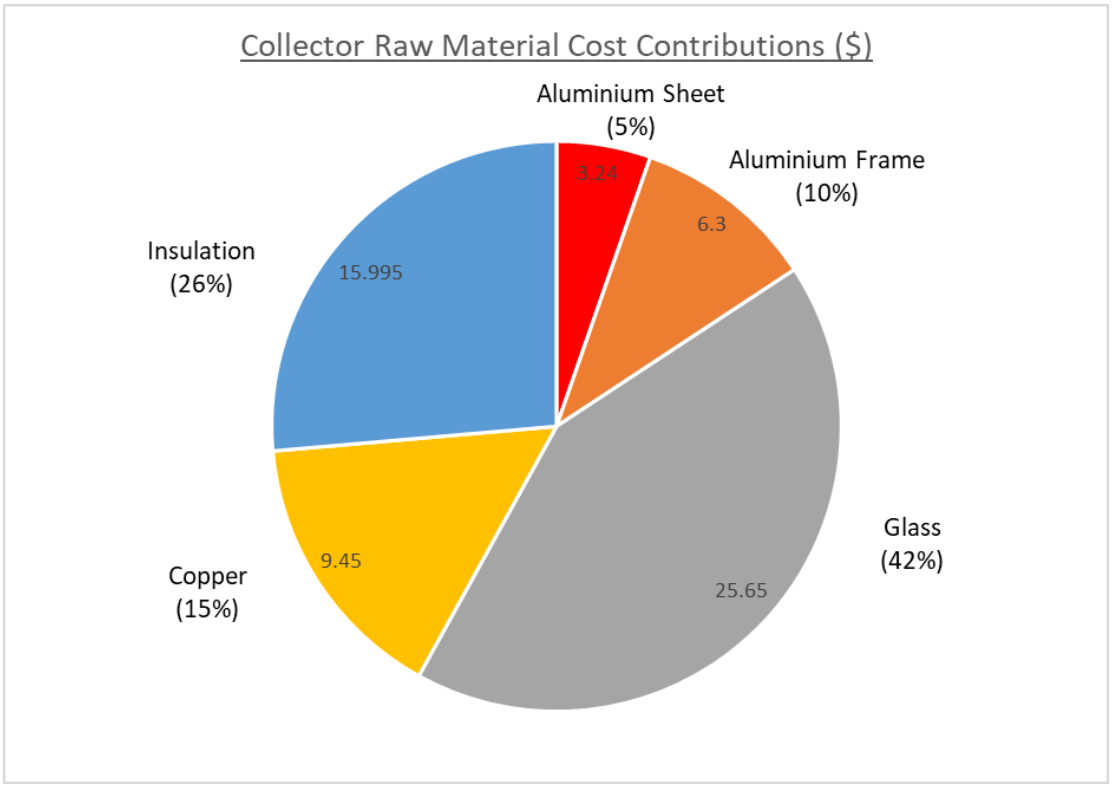

Figure 8. Chart of approximated cost contributions of components in a Joule Navitas 2m^2 Solar Thermal Collector

Figure 8 shows that:

- **Glass** contributes to 42% of the weight and 25.65% to the cost of the panel.
- **Copper** contributes to 15% of the weight and 9.45% to the cost of the panel.
- **Insulation** contributes to 26% of the weight and 15.99% to the cost of the panel.

- **Aluminium** contributes to 15% of the weight and 9.54% to the cost of the panel distributed between sheet aluminium and frame aluminium.

The glass component of the solar collector accounts for a large proportion (42%) of the overall cost of a solar thermal collector. The glass cover is usually 3 – 5mm thick soda-lime glass. Its main function is to provide protection to the absorber plate beneath it from the weather while still allowing solar radiation to pass through and be absorbed.

1.7.2 Weight Contribution Analysis

Similar to Section 1.7.1, a weight contribution analysis of the various components that make up a solar collector was carried out using a CAD model. This model allows the solar collector to be split into its individual components to identify which parts contribute most to the weight of the collector. Figure 9 shows a chart of the results obtained from this analysis.

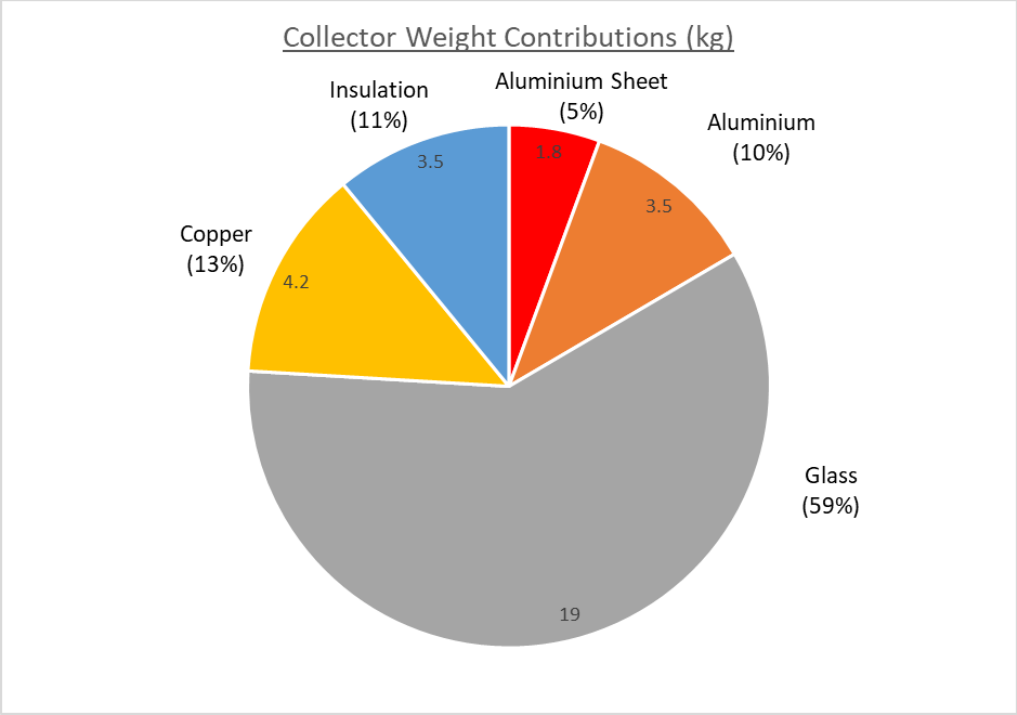

Figure 9. Chart of approximated weight contributions of components in a Joule Navitas 2m^2 Solar Thermal Collector

Figure 9 shows that:

- **Glass** contributes to 59% of the weight and 19% to the cost of the panel.
- **Copper** contributes to 13% of the weight and 4.2% to the cost of the panel.
- **Insulation** contributes to 11% of the weight and 3.5% to the cost of the panel.

- **Aluminium** contributes to 15% of the weight and 5.3% to the cost of the panel distributed between sheet aluminium and frame aluminium.

From this investigation, the glass component of a solar collector was identified the largest contributor to the weight of the collector. The function of the glass, as can be seen in Figure 7, is to protect the inner absorber plate of the solar collector from the weather while allowing the sun's radiation to still land on the absorber. In the analysis shown in Table 1, using a market available Joule Navitas solar thermal collector the glass cover accounted for 42% of the production costs and a 59% of the weight of the collector. The glass component was thus flagged as a potential area where modifications could be made to decrease the cost and weight of a market solar collector. By understanding its main function within the collector an investigation could be carried out to modify this component. While there are currently PVC solar collectors on the market, which have been produced to combat this issue, they are poorly insulated resulting in lower efficiency and significantly higher UV degradation.

Figure 10 shows a Joule Navitas $2m^2$ solar thermal collector which was dismantled by the author. The materials were individually weighed to verify the findings from the simulation. The process also allowed a deeper understanding of how a solar collector's individual components fit and worked together.

Figure 10. Dismantled solar thermal collector for individual component analysis

1.7.3 Current Market Availability and Analysis

It has been widely reported that the availability of fossil fuels will diminish in the coming years [30,31]. This is also common knowledge as everywhere in the world unsustainable energy practices can be seen daily. However, with global energy consumption set to dramatically increase by the year 2030 (Figure 11), a sustainable form of energy production in terms of both heat and electrical energy must be employed.

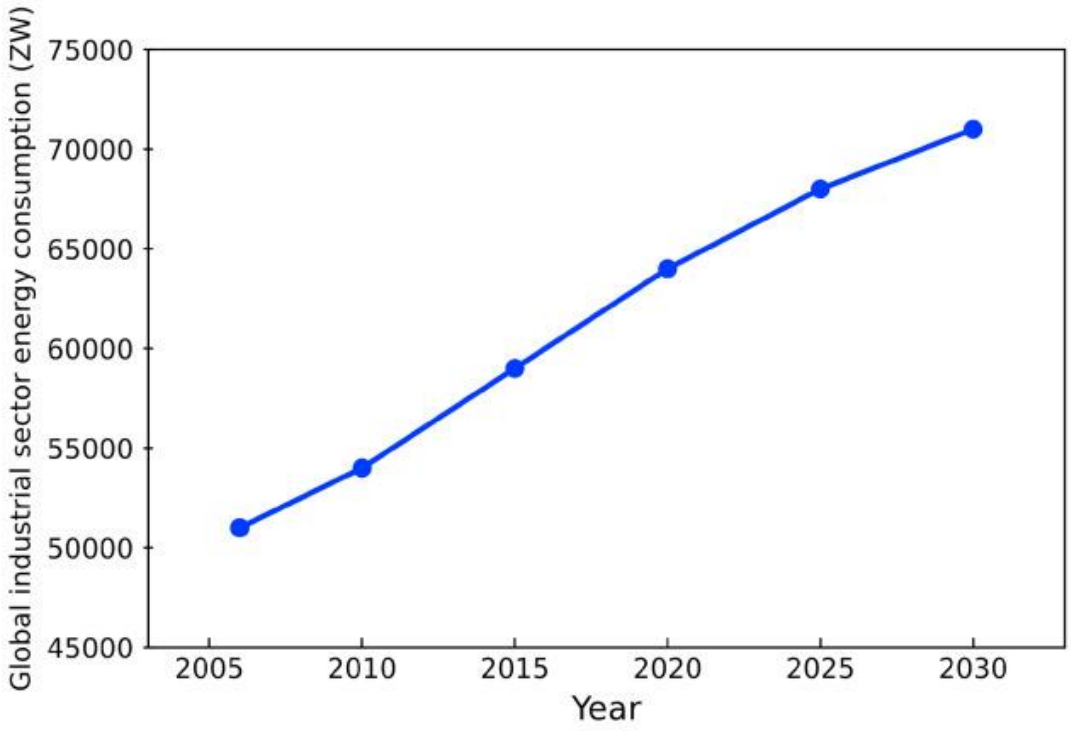

Figure 11. Global industrial sector energy consumption from 2006 – 2030 [32]

In 2003, Kalogirou *et al.* [33] identified solar thermal technology to be a viable option for household and industrial use. However, despite being identified as a viable solution almost 20 years ago, the market hasn't seen an uptake in solar thermal collector sales. This is largely due to the fact that common solar thermal collectors such as flat plate and evacuated tube collectors only have an efficiency in the range of 15 – 40% [34]. Other forms of solar thermal collectors such as parabolic dish collectors and concentrated solar collectors can reach a higher efficiency, however, they are largely impractical in most domestic and industrial settings due to their large size.

Another factor affecting the uptake in solar thermal technology is the price. In Ireland an installed solar thermal system costs on average €4,400. This price also assumes that the buyer has fully availed of the Irish government's solar installation grants. The current grant for installing solar technology domestically is €250 per m^2. Over the 25-year lifespan of a solar thermal system, this price just about makes the system profitable at the current efficiency. This statement is further investigated in the financial analysis section.

This drop in popularity of solar thermal in domestic settings can be seen all across Europe. Despite the fact that France and Denmark hold two of the top 3 spots for countries with the most installed solar thermal systems [35] across the world, solar thermal is less prominent

in other European countries, even within the same climate. The solar thermal market fell drastically from 2018 to 2019 in western European countries largely due to perceived lower efficiency of solar thermal collectors. Countries such as Ireland saw a 5.0% market decrease, United Kingdom saw a 22.1% decrease, and France saw a 14.1% decrease [36]. Meanwhile some southern European countries grew their solar thermal developments in the same time frame such as Greece (+ 10.0%), Portugal (+ 8.8%), and Cyprus (+ 23.7%). Denmark and Ireland are both in the Oceanic climate, however, despite Ireland being almost twice the size of Denmark it has 127.529% less operating solar thermal systems largely due to the perception and economics of solar thermal systems in Ireland.

The fall of popularity leads to a spiral as less and less people instal solar technology in their homes. With less need for installers, the cost of installing a solar system increases as the installers charge more for their services.

Unless the solar thermal industry is revitalised with a new product to bring solar thermal technology more in line with solar photovoltaic, it runs the risk of continue this spiral of becoming more expensive and less popular.

1.8 Techniques to Improve Efficiency in Solar Thermal Collectors

1.8.1 Convection Suppression

The concept of improving solar panel efficiency by suppressing convection in solar thermal panels has been around for many years, although an economically viable solution has yet to be found. Veinberg *et al.* [37] reported in 1959 that the first experimental studies using the concept of honeycomb structures for this purpose in flat plate collectors began in Russia as early as 1929. Hollands *et al.* [38] established in 1965 that natural convection losses could be potentially reduced under certain conditions. They performed a theoretical study proposing to insert a honeycomb structure between the absorber plate and glass cover. This structure was designed to frustrate the airflow and reduce heat loss via convection through the glass plate. Hollands e*t al.* research predicted that the efficiency of the collector could be substantially improved in the working temperature range of 90°C - 150°C. In the 1980s, Hollands *et al.* manufactured a honeycomb structure from fluorinated ethylene-propylene plastic (FEP) [38, 39].

1.8.2 Transparent Insulating Materials

These convection suppression honeycomb devices produced by Hollands *et al.* were amongst the earliest uses for a group of materials known as Transparent Insulating Materials (TIMs) [38]. TIMs were found to be extremely useful in solar applications as they can reduce convective losses in a cavity while also having a high solar transmittance and not increasing any losses due to conduction. Three main factors contribute to this unique property of TIMs to allow solar transmission while also suppressing convection: the geometry, the material, and the operating temperature [40]. The classifications of these TIM structures are shown below in Figure 12.

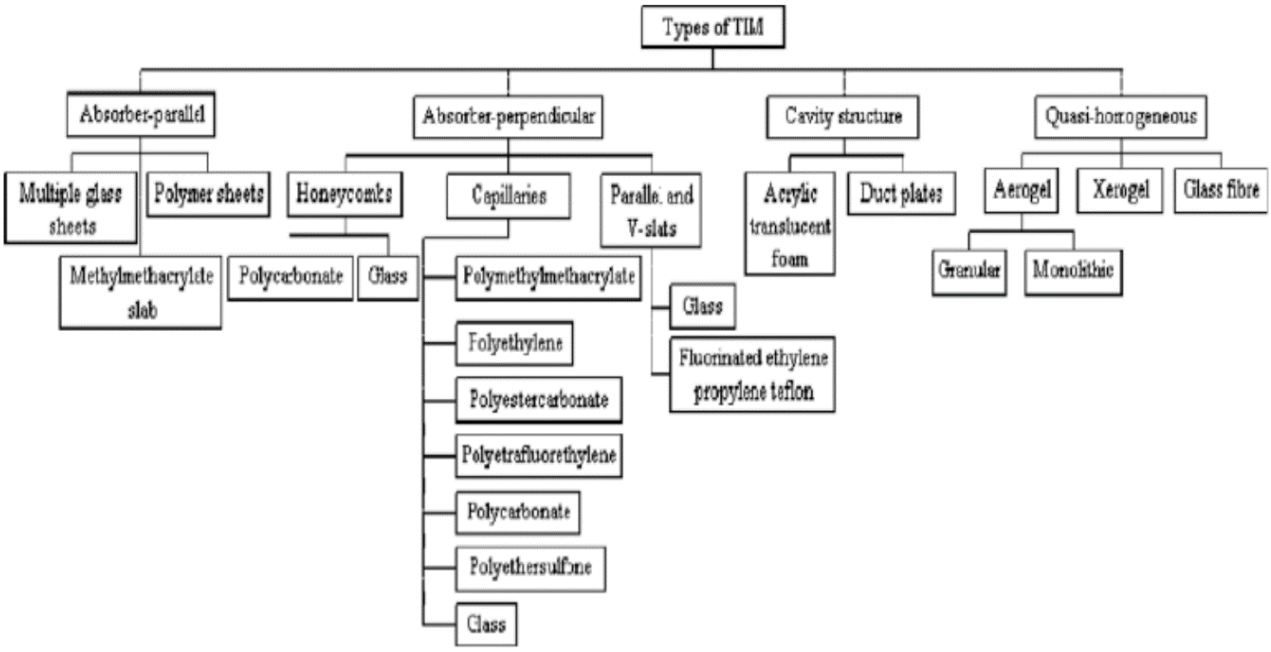

Figure 12. Geometries and associated losses of various transparent insulating materials [41]

Other attempts at creating convection suppressing devices were carried out throughout the 80s and into the early 2000s. These attempts largely fell into the category of absorber-perpendicular structures. Symons in 1982 produced a FEP Teflon film and tubular glass honeycomb [42, 43, 44]. In 1998, Platzer *et al.* reported that absorber-perpendicular structures were the most efficient in terms of solar transmittance and thermal resistance. Platzer also stated that while TIM technologies were yielding promising results, the relatively small market and high manufacturing and installation costs were limiting factors in the widespread uptake of this technology [45].

More recent studies on honeycomb structures have been focused on the optimal thickness of the honeycomb layer and the optimal cavity height between the honeycomb structure, the glass cover and absorber plate. In 2003, Abdullah *et al.* established that a single layer of polycarbonate honeycomb material with a 3mm gap between the TIM and the absorber plate is the highest performing gap height [46]. Abdullah *et al.* also found that the heat loss coefficient is most sensitive to the cavity between the absorber and the TIM structure. In 2005, Ghoneim *et al.* investigated the thermal performance of an FPC with different arrangements of square-celled honeycomb polycarbonate [47]. This study corroborated the findings of Abdullah *et al.;* that the optimum gap height is 3mm below the TIM. Ghoneim *et al.* also found that the best performance of the panel occurred when there was a gap both above and below the TIM insulation. In 2013, Tigi *et al.* produced large scale FPCs utilising honeycomb TIM structure which they have been deploying in Israel on several commercial sites [48]. Figure 13 shows a schematic of TIM structures implemented in a solar thermal collector.

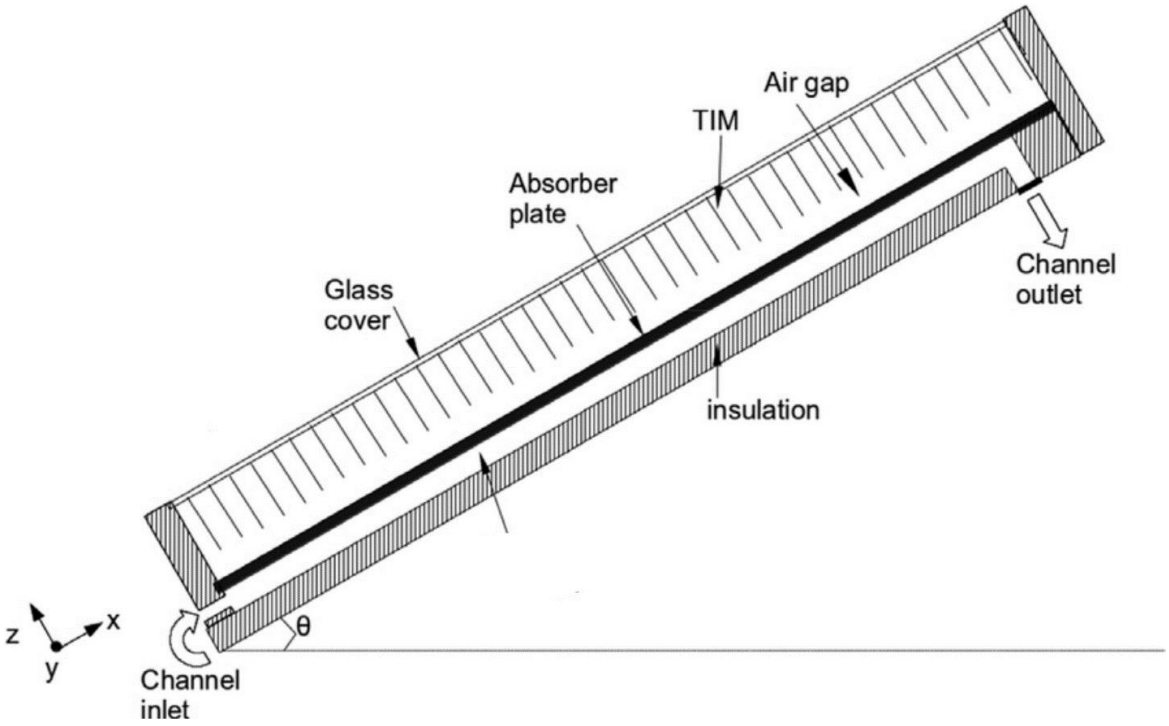

Figure 13. Schematic view of the flat plate solar collector with TIM structure [49]

The honeycomb structure has been utilised successfully for many years as a means of directing air flow. It has also been used to change turbulent airflow to laminar air flow. The structure is both light in weight and has a high strength. In Figure 14, the effect of a honeycomb structure within an air tank can be observed.

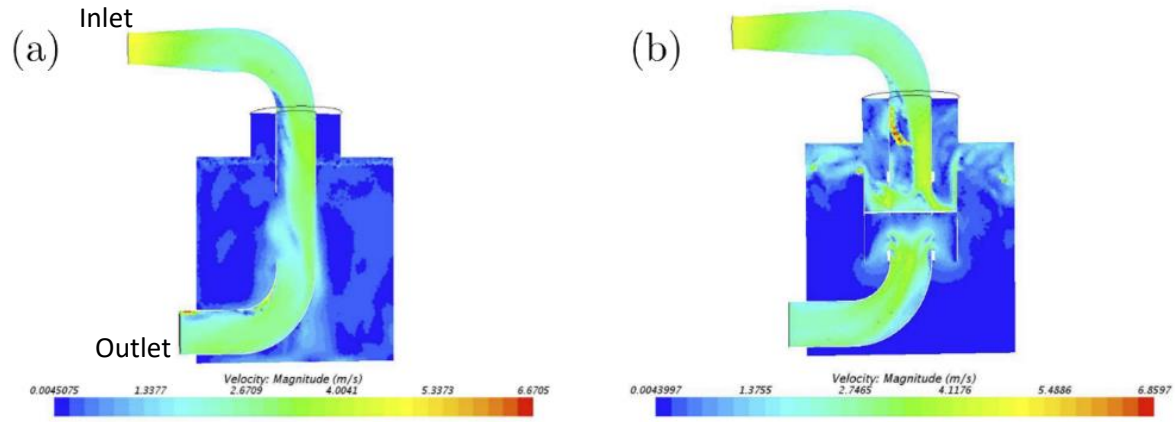

Figure 14. Velocity distribution in an air tank (a) **with** and (b) **without** honeycomb straightener [50].

As can be seen in Figure 14, the honeycomb structure changes the turbulent airflow to laminar flow. More interestingly for this project, we see that the honeycomb confines the convective flow to smaller cell sizes, resulting in lower air velocity and therefore lower heat transfer. In a solar thermal cell, this property should cause the hot air from the absorber plate to circulate away from the glass, meaning less heat will be lost through convection to the glass. This will hopefully increase the efficiency of the solar cell.

In recent years a new substance called aerogel has shown promising results as a TIM. Aerogels are the world's lightest solid materials, consisting of 99.98% air. Transparent super-insulating silica aerogels display the lowest thermal conductivity of any known solid [51]. Zhao *et al.* [52] created a transparent aerogel that was capable of maintaining a 265°C internal temperature in ambient conditions with 10mm thick aerogel and a glass cover similar to a solar thermal collector design. The drawback to silica aerogel is that it is extremely expensive, costing $12.50 per cubic centimetre [53]. This means that for a $2m^2$ solar collector size sheet of transparent aerogel would cost $250,000. Alongside the expensive nature of the material, due to the low density of the material, aerogel is very brittle [54].

1.8.3 Insulation Properties of Air

Air is a good thermal insulator due to its low density in gaseous form. Density is a large factor in a material's insulation capabilities. The larger the intermolecular distance within a substance the more difficult convective heat transfer is through it. This is because the molecules which are in a spread out molecular configuration from each other resist heat transfer to a certain degree. In solar collectors, there is an air cavity between the absorber plate and the glass plane for this purpose. The air within the cavity has very minimal movement, making it very difficult for heat to transfer through the medium and escape via the top of the collector. However, the air within the cavity still does move at a rate up to 0.16 m/s at the top surface of the solar collector, as seen in Figure 15. This causes a circulation of air heating up and cooling down, forming Rayleigh-Bénard Cells within the air cavity [55].

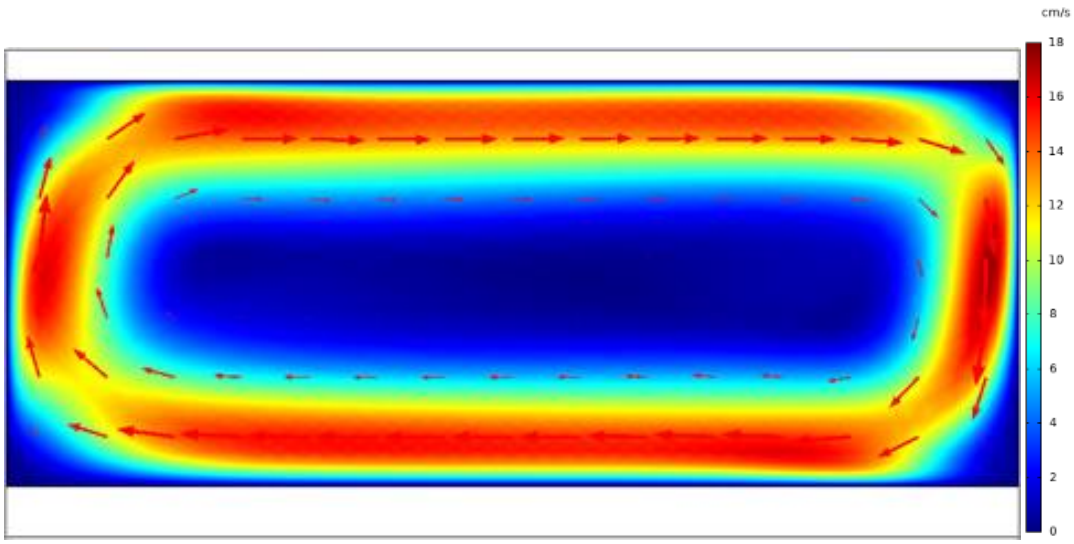

Figure 15. Velocity magnitude of circulating air within a solar thermal collector COMSOL simulation.

The slower that air moves, the better its insulation properties become. Stagnant or trapped air is a natural insulator and can reduce heat loss via both conduction and convection. This concept is used in many applications such as walls and fibreglass insulation. When small pockets of air become stagnant, convection cells can't be set up meaning that heat loss through convection is more difficult. By adding a honeycomb TIM (Figure 16) within the air cavity of a solar cell, stagnant air is created in the channels of the honeycomb. This greatly reduces convection losses while still allowing the sun's radiation to pass through and be absorbed. Figure 17 shows the velocity of air when a hexadic TIM is present within the solar collector air cavity which is reduced to almost stagnant.

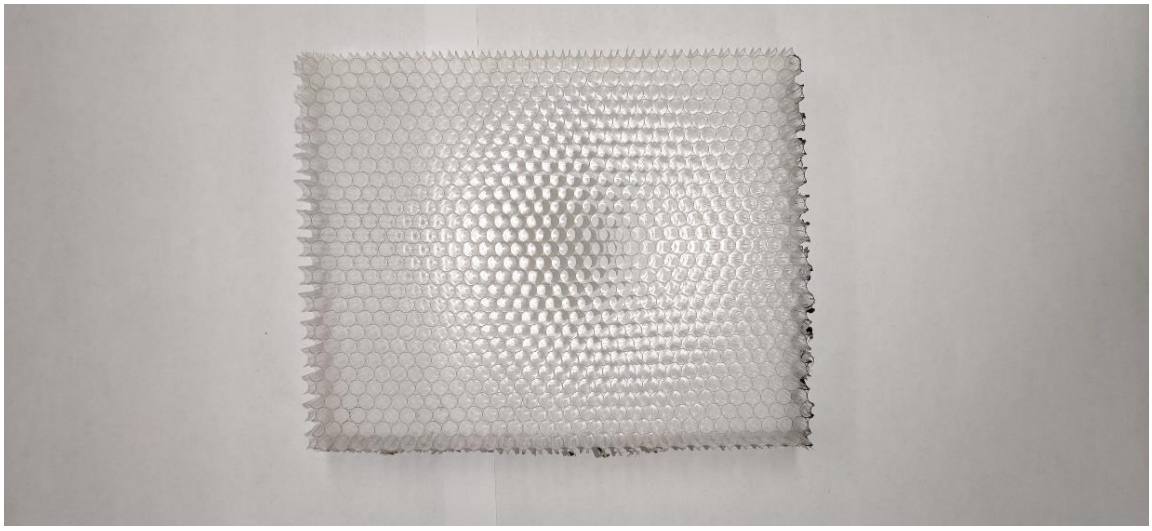

Figure 16. Sample of a polycarbonate honeycomb transparent insulating material.

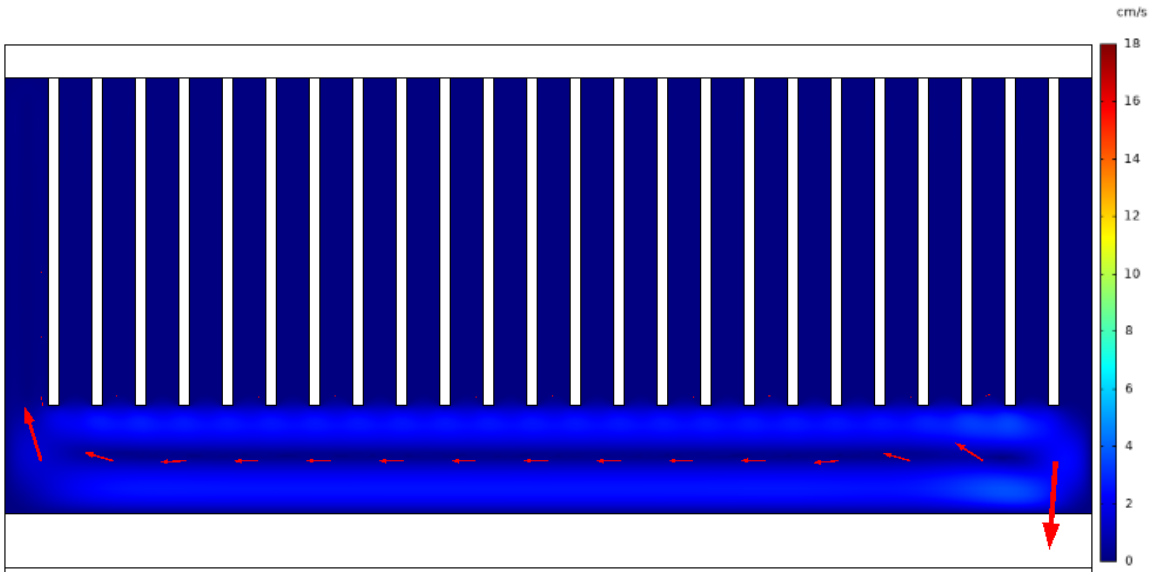

Figure 17. Velocity magnitude of circulating air within a solar thermal collector with a honeycomb TIM, COMSOL simulation.

1.8.4 Analysis of Polycarbonate as a TIM

As discussed in Section 1.8.2, the application of silica aerogel in solar thermal collectors is promising, however, it is not yet viable due to the cost of the material and its inherent properties.

It is proposed in this thesis that a cheaper alternative, with similarly good insulating properties could be employed. Polycarbonate (PC) sheets are already produced at a large scale for many different purposes across various industries. Horizontally channelled

polycarbonate is also use in some applications such as greenhouse and bus shelter roofs. Vertically channelled polycarbonate is less common; however, it is used in some industries such as commercial refrigeration, wind tunnels, climatic chambers, sterilised rooms, and laminar-flow ventilation. Honeycomb structure can be used to eliminate turbulence as seen in Section 1.8.2. If the cell size of the polycarbonate channels is small enough it induces stagnant air, which is an excellent natural insulator.

Polycarbonate honeycomb also has excellent structural properties. The uniform crushing of polycarbonate honeycomb absorbs kinetic energy at a constant compressive load until a 78% reduction of its initial volume is reached.

It is proposed that a hexadic transparent polycarbonate structure, with a small enough cell size could have similar optical and insulating properties as an aerogel, while having a better structural integrity for its application in solar thermal and costing a fraction of the cost.

A hexadic transparent polycarbonate 20mm thick honeycomb material, with 3mm honeycomb channels, weighing $1.8\frac{kg}{m^2}$, with a light transmission of 100 - 92% (IAM dependent) and a thermal conductivity of 0.069 $(\frac{W}{m\,K})$ tested to ISO 9050 and ISO 22007-2 standards was obtained and tested in this research. Its viability as a TIM structure in a solar thermal collector was analysed.

1.8.4.1 UV Degradation of Polycarbonate

Ultraviolet (UV) radiation can be a major issue when considering solar technology. When an organic material is exposed to large amounts of UV it can change the properties of the material. This can greatly affect the performance of solar thermal collectors as if the transparency of the materials change it can cause a drop solar in absorption.

UV radiation consists of packets of photons with high energy relative to visible light. The UV region lies in the wavelength range of 100 - 400 nm. It is divided into three sub-classifications known as UV-A (315-400 nm), UV-B (280-315 nm), and UV-C (100 - 280 nm). Exposure to UV light can cause degradation in the form of both physical and chemical changes in materials. An investigation into the degradation mechanisms with the materials showed that light transmission can be reduced which impacts the efficiency of the solar thermal collectors.

Glass – The dominant mechanism of UV degradation in borosilicate glass is related to the impurities present in the glass. These impurities may be metal compounds such as iron. These metallic atoms have free electrons which may be promoted to higher energy levels during UV exposure. This means that they are available to interfere with electromagnetic radiation, forming colour centres. Colour centre are defects in the regular lattice spacing of atoms within a solid compound. They absorb light of a particular wavelength, thus, lending a characteristic colour to the material. A build-up of colour centres causes a reduction of UV-transparency in the glass over time. This process is known as solarization.

Polymers – Polymers consist of covalently bonded organic constituents, making them susceptible to damage by UV. The most prevalent UV damage mechanism in relation to polymers is called chain scission by photolysis. This is the breaking of long chains into shorter ones due to high-energy photons breaking the main bond of the molecule. This degradation not only causes a reduction in molecular weight but also always results in a degradation of physical properties *i.e.,* strength, ductility and colour. This degradation can also release by-products into the surrounding environment causing other issues.

Other UV-induced damage mechanisms in polymers include the formation of radicals when the chemical bonds are broken. This happens during a process known as chain scission. These radicals will react with other available bonds nearby causing further degradation of the polymer molecules. Bonds dissociated by UV are also prone to react with available oxygen or water. This usually occurs at the surface of the polymer and causes degradation due to oxidation and hydrolysis.

The most dominant UV degradation mechanisms in PC are Photo-Fries rearrangement and photo-oxidation. The relative importance of these mechanisms depends on the irradiation wavelengths [56, 57]. It was shown that the photo-oxidation reaction is most significant when PC is exposed to the wavelengths present in the sun [58].

The underlying premise of all UV degradation is always that the absorption of high-energy UV photons can promote electrons to higher energy levels, dissociating chemical bonds and causing chemical or microstructural changes in the material. As FPCs are not vacuumed sealed, they are more affected by photo-oxidation than photo-fries rearrangement [59].

1.8.4.2 Photo-Oxidation of Polycarbonate

When PC is exposed to UV light, it can oxidise into compounds such as ketones, phenols, benzyl alcohol and other unsaturated compounds. The yellow colour formed after long exposure to the sun can also be related to further oxidation of phenolic end group forming free radicals [60]. In bisphenol A polycarbonate, photodegradation was attributed to two different mechanisms:

$$(OC_6H_4)_2C(CH_3)_2CO)_n + O_2\ ,\ R^* \rightarrow (OC_6H_4)_2C(CH_3CH_2)CO)_n$$

This product can be further oxidized to form smaller unsaturated compounds. This can proceed via two different pathways [61], the products formed depends on which mechanism takes place.

Pathway A

$$(OC_6H_4)_2C(CH_3CH_2)CO + O_2,\ H^*\ HO(OC_6H_4)OCO + CH_3COCH_2(OC_6H_4)OCO$$

Pathway B

$$(OC_6H_4)_2C(CH_3CH_2)CO)_n + O_2,\ H^*\ OCO(OC_6H_4)CH_2OH + OCO(OC_6H_4)COCH_3$$

1.8.5 Optimal Cavity Height

Another concept to explore while considering increasing the efficiency of solar thermal collector is to investigate the cavity height to see if adjustments in this height affect the heat transfer. From previous literature, the optimal cavity height is stated as the height between the absorber plate of a solar panel and the glass cover at which the system efficiency is highest [62, 63]. Previous studies by Paxton *et al.* [64] using finite element analysis determined that the optimal cavity height of a solar thermal air cavity is 2.5cm. At this height the highest absorber temperature and the lowest relative glass cover temperature was observed. This is shown in Figure 18 and Figure 19.

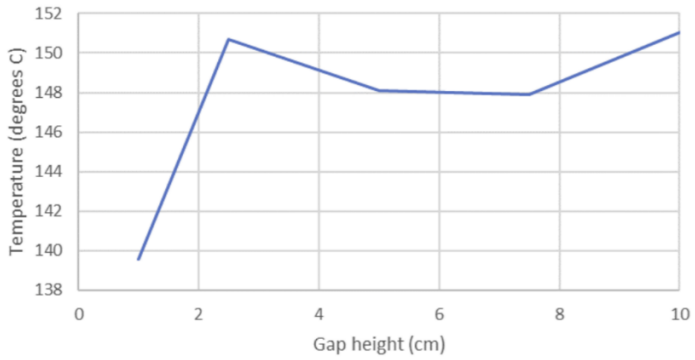

Figure 18. Average absorber surface temperature for flat plate solar collector for 1cm, 2.5cm, 5cm, 7.5cm and 10cm cavity heights at 1000s [46].

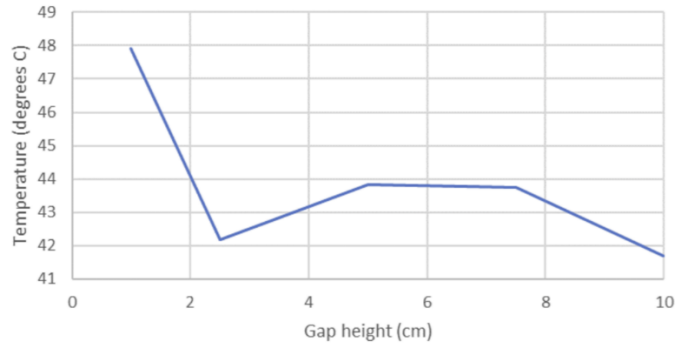

Figure 19. Average glass surface temperature for flat plate solar collector for 1cm, 2.5cm, 5cm, 7.5cm and 10cm cavity heights at 1000s [46].

From these results the lowest average heat transfer coefficient was from the 2.5cm gap height at 3.89 W/m^{2}K. A smaller air cavity is advantageous as it leads to less bulky solar panels hence less shading loss when the sun is at a low angle in the sky for solar panel arrays. A smaller cavity should lead to more attractive looking solar panels and a lower production cost due to less material being used. The optimal cavity height will be confirmed in this research.

1.8.6 Functionality and Application of Ultra-thin Glass

Ultra-thin glass such as BOROFLOAT® 33 was identified in this thesis as having potential applications in the solar collector industry. Borosilicate tempered glass is extremely strong and lightweight. Considering that two-thirds of the weight of a solar collector is contributed to the 3mm thick glass cover, a reduction in weight in this component could greatly reduce the overall collector weight. Borosilicate glass is widely available in a range of different

thicknesses. A 0.33mm sheet weighs only $0.2\,\frac{kg}{m^2}$, with a light transmission of 92% and a thermal conductivity of $1.2\ \left(\frac{W}{m\,K}\right)$.

Combining this ultra-thin glass with the polycarbonate TIM structure discussed in Section 1.8.4 could provide excellent convection suppression while also reducing one of the largest cost factors in solar panel creation and retaining the structural integrity needed for a solar collector. The structural support of the hexadic polycarbonate further reduces the need for a thick glass cover, meaning that the collector as a whole should be able to withstand the climate as usual.

1.9 Efficiency Performance Curve of a Solar Thermal Collector

The collector efficiency of a solar panel indicates how good a collector is at harnessing useful energy from the sun and being able to use that energy to successfully heat water for its use. It is defined as the ratio of useful heat gained per unit of aperture area (W/m^2) to the total irradiation incident on the collector (W/m^2) [65]. It is modelled as a quadratic curve depending on several factors:

- Maximum theoretical efficiency, η_0
- The heat transmission coefficient, a_1
- The temperature of the collector, T_{coll}
- The ambient external temperature, T_{amb}
- The area of the collector, A_{coll}
- The incident solar insolation, G
- The heat transmission dependent on temperature, a_2

It is calculated using the following equation [66]:

$$\eta = \eta_0 - a_1 \frac{T_{coll} - T_{amb}}{A_{coll}G} - a_2 \left(\frac{T_{coll} - T_{amb}}{A_{coll}G}\right)^2$$

The average monthly solar thermal efficiency on the market is between 30 – 45% efficiency [65]. This average, however, doesn't show that some months are much higher (sunnier months) and some months are much lower (less sunny months). The maximum theoretical efficiency limit is set do to the inherit properties of the materials used to create a solar collector such as the transparency of glass and the heat loss mechanisms of the various components. Figure 20, shows the standard efficiency performance curves for the different

types of solar thermal collectors; plastic absorbers, air collectors, flat plate collectors, and evacuated tube collectors. It can be clearly seen that evacuated tube collectors have the highest efficiency across the working range of a solar collector.

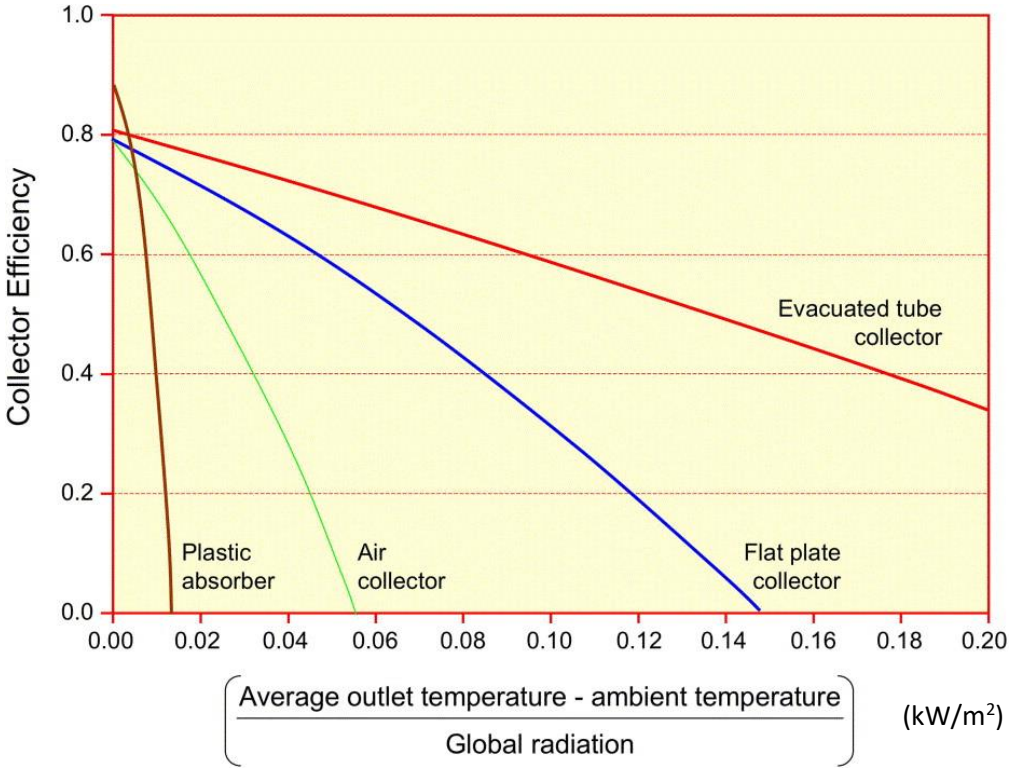

Figure 20. Efficiency performance curves of the various types of solar thermal collectors [67].

The heat losses are described in the collector efficiency curve equation by the parameters a_1 and a_2. The losses are mainly through convection and conduction through the top of the solar collector. This is due to the fact that the bottom of the collector is fully insulated, and the sides have a relatively small surface area, made usually of aluminium. The convection top losses through the glass cover were found to be the biggest cause of heat loss as outlined in Section 1.8.1.

1.10 Dual Glass TIM

Throughout the course of this research a dual glass system incorporated with the TIM structure was investigated as a potential solution. Initially the concept was explored with the hopes of reducing the heat that the polycarbonate TIM was exposed to within a solar thermal collector. This different application came about because the temperature induced within the solar cavity with the dual glass system was even greater than the regular hexadic TIM structure. While in theory a hotter temperature within the solar cavity was what we

hoped for from the TIM structure, the dual glass modifier pushed the temperature far beyond the melting point of polycarbonate. This would mean that the TIM would deform and melt making it unfit for its purpose. However, despite the results not proving positive for this application, it did spark an idea for employing the same concept in other applications such as greenhouses and windows. This idea was explored further throughout the research.

1.11 Scope of thesis

This thesis investigates how to increase the efficiency of flat plate solar thermal collectors using novel techniques. A novel honeycomb structure will be designed, and experiments and simulations will be conducted on its presence within the solar cell cavity. The viability of using a hexadic polycarbonate structure will be examined for its potential use as a TIM structure. An ultra-thin glass cover will be coupled with the TIM structure to examine the weight reduction implications for a solar collector. The performance of the novel solar collector will be analysed in terms of collector efficiency and its performance in a transient system. An economic analysis will be conducted to investigate the financial feasibility of this novel solar collector in the Irish market.

Investigations of different types of solar cells such as solar tube collectors and photovoltaics are beyond the scope of this thesis.

2. Experimental Methods

2.1 Laboratory Scale Testing Development

A computer-aided design (CAD) model was created for this experiment using SolidWorks. This design was then machined from clear 6mm acrylic and glued together using clear acrylic thermal glue. The model was 0.16m x 0.16m x 0.16m and manufactured from transparent acrylic. The prototype was produced to analyse and verify the optimal cavity gap between the absorber plate and glass cover from literature. The model included an adjustable height feature to accurately analyse the optimal cavity height. These heights ranged from 1cm to 10cm and were precision machined. The model can be seen in Figure 21.

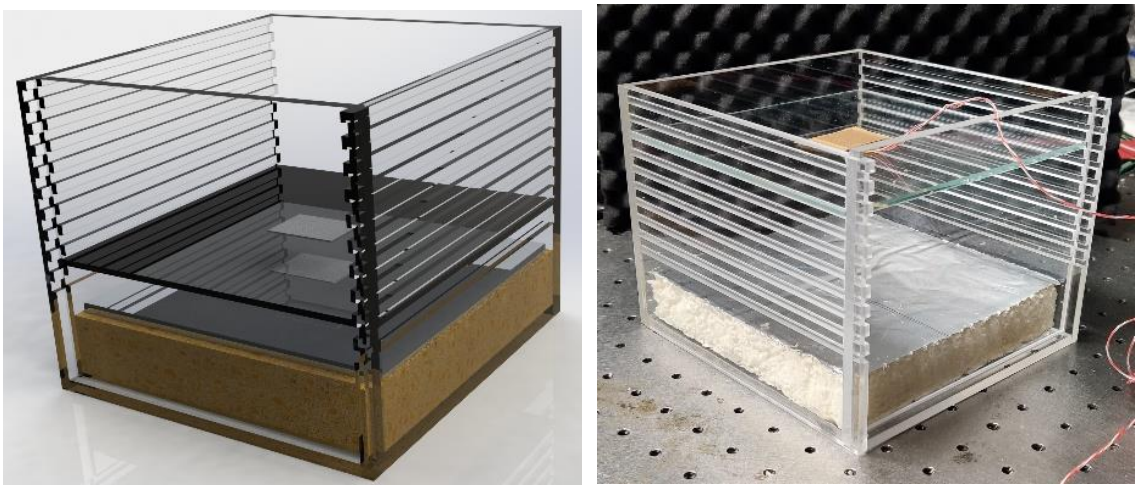

Figure 21. CAD mock-up and lab scale model of solar thermal collector with interchangeable glass cover and variable height.

The setup was designed with a hotplate in place of an absorber plate. The electrical energy inputted into the hot plate could be controlled and correlated to mimic the energy that would be absorbed if the sun's radiation was incident on a solar collector. This method gave a precise control over the energy input for more accurate data and took out the risks and variability of plumbing and water on a lab scale. There were also four thermocouples used in the system to measure the temperature and heat flux at various point of the model collector.

- Thermocouple #1 was placed inside the hot plate.
- Thermocouple #2 was placed on the inside of the glass cover.
- Thermocouple #3 was placed on the outside of the glass cover.
- Thermocouple #4 was placed externally to monitor the ambient air temperature.

The setup was also insulated at the bottom and on all four sides to ensure only the heat loss through the top glass cover was being analysed.

2.2 Novel Flat Plate Solar Collector (NFPC)

The novel solar thermal collector used in this study was created in the McCloskey Nanothermal Research Group. The collector follows the same design as a regular solar thermal collector, except for two key changes regarding the glass cover and the inclusion of a transparent insulating material. The glass cover is a 0.33mm tempered borosilicate glass sheet weighing $0.2\frac{kg}{m^2}$, with a stated light transmission of 92% and a thermal conductivity of 1.2 $(\frac{W}{m\,K})$ [68] tested to ISO 9050 [69] and ISO 22007-2 [70] standards. The transparent insulating material is a polycarbonate 20mm thick honeycomb material, with 3mm honeycomb channels, weighing $1.8\frac{kg}{m^2}$, with a light transmission of 100 - 92% (IAM dependent) and a thermal conductivity of 0.069 $(\frac{W}{m\,K})$ tested to ISO 9050 and ISO 22007-2 standards. Figure 22 shows the lab scale model of the NFPC.

Figure 22. Overhead view of lab-scale model of the Novel Flat Plate Solar Collector (NFPC)

2.2.1 Aluminium Hexadic Structure

For initial designs an aluminium hexadic structure was used, as seen in Figure 23. This structure had 3mm channels and was 20mm thick. This material allowed conceptual testing to occur without the risk of melting or deformation of a polymer due to heat. The insulating properties of the structure were found to be quite impressive, however, it clearly lacked the optical properties required of a TIM used in solar thermal collectors.

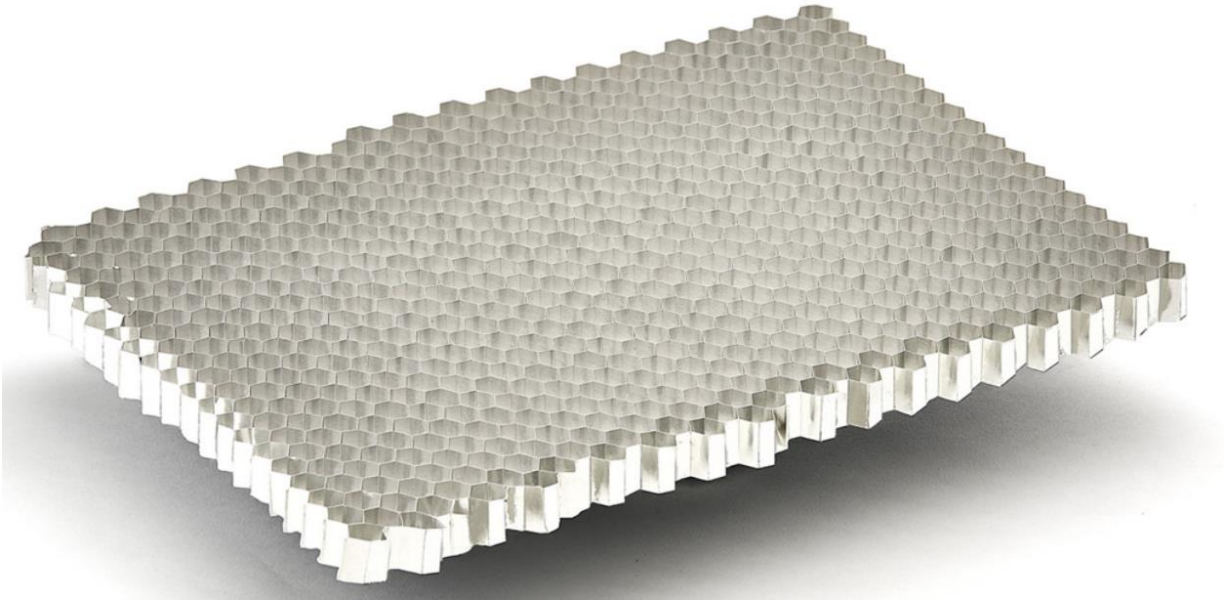

Figure 23. Aluminium hexadic structure with 3mm channel size and 20mm thick

2.2.2 Polycarbonate Hexadic Structure

Building upon the proof of concept using the aluminium structure in Section 2.2.1 a polymer design was obtained. This structure consisted of a 20mm thick transparent polycarbonate (PC), with hexadic capillaries similar to a honeycomb design. The PC structure weighed $1.8\frac{kg}{m^2}$, with a light transmission of 100 - 92% (IAM dependent) and a thermal conductivity of 0.069 $(\frac{W}{m\,K})$ tested to ISO 9050 and ISO 22007-2 standards. It was used to examine its potential as a TIM within a solar cell. The components convection suppression properties, optical properties, UV properties and heat resistant properties were all examined. The structure can be seen in Figure 24.

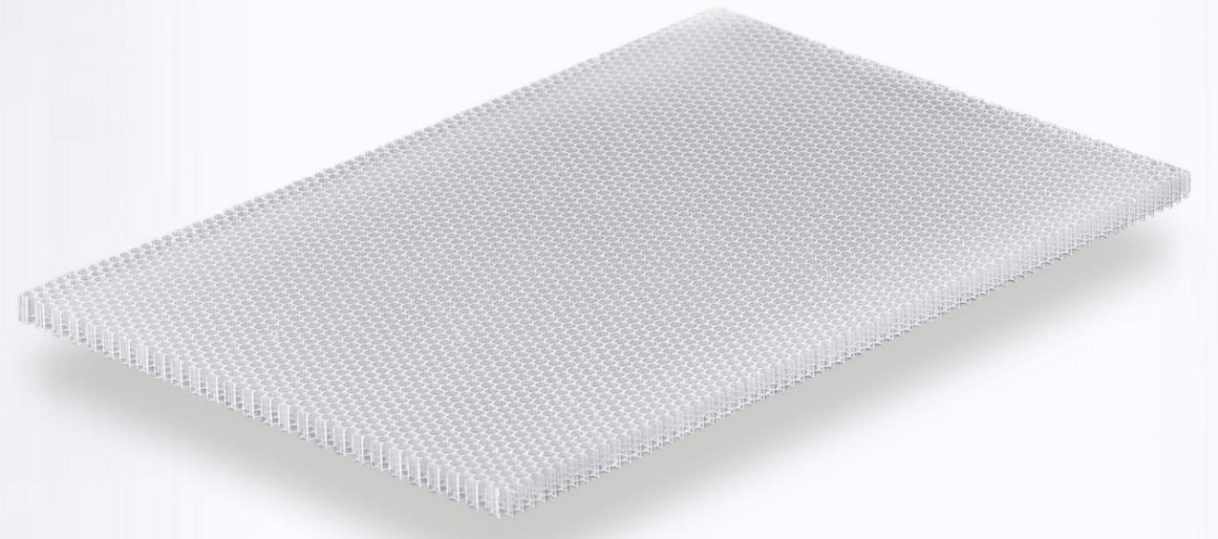

Figure 24. Transparent polycarbonate hexadic structure with 3mm channels and 20mm thick

2.3 Market Flat Plate Collector (MFPC)

The flat plate collector that was available on the market was a $2m^2$ Joule Navitas solar thermal collector. This is a commercially available collector that has been tested to EN 12975 [71] standards and certified by NSAI Ireland. The efficiency constants stated for the collector for an irradiance of $G = 800\frac{W}{m^2}$ were $\eta_0 = 0.799, a_1 = 4.173, a_2 = 0.008$ $(\frac{W}{m^2K})$. The glass cover of the collector was 3.2mm tempered solar safety glass weighing 20kg with a stated light transmission of 92% [72].

2.4 Finite Element Analysis

COMSOL Multiphysics® was used to simulate fluid flow and heat transfer within the solar collector in this study. Due to the design of solar thermal collectors, there is an air cavity between the absorber plate which collects the sun's radiation and the glass cover which protects the absorber from the weather conditions. This air cavity is where the majority of the physics occurs and where energy is lost from the collector through convection and conduction. This FEA software uses a computational fluid dynamics (CFD) model to analyse the complex fluid flow within the cavity. A Navier-Stokes equation [73] is used to model the laminar flow and a k-ε model [74] is used for the turbulence flow, although the flow is this regime is mainly laminar. A model was created for the MFPC and NFPC (Figure 25) to simulate a solar thermal collector in real-world conditions. A physics-controlled mesh size of $1.25x10^{-5}$ - 0.0037 m was implemented in this study.

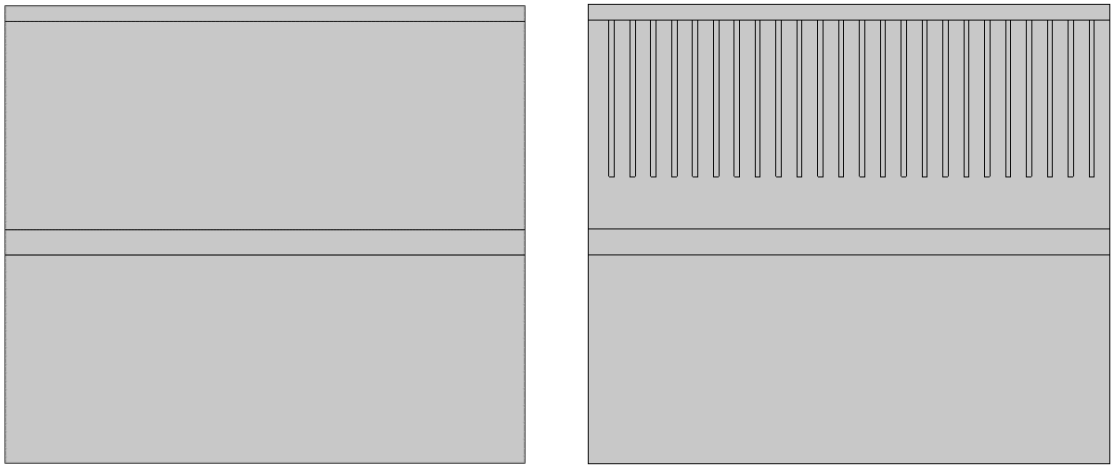

Figure 25. COMSOL models of i) MFPC and ii) NFPC

2.5 System Level Modelling

TRNSYS is a transient system simulation tool which allows you to simulate the behaviour of transient systems. The software was used in this study to simulate a solar thermal collector as part of a domestic hot water system. The hot water demand profile used was the EU reference tapping cycle number 3 [75]. This profile is based on the hot water usage of an average European household in accordance with the EU M324EN standards. It is equivalent to a daily energy output of 11.7 kWh representing 199.8 litres of water at 60°C.

An auxiliary heating system was also employed to heat the hot water tank to 60°C when the solar thermal system failed to do so. The auxiliary heat was set to turn on whenever the tank temperature dropped to 55°C and turn off when 60°C was achieved during the daytime hours of 8am and 10pm (Figure 26).

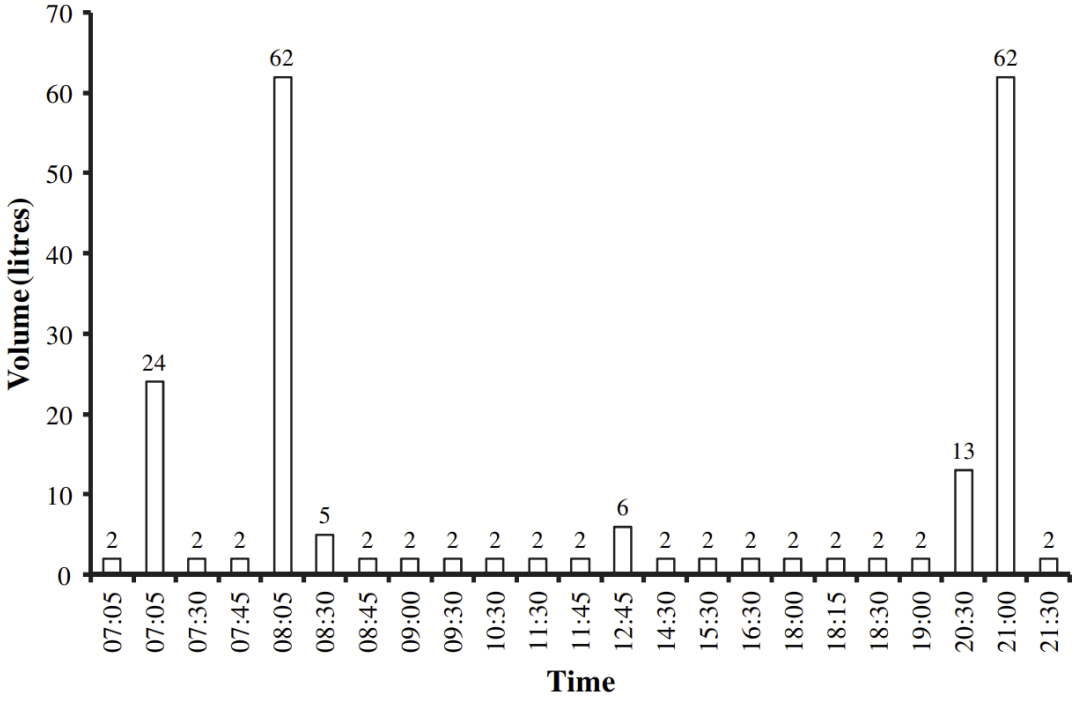

Figure 26. Volume of hot water draw off as per EU M324EN standards [75]

A schematic of the TRNSYS simulation diagram is shown in (Figure 27). The schematic shows a breakup of the system into its individual components plus the location of the thermocouple sensors used in the energy analysis. These parameters include:

- Temperature at the collector inlet, *T1*
- Temperature at the collector outlet, *T2*
- Temperature at solar coil inlet, *T3*
- Temperature at solar coil outlet, *T4*
- Temperature of cold-water inlet from mains, *T5*
- Temperature at the bottom of the hot water tank, *T6*
- Temperature at the 70% up the hot water tank, *T7*
- Temperature of hot water supplied to house, *T8*

The flow rate of the solar collector was $40\,\frac{kg}{h\,m^2}$ and Irish weather data from Dublin Airport was used from TRNSYS typical meteorological year (TMY) weather files.

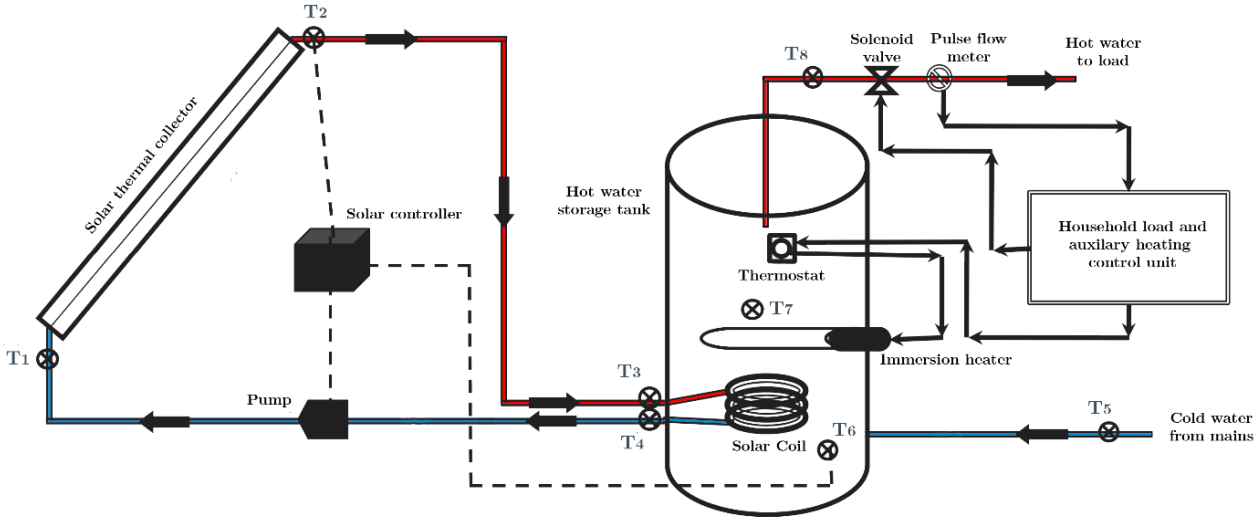

Figure 27. Schematic diagram of TRNSYS simulation experimental setup

2.6 Energy Analysis

The performance analysis of the solar collectors in this study was evaluated based on several different factors including useful energy gained, auxiliary heating required, solar fraction, and collector efficiency.

2.6.1 Useful Energy Gained

This is the amount of energy collected by the solar collector from the sun. It is given by [76]:

$$Q_{collector} = \dot{m}C_p(T_2 - T_1)$$

2.6.2 Auxiliary Heating Required

The auxiliary heating required is the amount of additional heat that the immersion must supply to the hot water tank for it to reach its desired temperature set at 60°C. The additional energy is usually supplied via gas, oil, or electricity from an external source to an immersion heater. It is given by:

$$Q_{aux} = Q_{load} - Q_{solar}$$

2.6.3 Solar Fraction

The solar fraction of this system is the ratio of solar energy collected to the total energy demand for sufficient hot water in the domestic hot water system. It is given by [76]:

$$Solar\ Fraction = \frac{Q_{solar}}{Q_{solar} + Q_{aux}}$$

2.6.4 Collector Efficiency

The efficiency of flat plate solar thermal collectors is modelled as a quadratic performance curve which depends on the incident solar insolation (G), the ambient external temperature (T_{amb}), the maximum theoretical efficiency (η_0) and two parameters a_1, the heat transmission coefficient, and a_2, the heat transmission dependent on temperature. It is calculated using the following equation [66]:

$$\eta = \eta_0 - a_1 \frac{T_{coll} - T_{amb}}{A_{coll}G} - a_2 \left(\frac{T_{coll} - T_{amb}}{A_{coll}G}\right)^2$$

This can be simplified to:

$$\eta = \frac{Q_{solar}}{A_{coll}G}$$

2.7 Economic Analysis

One of the major constraints in the solar thermal industry is the financial viability of collectors for consumers. In order for performance increases to be worth it, the cost of the collector must not increase for the end customer. To analyse the economic viability of the MFPC and NFPC the annual savings, simple payback period and net present value was calculated along with annual savings for a household.

The data shown in Table 2 was used to define the economic parameters are the market prices for electricity and heating in Ireland in 2022 [77]. The load used by a household was based on the hot water usage of an average European household in accordance with the EU M324EN standards. The lifetime of the system was assumed to be 25 years based on the guarantee quoted by manufacturers ranging from 20 – 30 years. The annual operation and maintenance costs were 1% of the initial cost and the costs increased at a rate of 1% per year [78] and the discount rate of 4% is in line with Irish government guidelines [79].

Table 2. Economic parameters of a solar thermal system in a domestic setting in Ireland

Parameter	Value	Units
Cost of electricity	0.2396	€/kWh
Cost of heating (oil)	0.098	€/kWh
Inflation rate of energy	5.6	%
Cost of FPC system	4400	€/kWh
Government grant	1200	€/kWh
FPC size	6	m^2
System lifetime	25	years
Discount Rate	4	%

2.7.1 Annual Savings

The annual savings are the amount of energy and money an average household can save by implementing a solar thermal system. This is measured in terms of kWh and cost per kWh (€) for a house in Ireland.

2.7.2 Simple Payback Period

The simple payback period (SPP) is a useful metric as it shows the public how long it will take for their investment to pay for itself. It is given by the ratio of the initial cost of purchasing the solar system ($C_{initial}$) to the savings made annually by the collector (S) [79]:

$$SPP = \frac{C_{initial}}{S}$$

2.7.3 Net Present Value

The net present value (NPV) is a financial analysis technique used to determine whether a product is financially viable to pursue. In this study it is used to determine if the NFPC is a product that would perform well in the Irish market.

It is calculated using the total cost of the solar system over its entire lifespan (C), including the initial costs ($C_{initial}$) and the upkeep costs of operation and maintenance (C_{upkeep}).

It is then divided by the total revenue the solar system accrues over its lifespan (R). It is given by [26]:

$$NPV = \frac{Q_{useful}}{\eta_{aux}} \sum_{n=1}^{n=N} \frac{(1+e)^n}{(1+d)^n} - C_{initial} + \sum_{n=1}^{n=N} \frac{C_{upkeep}(1+e)^n}{(1+d)^n}$$

Which can be simplified to:

$$NPV = R - C$$

Where η_{aux} is the auxiliary heater efficiency, N is the product lifetime, e is the annual fuel inflation rate, and d is the discount rate.

3. Results

3.1 Determination of Optimal Cavity Height

3.1.1 Determination of Optimal Cavity Height

This experiment was carried out as three independent tests. The experiments were carried out using the model lab scale solar collector shown in Figure 21 to determine the desired air gap before employing any TIM technology. Measurements were taken at each height increment ranging from 1cm – 10cm to determine the optimal cavity height. The tests were carried out from 10cm down to 1cm, and from 1cm up to 10cm. This was done to ensure consistency throughout as the thermal setup takes a long time to reach equilibrium. The results of these experiments are shown below in Figure 28 - 31. The key results are shaded within Table 3 and show the lowest U-value at a cavity height of 1cm.

Table 3. Experimental data for flat lab-scale solar collector at steady state.

Distance	Avg GT	Avg GF	Avg PT	Avg PF	U - Glass	U - Plate	Uval - G	Uval - P
cm	K	W / m^2	K	W / m^2	W / mK	W / mK	W / m^2K	W / m^2K
0.5	57.63	377.09	100.83	779.16	1.13	1.34	9.64	9.64
1	54.63	311.25	121.18	838.42	1.97	2.39	10.18	8.29
2	51.29	260.72	117.65	994.39	3.52	5.85	8.29	10.18
3	51.36	271.76	117.15	848.07	5.49	7.51	8.73	8.73
4	49.48	254.90	115.84	790.90	7.13	9.45	8.35	8.25
5	47.73	228.63	113.97	844.13	8.29	12.81	8.98	8.98
6	45.78	213.37	112.39	869.74	9.68	16.07	9.41	9.41
7	45.01	204.57	111.38	867.70	11.01	18.87	9.50	9.50
8	43.18	199.96	109.87	855.00	12.82	21.54	9.51	9.51
9	40.68	170.19	108.49	868.30	13.03	24.92	9.81	9.81
10	37.82	140.14	106.85	905.73	12.82	29.33	10.43	10.43

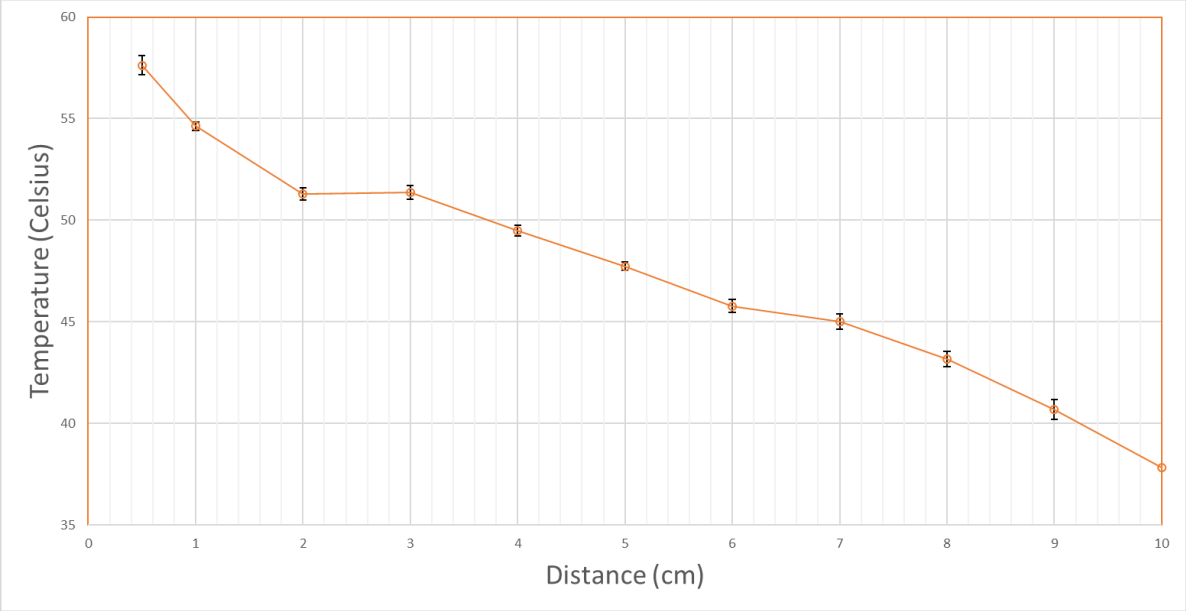

Figure 28. Experimental data of **glass cover temperature** for flat lab scale solar collector at steady state. SD indicated. n=3.

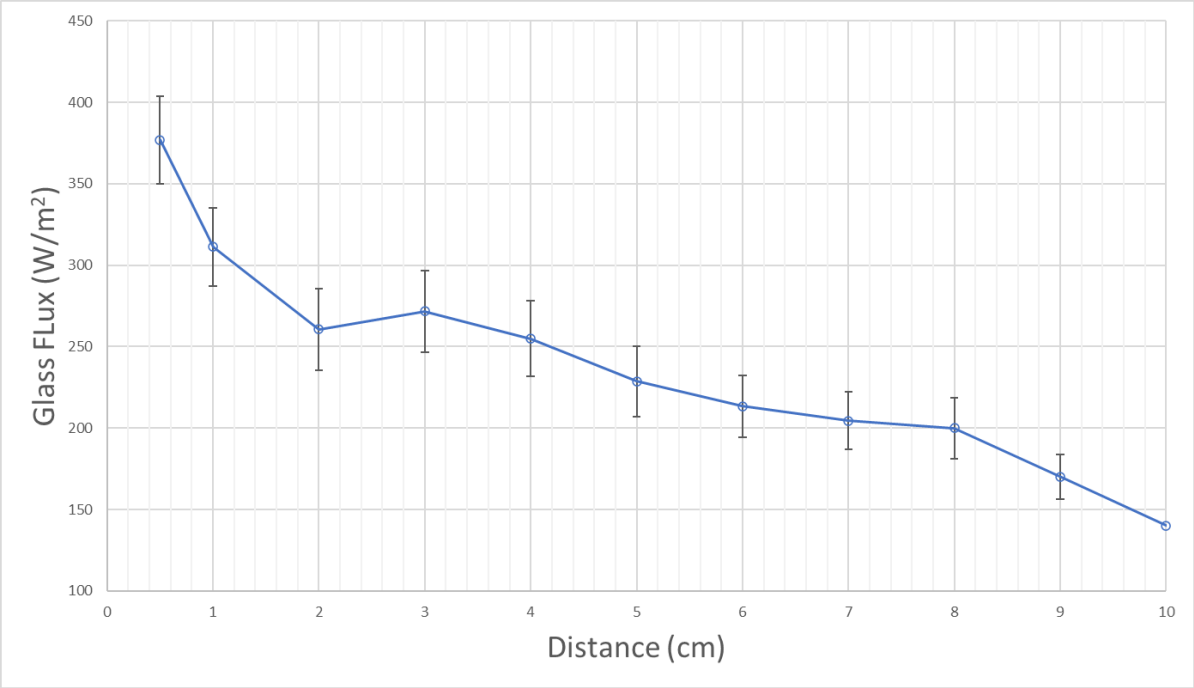

Figure 29. Experimental data of **glass cover flux** for flat lab scale solar collector at steady state. SD indicated. n=3.

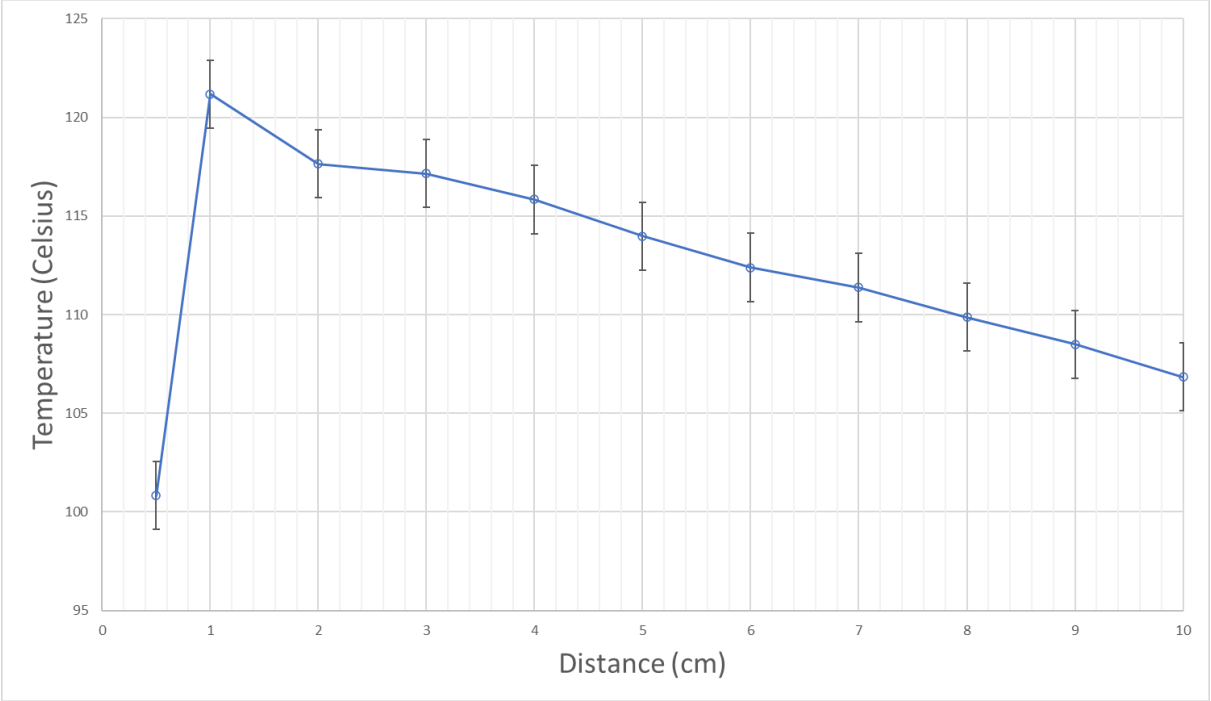

Figure 30. Experimental data of **absorber plate temperature** for flat lab scale solar collector at steady state. SD indicated. n=3.

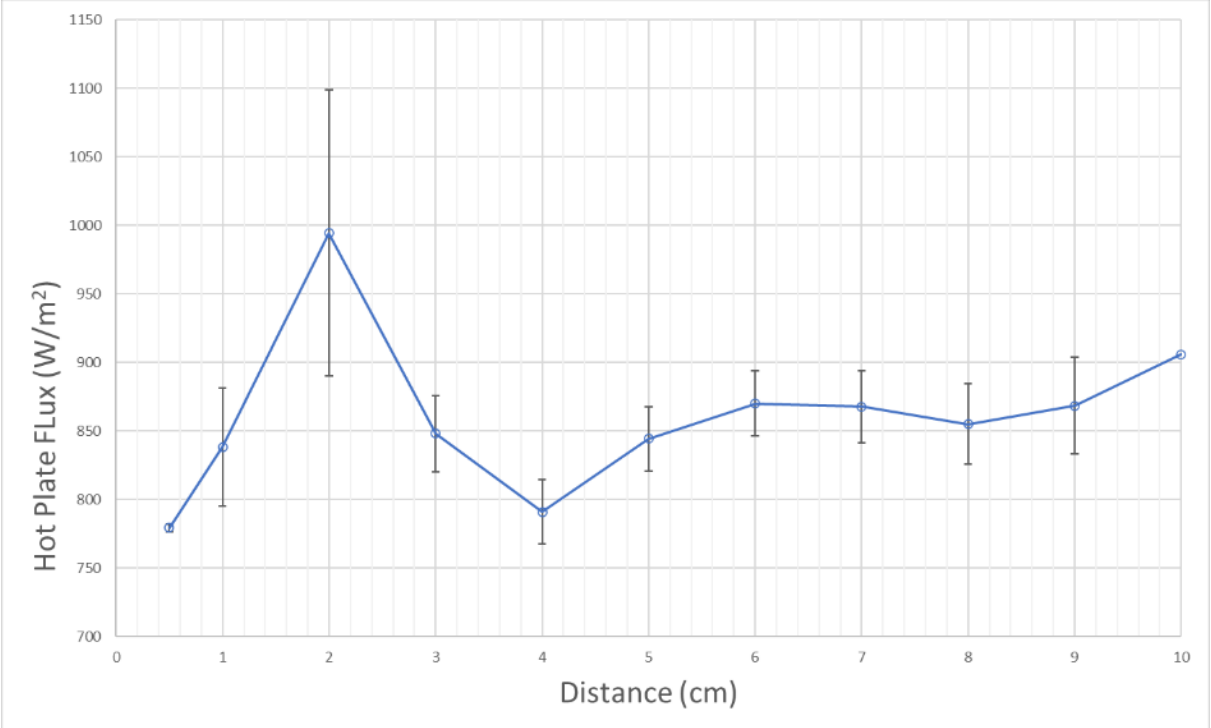

Figure 31. Experimental data of **absorber plate flux** for flat lab scale solar collector at steady state. SD indicated. n=3.

Based on these Figures 28 - 31, the optimal cavity height in the model solar collector was determined to be 1cm. At this height the absorber plate temperature was found to be at its highest at 121.18 ± 0.44°C, with a relatively low flux of 838.42 ± 3.00W/m^2.

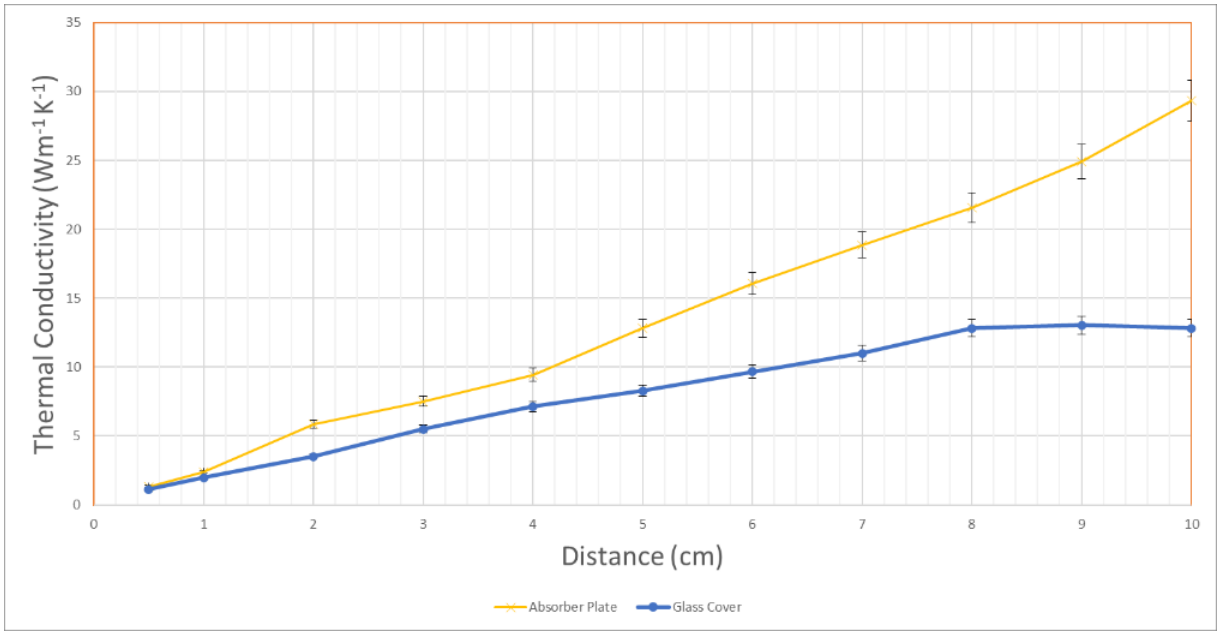

Figure 32. Data of **absorber plate and glass cover thermal conductivity** for flat lab scale solar collector at steady state. SD indicated. n=3.

By examining the data in more depth, the effective thermal conductivity can be determined. In Figure 32, the lowest thermal conductivity was found when the cavity height was 0.5cm. However, as can be seen in Figure 33, the temperature of the absorber plate was significantly lower at 0.5cm cavity height. The optimal height was determined at 1cm, which is in contrary to the experiments performed by Paxton *et al.* This value of 1.97 $Wm^{-1}K^{-1}$ (Glass) and 2.39 $Wm^{-1}K^{-1}$ (Absorber Plate) verified that the 1cm cavity height has a lower ability to conduct heat, hence more heat energy remaining in the solar cell and increasing the efficiency.

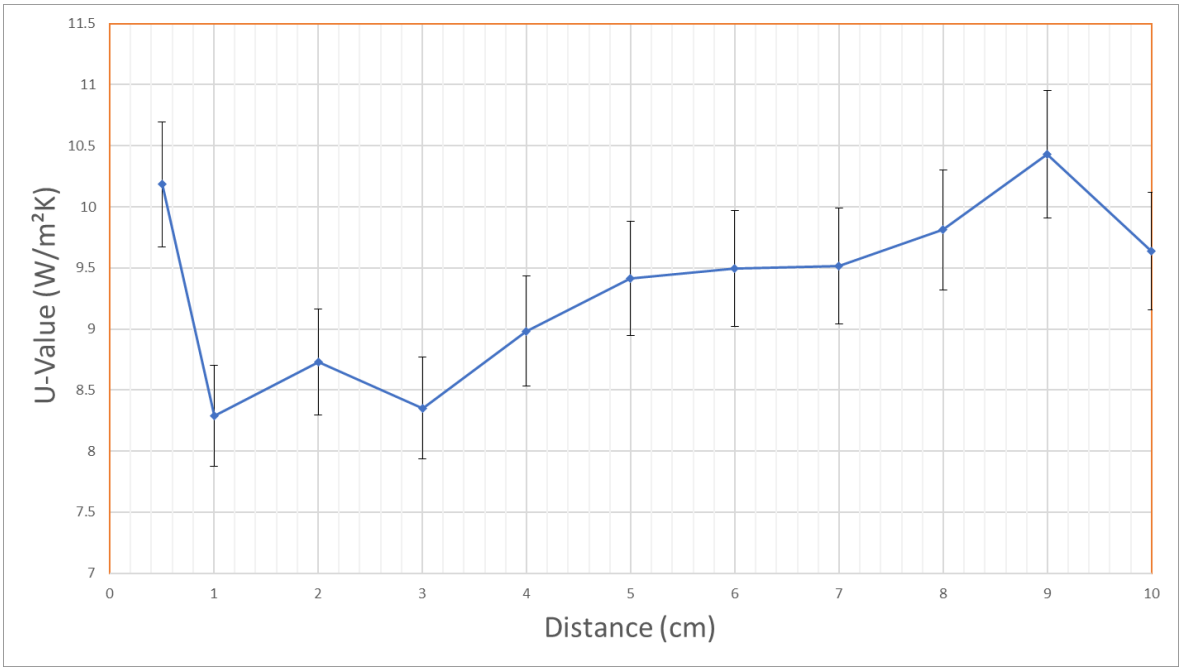

Figure 33. Experimental data of **absorber plate U-value** for flat lab scale solar collector at steady state. SD indicated. n=3.

The U-value of a material is a measure of how effective a material is as an insulator. The lower the U-value, the less heat that is lost and the more insulation that the material provides. By computing the U-value of the solar cell as a function of cavity height one can clearly and effectively portray the height at which the solar cell is optimally reducing heat loss, hence increasing efficiency. The value of 1cm cavity height was again verified to be the optimal cavity height with a U-value of 8.29 ± 0.68 W/m^{2}K as shown in Figure 33.

From Table 4, a 1cm cavity height was identified as the optimal height providing the greatest efficiency for the flat plate solar cell. The most important data point of the U-value of a 1cm cavity height solar cell is shaded. This value of 8.29 ± 0.68 W/m^{2}K was significantly lower than all other values. A lower U-value indicates a higher total heat transfer coefficient.

Table 4. Summary of important experimental data for flat solar cell at steady state as identified from this research

Distance	Avg GT	Avg GF	Avg PT	Avg PF	U - Glass	U - Plate	Uval - G	Uval - P
cm	K	W / m^2	K	W / m^2	W / mK	W / mK	W / m^{2}K	W / m^{2}K
1	54.63	311.25	121.18	838.42	1.97	2.39	10.18	8.29

Next, the temperature change depending on the cavity height was examined. From the above figure, it is shown that the cavity height decreases the efficiency increases. However, at a certain point from 1cm to 0cm the collector efficiency gets worse. A higher temperature

within the solar air cavity is desired as it means that more heat can be absorbed by the collector and transferred to the water. All the while the glass cover temperature should be as low as possible because that indicates that less heat is escaping through top losses. A comparison of the stagnation temperature of the absorber plate and the glass cover is shown in Figure 34 as a function of cavity height.

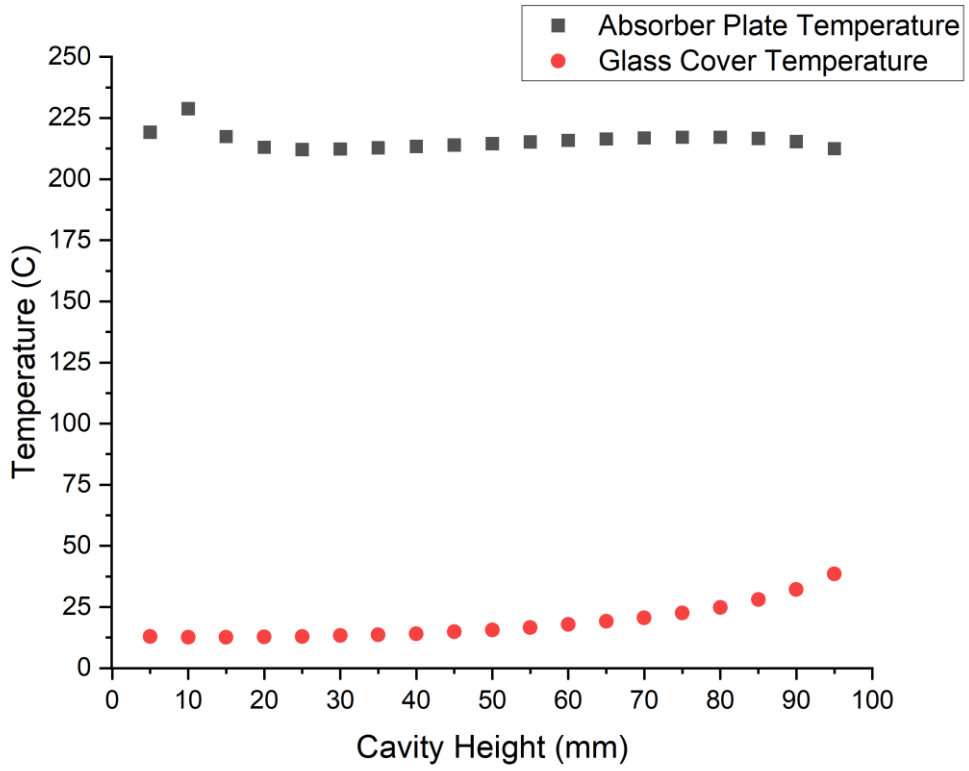

Figure 34. Experimental data of **internal cavity temperature** for flat MFPC at steady state.

Figure 34 shows that a 1cm is the most optimal as it provides the highest temperature for the absorber plate and maintains the lowest relative glass cover temperature.

3.1.2 Optimal Cavity Height at Various Angles

The same solar collector model was then mounted at various angles ranging from 45° to 10° to replicate a real-world environment of a solar panel mounted on a roof. Due to the location of Ireland at 53.1424° N, 7.6921° W, there is an optimal mounting angle of approximately 35° [80]. This angle is determined by the height of the sun as it passes through the sky. It can be determined by the general rule of thumb of:

$$Latitude\ of\ location - 20°$$

Therefore, tests were carried out at a selection of intervals ranging from 10° to 45° to determine how the convection process might differ between the various angles of solar panels in Ireland. The results of these experiments are shown in Table 5.

Table 5. Experimental data of absorber plate temperature and U-value for lab scale solar collector at various angles ranging between 0° and 45° at steady state. n=5

	Absorber Plate Temperature					U-Value				
Distance	0°	10°	20°	35°	45°	0°	10°	20°	35°	45°
cm	°C	°C	°C	°C	°C	W / m^{2}K	W / m^{2}K	W / m^{2}K	W / m^{2}K	W / m^{2}K
0.5	100.83	102.69	100.24	102.82	102.69	10.18	9.08	10.36	9.73	9.68
1	121.18	119.11	122.52	119.30	121.64	8.29	8.57	8.53	8.59	8.17
2	117.65	115.50	121.35	115.35	119.12	8.73	9.92	9.08	9.27	8.48
3	117.15	114.37	120.12	113.93	118.11	8.36	9.83	10.03	9.40	8.85
4	115.84	112.31	117.76	112.57	115.31	8.98	9.78	9.98	9.99	9.35
5	113.97	112.95	116.34	110.83	114.05	9.41	9.86	10.04	10.32	9.64
6	112.39	109.74	113.83	109.28	112.93	9.50	10.34	10.24	10.44	9.93
7	111.38	108.59	112.21	108.35	111.54	9.51	10.50	10.48	10.62	10.12
8	109.87	107.73	111.54	108.09	110.04	9.81	10.62	10.74	10.78	10.28
9	108.49	106.63	110.33	107.34	108.66	10.43	10.81	10.99	10.89	10.38
10	106.85	106.17	109.33	107.64	107.91	9.64	11.14	11.20	10.92	10.55

Figure 35 and Figure 36 show the key experimental results from performing the same tests as with a solar collector on a flat surface, however, these experiments were performed at various angles from 0 to 45°.

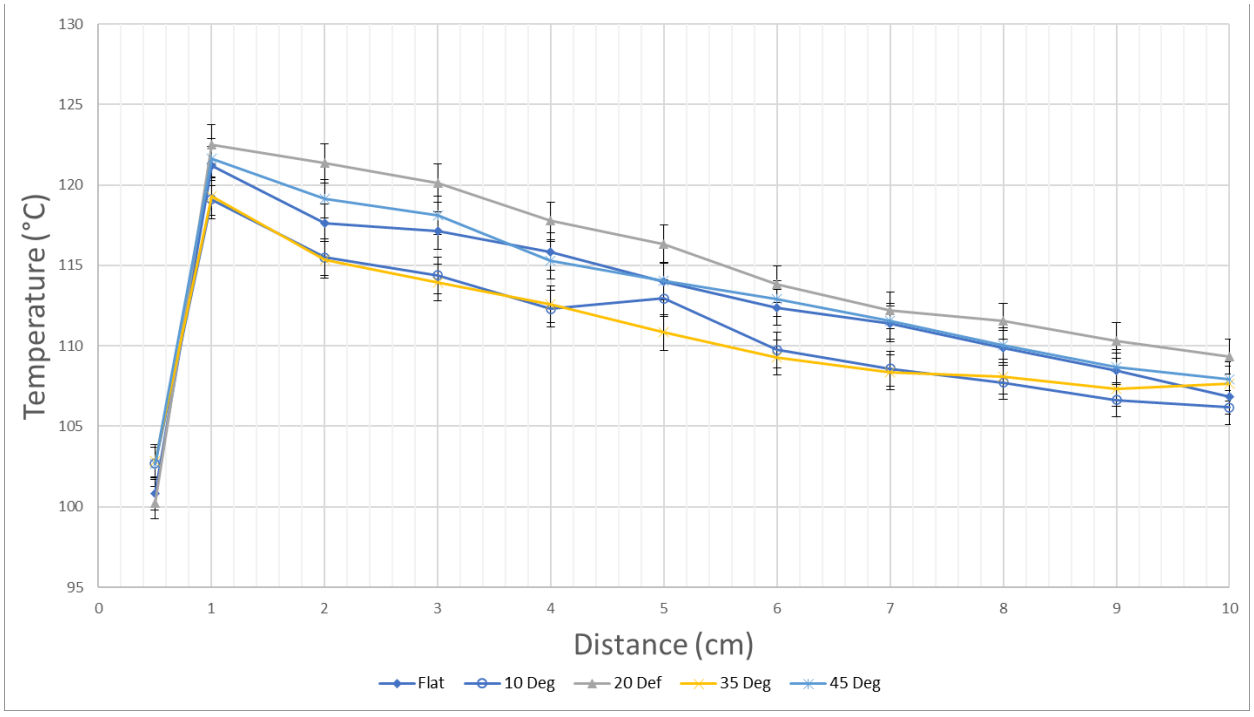

Figure 35. Experimental data of **absorber plate temperature** for lab scale solar collector at various angles ranging between 0° and 45° at steady state. n=5, SD indicated.

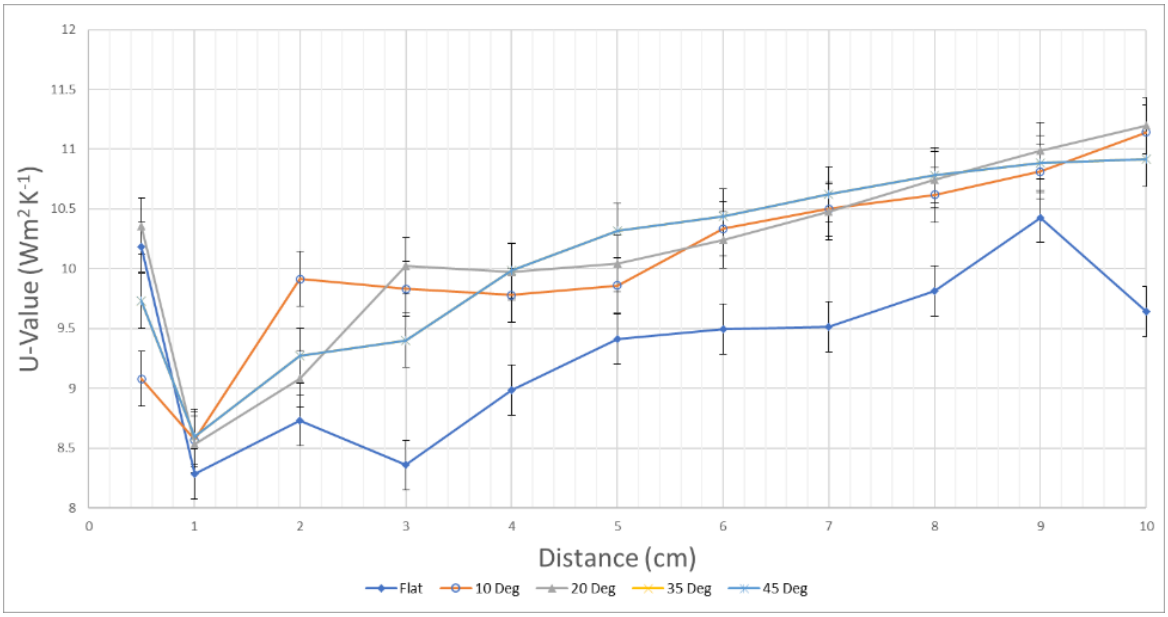

Figure 36. Experimental data of **U-value** for lab scale solar collector at various angles ranging between 0° and 45° at steady state. n=5, SD indicated.

Figure 35 and 36, confirm the findings from Section 3.1 and substantiate that at all working angles for the solar thermal collector model, the U-value at 1cm was found to be the lowest at 8.17 ± 0.75 W/m^{2}K. This further confirms that the optimal cavity height for flat plate solar collectors is 1cm. This is important as this set of experiments demonstrates triangulation of methodologies verifying the results.

3.2 Polycarbonate as a TIM

Once the optimal cavity height was identified experimentally, the properties of polycarbonate were analysed to determine if it was a viable material for used as a TIM.

The properties of polycarbonate that were analysed were: optical transmission, IAM dependence, absorption, UV degradation, and thermal conductivity.

3.2.1 PC Hexadic Structure Transmission Analysis

A Perkin Elmer UV-VIS-NIR spectrometer was used to measure light transmission across the ultraviolet, visible, and near-infrared ranges of the electromagnetic spectrum. The spectrometer measured the amount of light transmitted through a sample compared to a reference measurement in the range of 800nm – 230nm. The following results shown in Figure 37 were obtained.

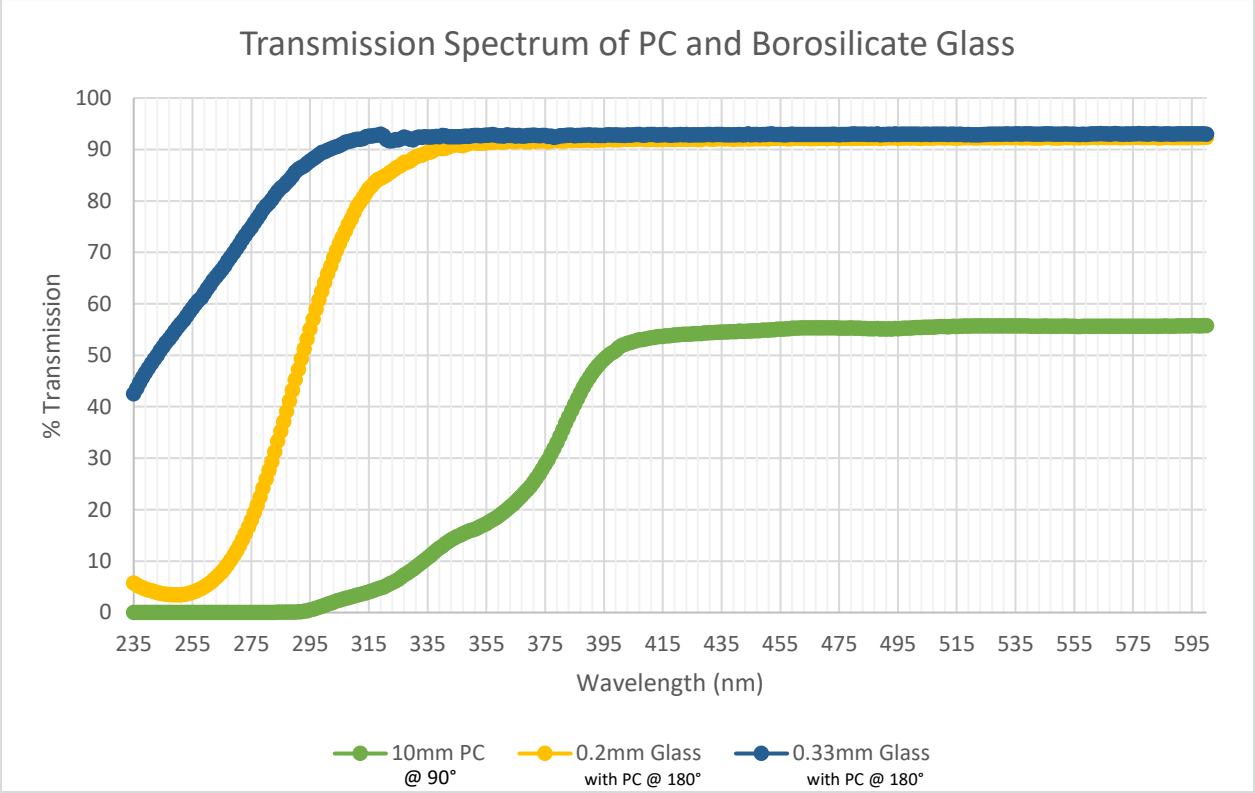

Figure 37. Transmission spectra of polycarbonate and borosilicate glass from 600 – 235nm

This result shows us that at direct incident angles, the combination of polycarbonate TIM and ultra-thin glass allow over 92% of the light to pass through in the visible and near-IR ranges. This is a positive result as it is in line with the transmission of regular solar glass is also ~ 92%.

3.2.2 PC Hexadic Structure IAM Dependent Transmission

As the sun moves across the sky on a daily basis the incident angle of radiation also changes for a solar collector. The sun also moves perpendicularly to the horizon axis depending on the time of the time. This means that the sun is rarely shining directly incident to the absorber plate in the solar thermal collector. Therefore, we must investigate the angle dependent transmission of the system to understand its performance in a real-world climate.

As the incidence angle increases, the amount of radiation reflected from the glass cover and the polycarbonate structure increases. The effect of reflection and absorption as a function of incidence angle is expressed in terms of the incidence angle modifier (IAM), K_θ. This is

defined as the ratio of the radiation absorbed by the cell at incidence angle θ divided by the radiation absorbed by the cell at normal incidence [81]. The IAM at angle θ is found by:

$$K_\theta = \frac{(\tau\alpha)_\theta}{(\tau\alpha)_n}$$

The IAM value for this system was measured experimentally using a PV cell and a light source. Initially the IAM was measured for the PV cell alone at various angles, then the glass cover and the glass cover with the hexadic polycarbonate were placed in front of the PV cell. The amount of energy absorbed by the PV cell was recorded in each incidence and therefore the IAM for the NFPC system could be determined. Figure 38 and Figure 39 shows the IAM value for the MFPC and the NFPC systems. The values are seen as 2.305 for the MFPC and 2.264 for the NFPC. The value for an undisturbed PV cell was 2.444, meaning that there is a slight decrease due to the addition of the polycarbonate hexadic structure. This would affect the transmission of light and hence the absorbance of heat by the solar collector at lower angles. Figure 38 and 39 show the incident angle modifier (S_i) against the voltage (V) that was seen by the PV cell at a specific angle.

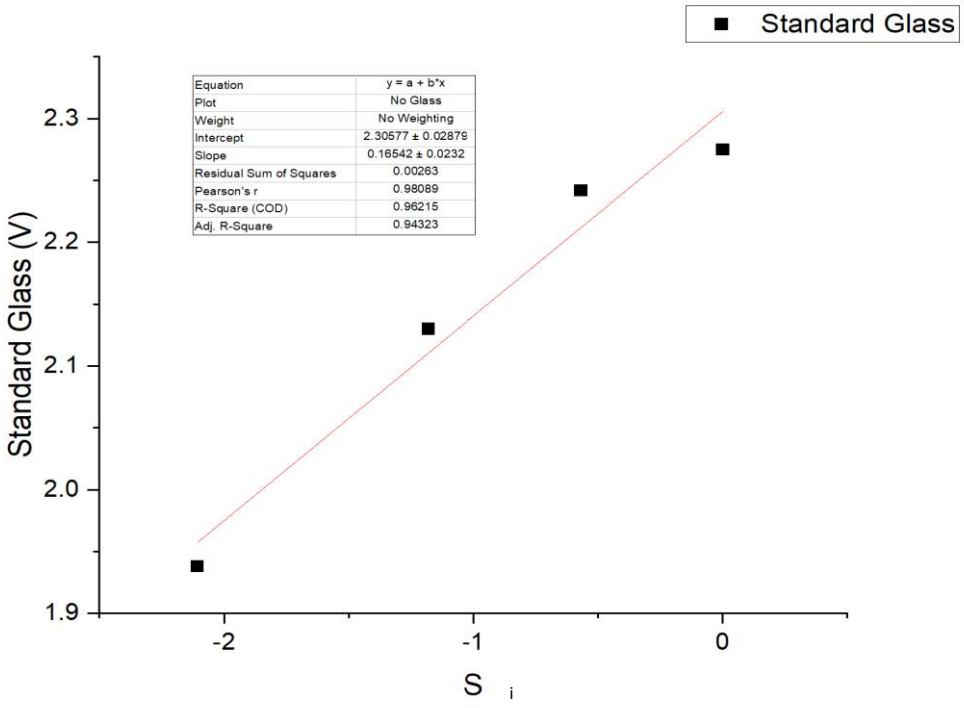

Figure 38. Incident Angle Modified (IAM) graph of Joule Navitas solar thermal collector (MFPC), y-axis is voltage

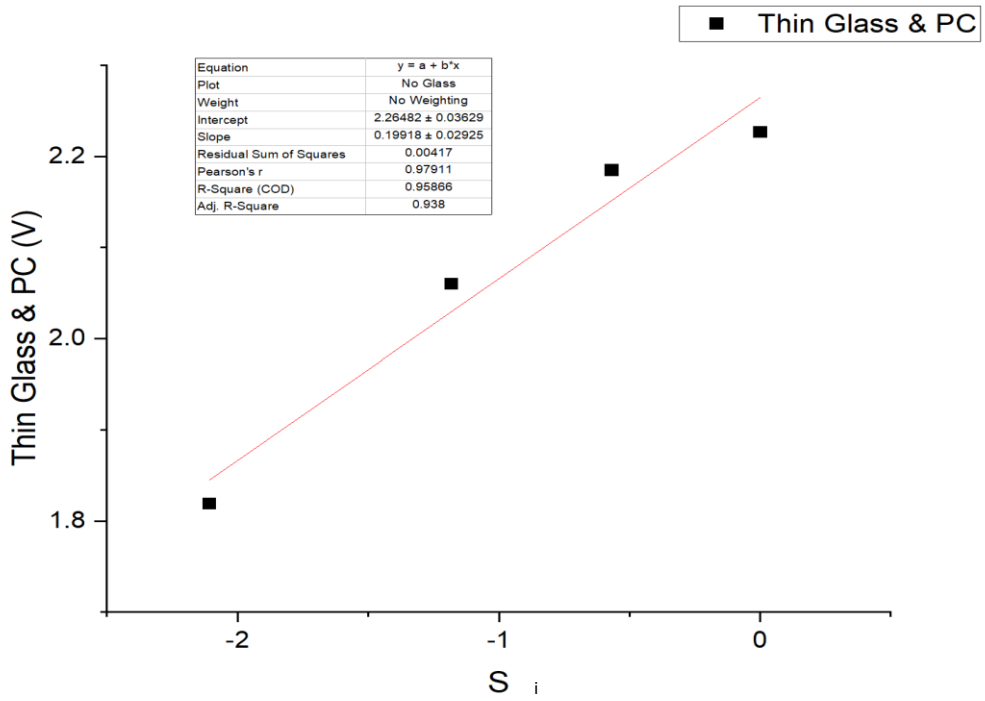

Figure 39. Incident Angle Modified (IAM) graph of novel solar thermal collector (NFPC), y-axis is voltage

3.2.3 PC Hexadic Structure Absorption Analysis

According to the Beer-Lambert Law there is a relationship between the attenuation of light through a substance and the properties of that substance. From this law, we find a logarithmic relationship between absorption and transmission.

$$A = -log_{10}T$$

Figure 40 shows the absorption spectrum, calculated using the above equation. This graph shows that the ultra-thin glass absorbs a significant amount of UV radiation. This is a promising result as from Section 1.8.4.1 we know that UV can cause a significant degradation in polycarbonate affecting both its mechanical and optical properties. However, as we can see by placing the polycarbonate beneath the glass cover, up to 1.5AU of UV radiation is absorbed before it reaches the polymer. This greatly reduced the risk of discolouration of the polymer.

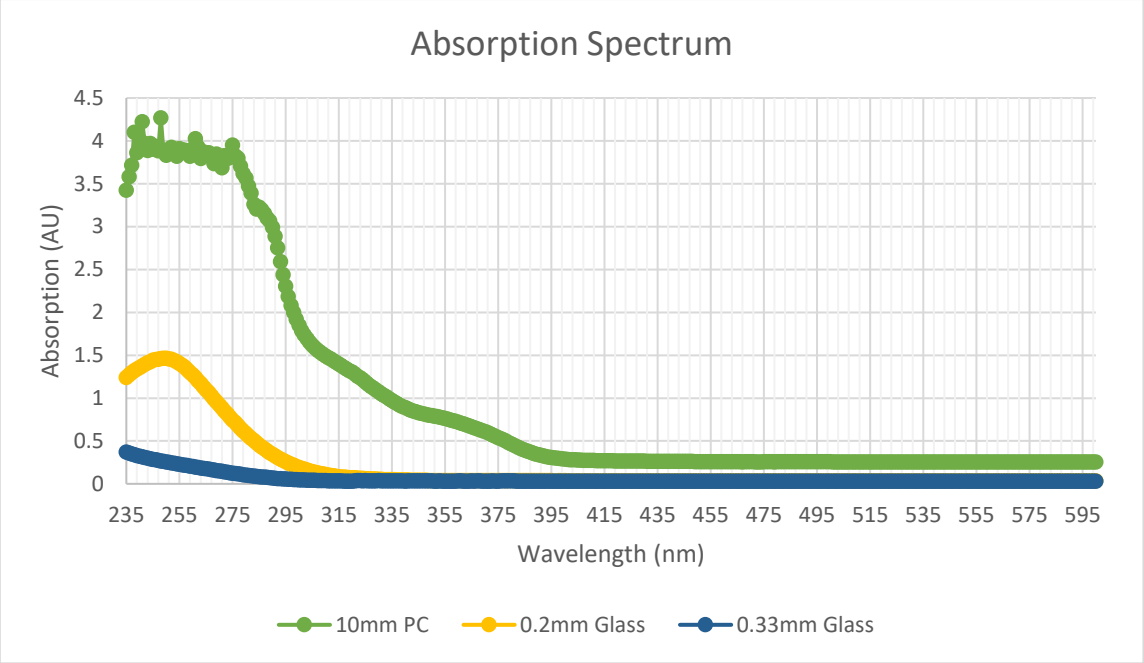

Figure 40. Absorption spectra of polycarbonate and borosilicate glass from 600 – 235nm

3.2.4 Lifetime UV Testing of PC Hexadic Structure

A lifetime UV exposure test was carried out on the PC hexadic structure. This was done to analyse the performance of the polycarbonate in real world conditions. To reach the ISO 4892-3 [82] requirements the UV exposure and temperature need to be controlled. The accelerated lifetime testing was done using an 8W, 50Hz multifunctional UV lamp. The lamp produced light at 365nm (UV-A), 302nm (UV-B), and 252nm (UV-A) wavelengths with a wide area of illumination. A 600W digital hotplate was used to maintain a constant and uniform heat across the polycarbonate sample of 50°C. An enclosure for the experiment was also designed using SolidWorks and produced using wood as shown in Figure 41.

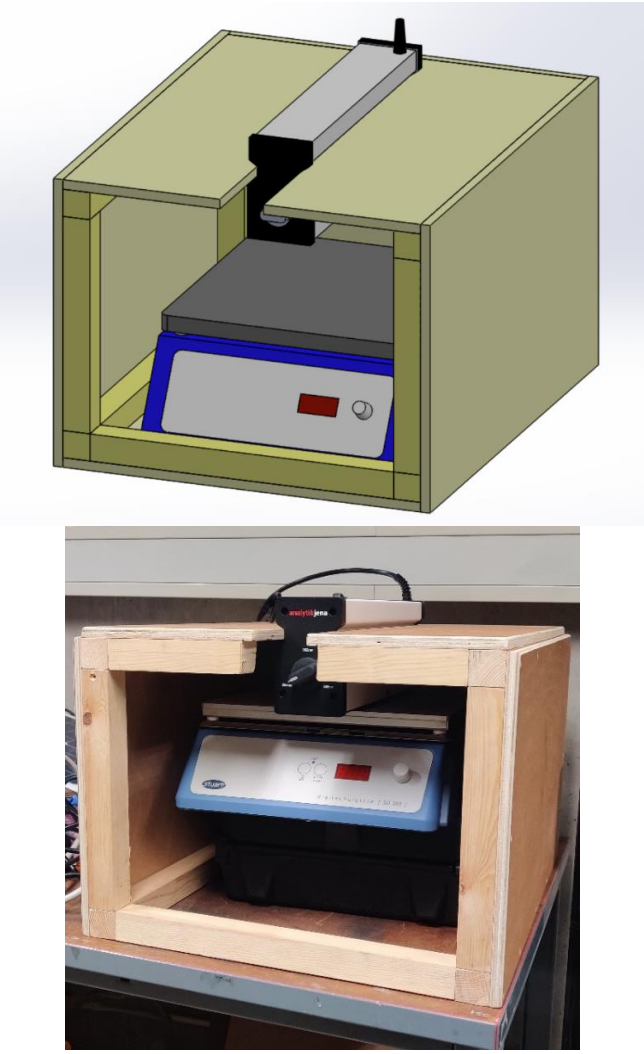

Figure 41. CAD and physical model of UV accelerated lifetime test experiment enclosure

The length of the experiment and the distance of the sample from the light source were calculated using the following relation:

$$I \propto \frac{1}{r}$$

From this relation, the following equation can be derived:

$$I = \frac{P}{L\pi}\frac{1}{r}$$

Where P = power, L = length of light source, and r = distance from source to sample.

The UV proportion of the solar spectrum is broken down into UV-A, UV-B, UV-C. Only 5% of solar terrestrial radiation is UVR. However, UVC and most of UVB are removed from extra-terrestrial radiation by stratospheric ozone. Therefore, the radiation from the sun which lands on a solar collector comprises of about 95% UV-A, 4.95% UV-B and 0.05% UV-C [83]. The visual results of the experiment are shown in Figure 42.

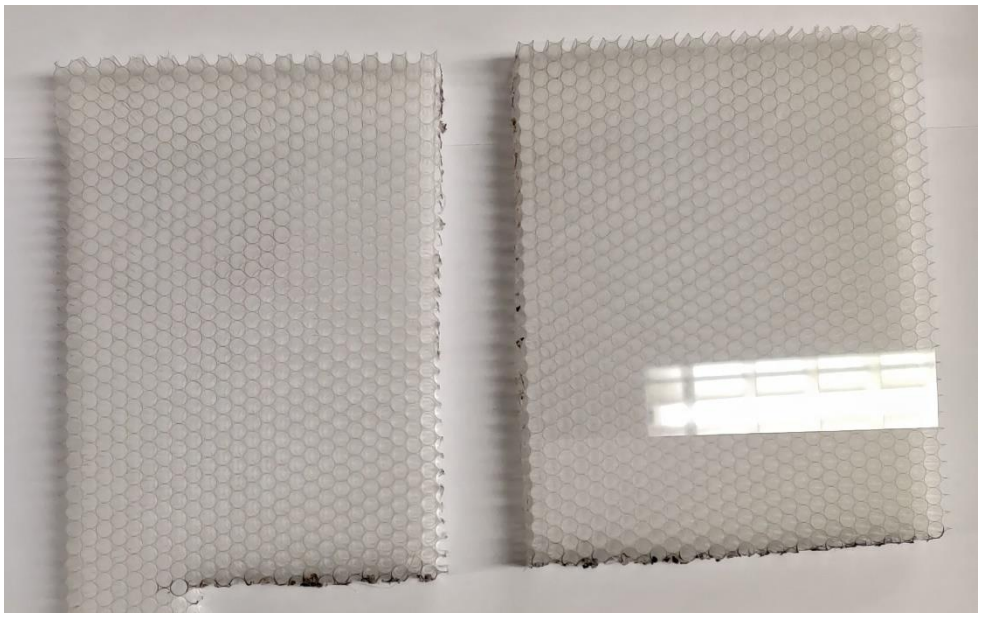

Figure 42. Accelerated UV ageing polycarbonate samples i) with and ii) without glass cover

As can be seen in Figure 42, no discernible difference can be identified between the samples. This was confirmed in a transmission test with both samples giving the same transmission to each other and a sample that had not underwent UV accelerated ageing. After further investigation including speaking to the manufacturer of the polycarbonate it was identified that a UV protective coating was applied to the polymer. This coating was affecting the results of the UV ageing test. However, it did mean that the high-end UV treated polycarbonate did not degrade whatsoever with a lifetime exposure to UV. This is a very positive result and further shows that polycarbonate may be a viable TIM structure for a solar thermal collector.

3.2.5 Differential Scanning Calorimetry Analysis of PC Hexadic Structure

Differential Scanning Calorimetry (DSC) is a thermo-analytical technique which measures the energy transferred to/from a sample undergoing a physical or chemical change. It

calculates the difference in the amount of energy needed to increase the temperature of a sample and a reference sample with a well-defined heat capacity, as a function of temperature. There are two different variations of DSC: Heat Flux DSC and Power Differential DSC. In this research, a Perkin Elmer Heat Flux DSC 400 was used to determine the thermal resistance properties of polycarbonate.

A Heat-flux DSC measures the heat flux difference between the sample and the reference. This is calculated by integrating the ΔT_{ref} curve. The experiment is conducted in a temperature-controlled environment. The results for the polycarbonate hexadic structure are shown in Figure 43. The melting point of the structure was found to be 146.69 – 148.97°C.

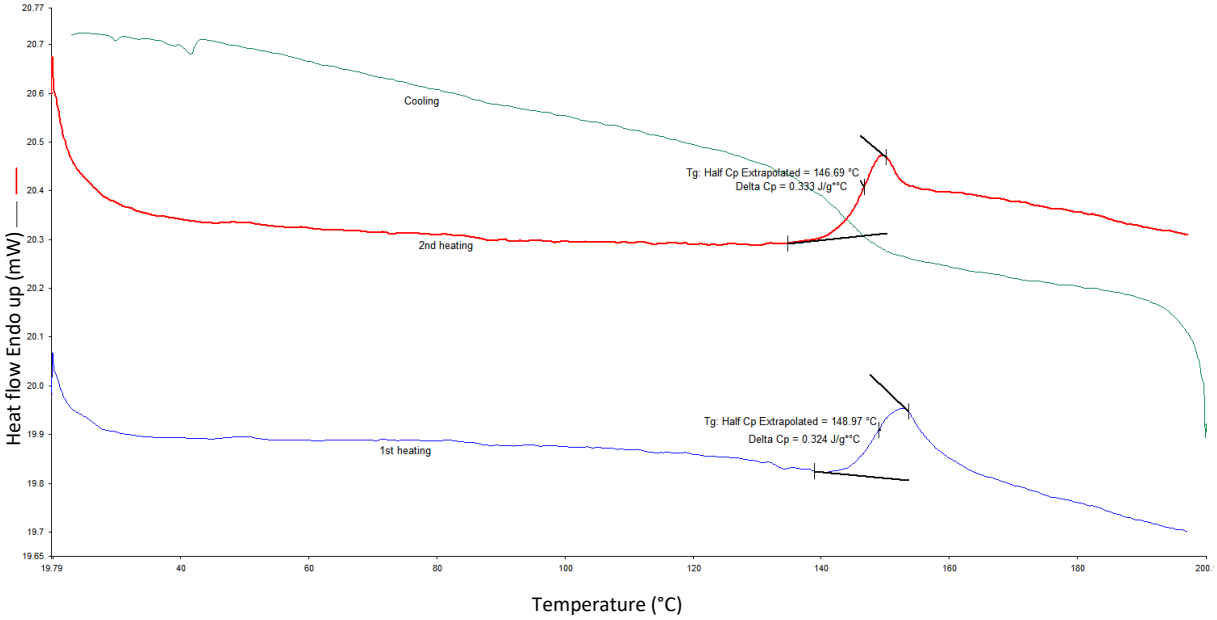

Figure 43. Differential Scanning Calorimetry analysis of polycarbonate hexadic structure

3.2.6 Thermal Conductivity of PC Hexadic Structure

The thermal conductivity of the PC hexadic structure was experimentally determined. This was done using a FOX 50 Heat Flow Meter. This is a microprocessor-based instrument that has the capabilities of measuring the thermal conductivity of a sample within the in the conductivity range of 0.1W/mK to 10W/mK. The data is measured and analysed using WinTherm50 software.

The sample of polycarbonate was smeared with thermal grease to ensure a better contact area (Figure 44) and was placed in between two plates of known temperature. The change in temperature between both plates and the amount of energy needed to keep them at that temperature were used to identify the thermal conductivity of the sample. Table 6 shows the parameters of the experiment and Table 7 shows the thermal conductivity of the sample at various temperature differences.

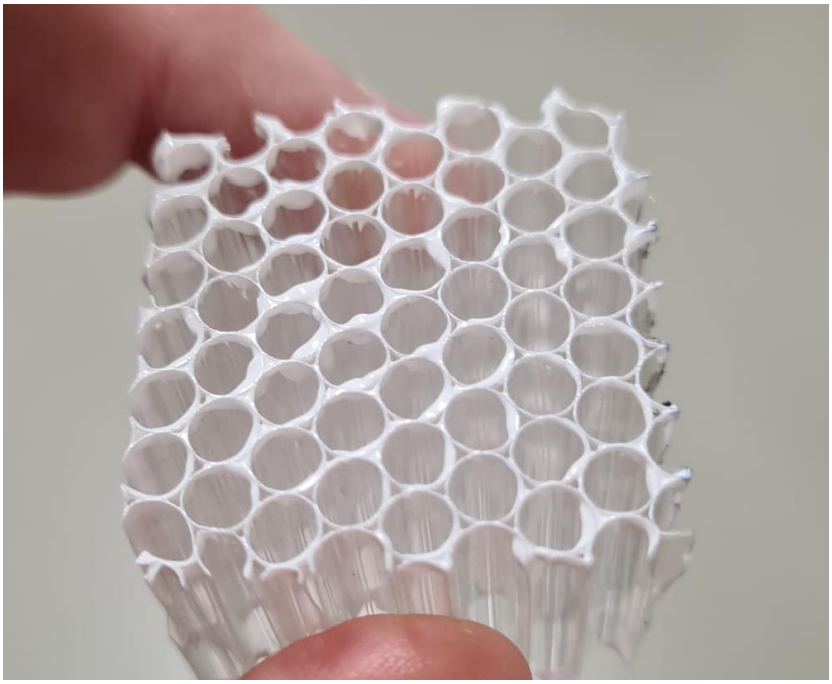

Figure 44. Hexadic PC sample prepared with thermal grease for thermal conductivity experiment

Table 6. Experimental parameters for thermal conductivity of hexadic PC structure

Thickness of Sample	19.79mm
Setpoint Upper	20.0°C
Setpoint Lower	5.0°C
Temperature Average	12.5°C
Total Thermal Resistance	0.285 m^2K/W
Results Average	0.284 m^2K/W

Table 7. Experimental results for thermal conductivity of hexadic PC structure

T_upper [°C]	T_lower [°C]	Q_upper [µV]	Q_lower [µV]	Lamba [W/mK]
20.02	5.01	619	-691	0.06972
20.02	5.01	618	-691	0.06971
20.02	5.01	617	-692	0.06968
20.02	5.01	616	-693	0.06966
20.02	5.01	615	-694	0.06967
20.02	5.01	614	-694	0.0696
20.02	5.01	614	-695	0.06966
20.02	5.01	613	-696	0.06965
20.02	5.01	612	-695	0.06958
20.02	5.01	612	-696	0.06959

From Table 7, we can see that the thermal conductivity of the hexadic polycarbonate sample is 0.06965 W/mK. We can examine this figure in the context of windows to see where the thermal conductivity of this sample is comparatively. Double-glazed windows with an air cavity, which are standard in many homes, have a thermal conductivity of approximately 0.0672 W/mK. Newer triple-glazed windows with an air cavity have a thermal conductivity of around 0.031 W/mK. This means that the thermal conductivity of the hexadic polycarbonate structure is in line with a double-glazed window.

3.3 Convection Suppression

Using the knowledge gained throughout Section 3.2, a novel polycarbonate hexadic structure was produced (the NFPC). This novel flat plate solar collector was used from here on out in this study as opposed to the model lab-scale solar collector that was used previously. The NFPC consists of a layer of ultra-thin borosilicate glass, mounted on 20mm thick transparent hexadic polycarbonate acting as a TIM structure as described in Section 2.2. The NFPC is compared again a market flat plate collector (MFPC) from here on out in this study. The MFPC is a Joule Navitas solar collector which can be purchased on the market in Ireland as described in Section 2.3.

3.3.1 Convection Suppression Tests

The convection suppression qualities of the hexadic transparent insulating structure could be clearly seen in the COMSOL Multiphysics® simulations. The circulation of air heating up and cooling down within the solar cell forms Rayleigh - Bénard Cells within the air cavity [84]. In the MFPC the air can circulate at speeds of up to 18 cm/s (Figure 45) allowing heat to escape more readily via convection through the top glass surface of the

solar collector. However, with the addition of the hexadic TIM structure the air flow speed was reduced to 3.75 cm/s (Figure 45). This is a 79.16% decrease in air speed at its maximum within the cell. Additionally, the air speed close to the glass cover boundary was reduced to ~ 0 m/s and this stagnant air extended down two-thirds of the air cavity. This stagnant air is a natural insulator and greatly reduces heat losses via convection and conduction through the top of collector. A decrease in heat loss causes an increase in temperature within the solar collector which enhances the heat collected by the absorber plate. This simulation was replicated experimentally, and a temperature increase of 15.12% was seen (Figure 46). Table 8 shows the stagnation temperature data of the simulation and experimental tests.

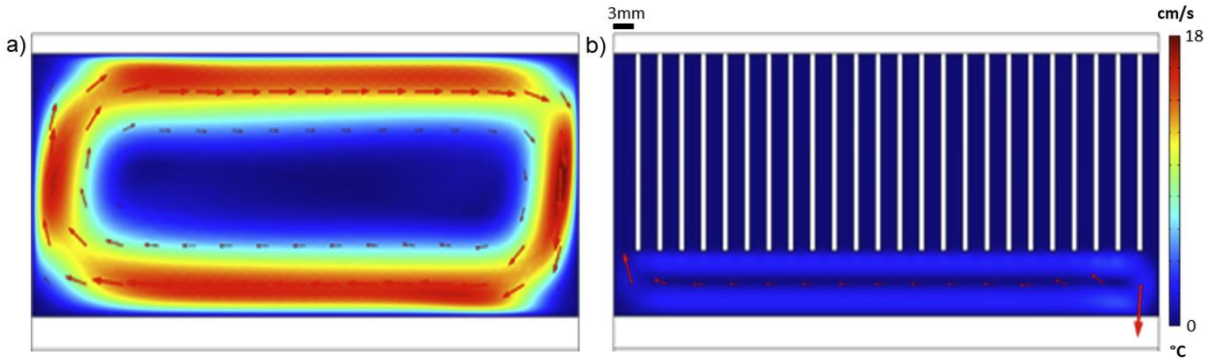

Figure 45. COMSOL simulations of i) MFPC and ii) NFPC showing air flow within a solar thermal collector

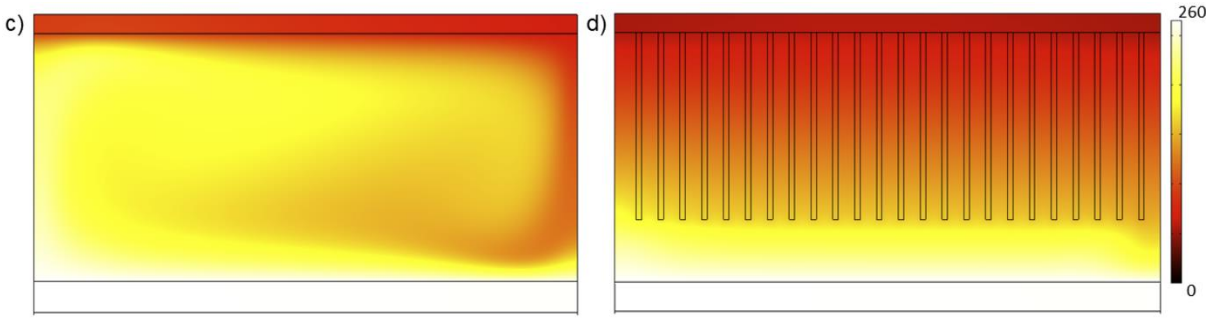

Figure 46. COMSOL simulations of i) MFPC and ii) NFPC temperature within the air cavity, temperature unit in scale

Table 8. Temperature data for solar thermal collector in simulation and experimental tests after 30 minutes

Item	Temperature	Units
COMSOL Simulation		
MFPC	125.71	°C
NFPC	137.81	°C
Lab Scale Experiments		
MFPC	121.18	°C
NFPC	139.50	°C

Once shown in simulations, the convection suppression properties of the novel hexadic TIM structure were examined in lab-scale experiments. Determination of the optimal cavity height was carried out at both a flat and a mounted angle to analyse the effects that the novel TIM structure could have to optimise the efficiency of a solar cell. Experimentation was carried out independently three times at each height increment ranging from 1cm – 10cm to determine the optimal cavity height with the honeycomb structure within the cavity. The experiments were also conducted to observe if there was an increase in absorber plate temperature due to the convection frustrating properties of the honeycomb structure.

The U-value of the system decreased from 1.55 ± 0.68 W/m^{2}K for the MFPC to 0.9 ± 0638 W/m^{2}K for the NFPC with the hexadic structure within the cavity. This 53.06% decrease in the U-value, corresponding to a very significant increase in the efficiency of the solar cell system. This can be seen in Figure 47.

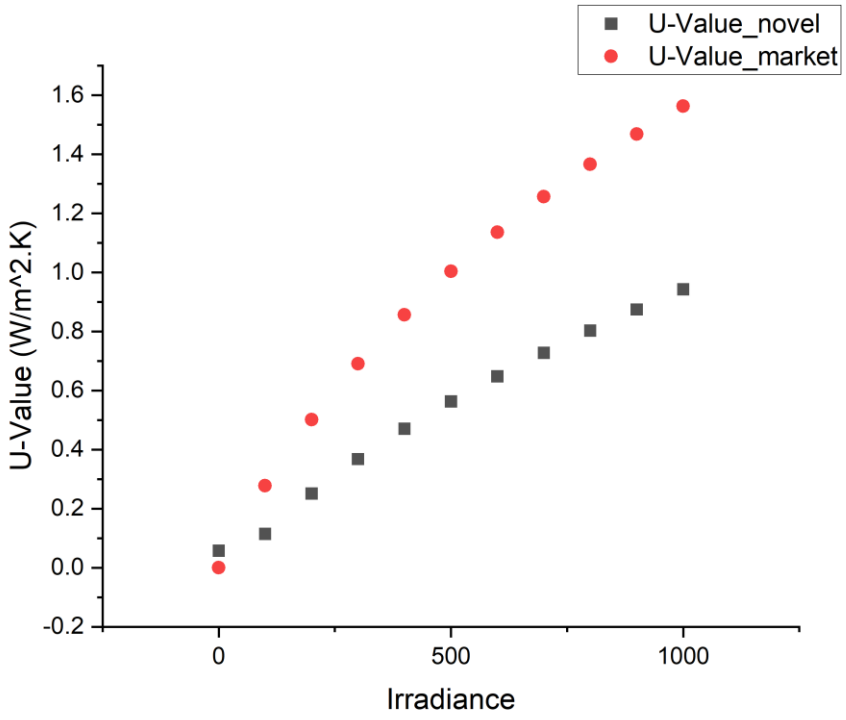

Figure 47. Experimental data of **U-value for MFPC and NFPC** at steady state

We will see in Section 3.4 the effect that this lower U-valve as an entire system has on the efficiency of the solar thermal collector.

3.4 Efficiency Performance Curve

The efficiency performance curve of the NFPC was found to be superior to the MFPC and brought the collector more in line with the more expensive evacuated tube collector efficiencies. Figure 48 shows the experimental setup for testing the efficiency of the MFPC and NFPC. This part of the study was initially carried out using FEM analysis simulations and then verified using lab-scale experiments.

Figure 48. Experimental setup for the efficiency performance curve of solar thermal collector experiments

While the theoretical maximum efficiency of both MFPC and NFPC were approximately equal (80%), the NFPC outperformed the MFPC at higher temperatures and more importantly in the working temperature range of solar thermal collectors. The heat transmission coefficients as described in the equation for the MFPC and the NFPC were $a_1 = 2.69\text{x}10^{-3}$ W/(m^{2}K), $a_2 = 7.45\text{x}10^{-6}$ W/(m^{2}K), and $a_1 = 1.56\text{x}10^{-3}$ W/(m^{2}K), $a_2 = 6.52\text{x}10^{-6}$ W/(m^{2}K) respectively. Figure 49 and Figure 50 shows a comparison between both efficiency performance curves. It also shows the efficiency performance curve of an evacuated tube collector [67] to visualize how the NFPC is more in line with the evacuated tube solar thermal collector efficiency.

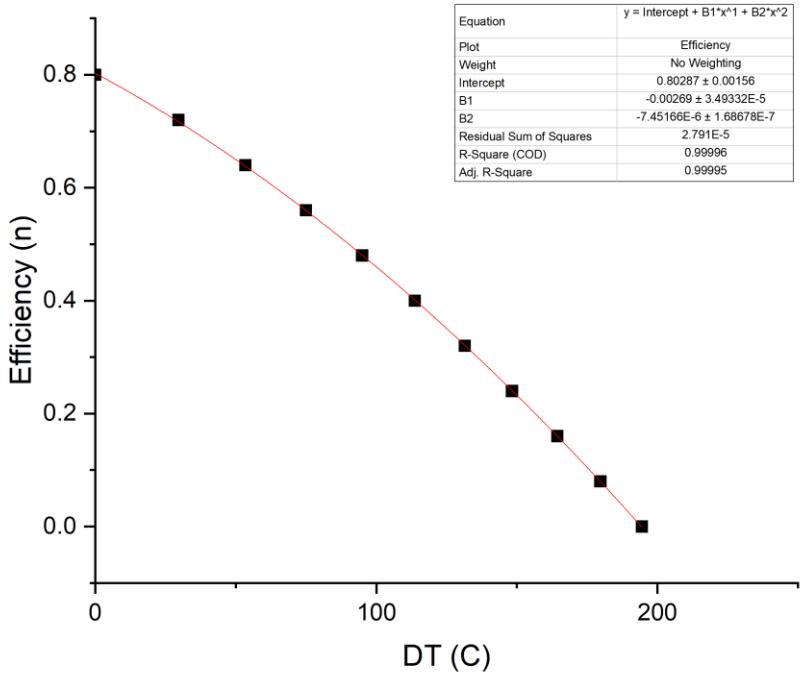

Figure 49. Efficiency performance curve of MFPC solar thermal collector

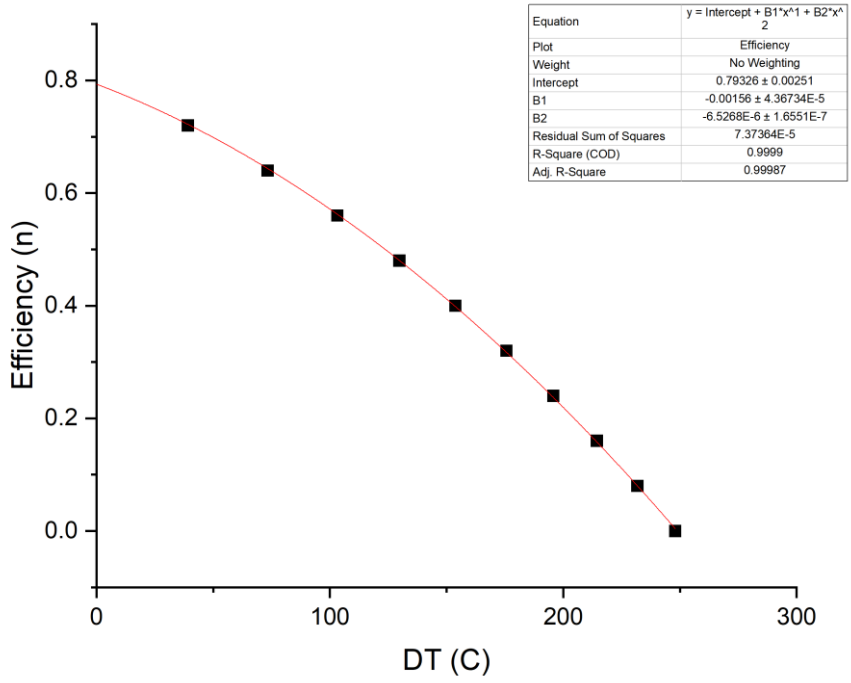

Figure 50. Efficiency performance curve of NFPC solar thermal collector

The efficiency performance curves were also verified experimentally using the lab scale model. The experiments showed a very near correlation to the COMSOL simulations

suggesting that the simulation results could be replicated in a real-world environment. Figure 51 shows a comparison of the simulation data vs. the experimental data for the NFPC and the MFPC. It also shows a performance comparison with an evacuated tube collector efficiency. This is done to visually represent the improvement that the novel hexadic TIM structure has provided over the MFPC and how much closer it brings the technology to being in line with evacuated tube collectors (ETC). ETCs are more efficient than FPCs as they have all the air removed from within the solar cavity by vacuum. They are more expensive due to the vacuum process and the need for different materials to maintain the vacuum. They are also more vulnerable than FPCs as any damage can break the vacuum seal and render the system unusable. This type of damage has been caused previously be hail, heavy rain, and wind. The NFPC essentially provides the similar thermal properties to the ETC without all the issues including the cost of the product, the maintenance and upkeep required, and the weight of heavy glass tubes.

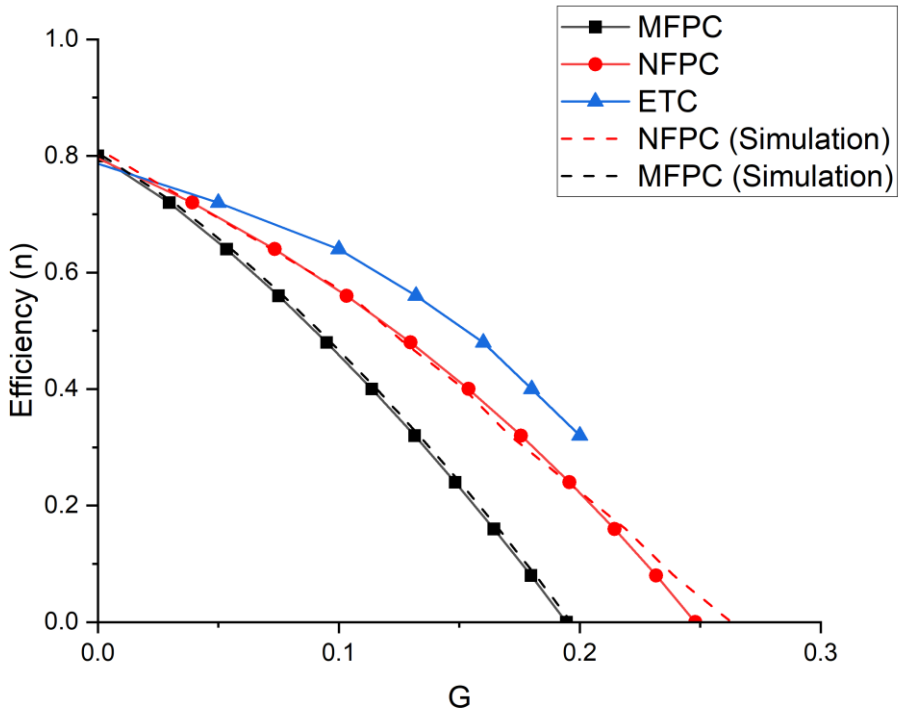

Figure 51. Efficiency performance curve comparison of a MFPC, NFPC, and Evacuated tube solar thermal collector plus the correlation to the simulation results. G = Solar irradiation in W.

This efficiency increase for the NFPC is extremely promising as it means that more of the sun's energy can be harnessed by the solar collector. For the consumer, this means that they

will receive more useful energy and hence more available hot water from the same or less investment in terms of costs and space.

This result was the ultimate goal of this research to identify a method of increasing the efficiency of solar thermal collectors while not increasing the cost of investment to reduce to overall payback period for consumers. This was done to make solar thermal a more viable option for the public and incentivise affordable decarbonisation of hot water heating. While this study mainly focuses on the domestic setting, the efficiency improvements are transferrable to the commercial industry and if the same technology was employed there the same benefits should be seen.

3.5 System Level Modelling

A transient model of both the MFPC and NFPC were analysed to understand their performance in an average DWHS in Ireland. Figure 52 shows the output temperature from the MFPC, and the useful energy gained throughout the day on January 15th and June 15th. It also shows the corresponding information for the NFPC. It can be clearly seen that across an average day in both a winter month and a summer month, the NFPC performs much more efficiently. On January 15th, the NFPC reached a temperature of 100◦C, while the MFPC only reached 65◦C without additional auxiliary heating. The NFPC gained 1.5 kWh more than the MFPC. On June 15th, the NFPC was consistently above 100◦C from 09:00 am to 7:00 pm, while the MFPC only maintained this output temperature from 10 am to 11:30 pm. The NFPC gained 0.3 kWh more than the MFPC on this day.

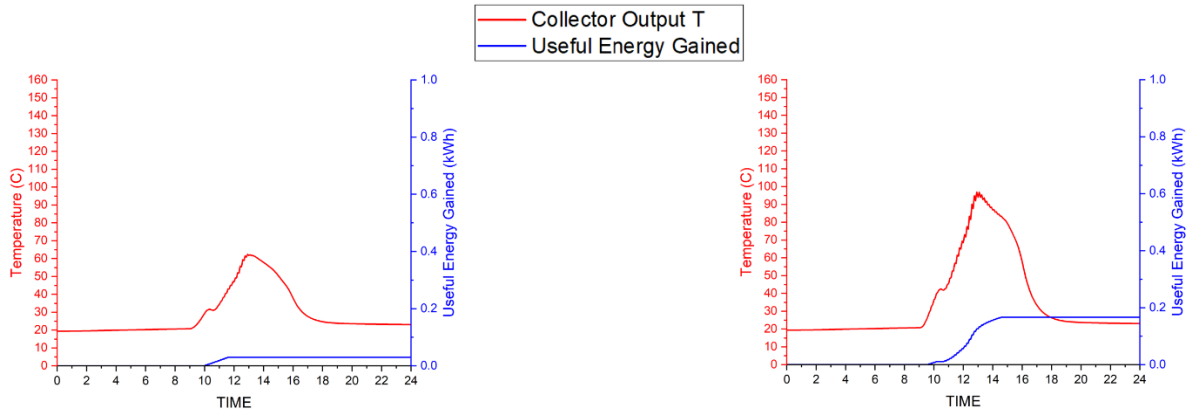

Figure 52. Collector output temperature and useful energy gained of a) Market flat plate collector (MFPC) in January and b) Novel flat plate collector (NFPC)

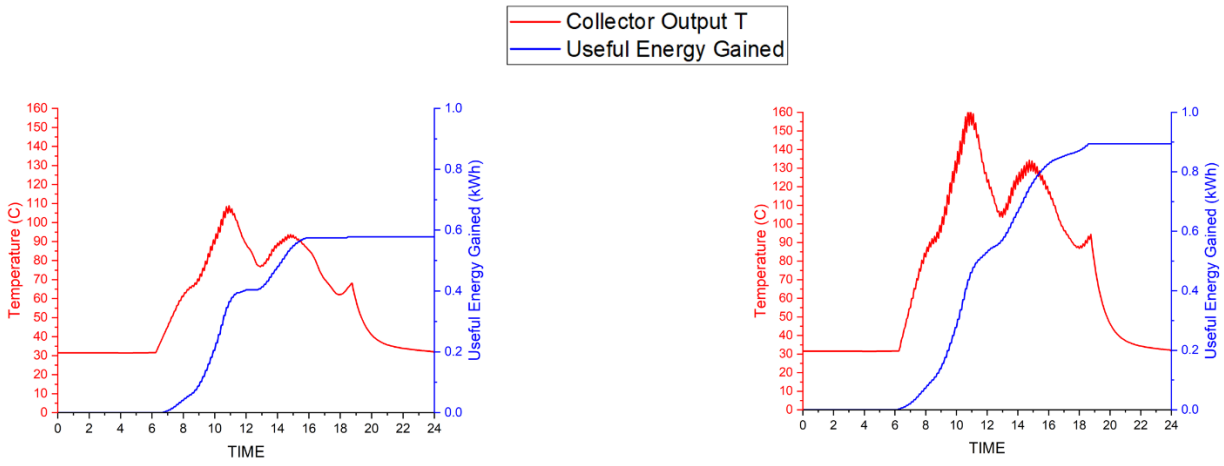

Figure 53. Collector output temperature and useful energy gained of a) MFPC in June and b) NFPC in June

3.6 Energy Analysis

3.6.1 Useful Energy Gained

Table 9 and 10 shows the average monthly useful energy, auxiliary heating required, solar fraction, and storage tank thermal losses for the MFPC and NFPC respectively. Although the NFPC collected more useful energy from the sun consistently throughout the entire year, the rise in temperature caused a greater heat loss in the storage tank. The useful energy could become more efficient if the water load was used more consistently throughout the day, hence reducing the temperature of the storage tank.

Table 9. Energy gained, Auxiliary heating required, Solar fraction, and Tank losses of a Market Flat Plate Solar Collector (MFPC)

Month	Q_{useful} (kJ)	$Q_{auxilary}$ (kJ)	Solar Fraction	Tank Losses (kJ)
January	1.27E+05	7.76E+05	14%	3.56E+05
February	1.54E+05	6.69E+05	19%	3.56E+05
March	3.28E+05	7.03E+05	32%	4.97E+05
April	4.00E+05	7.29E+05	35%	6.29E+05
May	4.93E+05	7.50E+05	40%	7.32E+05
June	4.46E+05	7.65E+05	37%	7.05E+05
July	4.86E+05	7.53E+05	39%	7.31E+05
August	4.10E+05	7.75E+05	35%	6.76E+05
September	3.49E+05	7.22E+05	33%	5.63E+05
October	2.56E+05	7.21E+05	26%	4.73E+05
November	1.35E+05	7.38E+05	15%	3.63E+05
December	9.69E+04	7.74E+05	11%	3.52E+05

Table 10. Energy gained, Auxiliary heating required, Solar fraction, and Tank losses of a Novel Flat Plate Solar Collector (NFPC)

Month	Q_{useful} (kJ)	$Q_{auxilary}$ (kJ)	Solar Fraction	Tank Losses (kJ)
January	1.53E+05	7.67E+05	16.62%	3.73E+05
February	1.90E+05	6.55E+05	22.51%	3.81E+05
March	3.90E+05	7.05E+05	35.60%	5.61E+05
April	4.90E+05	7.28E+05	40.25%	7.19E+05
May	5.99E+05	7.07E+05	45.88%	7.98E+05
June	5.42E+05	7.13E+05	43.17%	7.49E+05
July	5.90E+05	7.00E+05	45.76%	7.84E+05
August	4.94E+05	7.52E+05	39.67%	7.36E+05
September	4.18E+05	7.40E+05	36.07%	6.50E+05
October	3.05E+05	7.17E+05	29.89%	5.22E+05
November	1.63E+05	7.28E+05	18.29%	3.83E+05
December	1.20E+05	7.63E+05	13.56%	3.66E+05

3.6.2 Auxiliary Heating Required

The additional auxiliary heating required for the MFPC and NFPC is shown in Table 9 and Table 10 respectively. The NFPC auxiliary heat demand was on average 2.3% lower than that of the MFPC to reach the required temperature for the domestic hot water load.

3.6.3 Solar Fraction

The solar fraction for the NFPC was on average 15.25% higher than that of the MFPC. Although the NFPC collected more useful energy from the sun and brought the tank to a higher ambient temperature, this caused an increase in the thermal losses of the storage tank which depends on the temperature difference between the water and external ambient. The increased useful energy absorbed would have a much greater impact if the water from the tank was being drawn off on a more consistent basis.

3.6.4 Collector Efficiency

The efficiency of the flat plate collectors was calculated using the values for a_1 and a_2 that were obtained in Section 3.4. The overall efficiencies of the collector with A = 6 m^2 and G = 1000 W/m^2 averaged over the entire year were 40.93% for the MFPC and 49.46% for the NFPC. This is a relative percentage increase of the NFPC collector's efficiency was 20.84%. The maximum efficiency of the MFPC was 65.73% in May and 79.86% for the NFPC also in May. This is a promising result for the Irish market and also if the technology was implemented in sunnier climates, households could experience a much higher efficiency rate year-round.

3.6.5 Annual Savings

Using the parameters given in Table 2, the annual savings for a household were calculated to be €13.50 greater per year for the NFPC compared to the MFPC. This saving is due to the fact that the NFPC uses 70 kWh less auxiliary heating per year. Over the lifetime of a solar thermal system this amounts to €337.50 and 1750 kWh in savings for using the NFPC instead of the MFPC. The weight of the collector was also reduced by a full order of magnitude by reducing the weight of the glass cover from approx. 20kg to 2kg. From analyzing the individual component weight contribution of the solar collector in SolidWorks®, the glass cover was found to account for 60% of the weight of a collector. Reducing this weight ten-fold could have significant impacts on the cost of transport and installation of a solar thermal system. The overall weight of the MFPC was 33kg compared to 15kg for the NFPC. Figure 54 shows the weight contribution of the components in a solar collector.

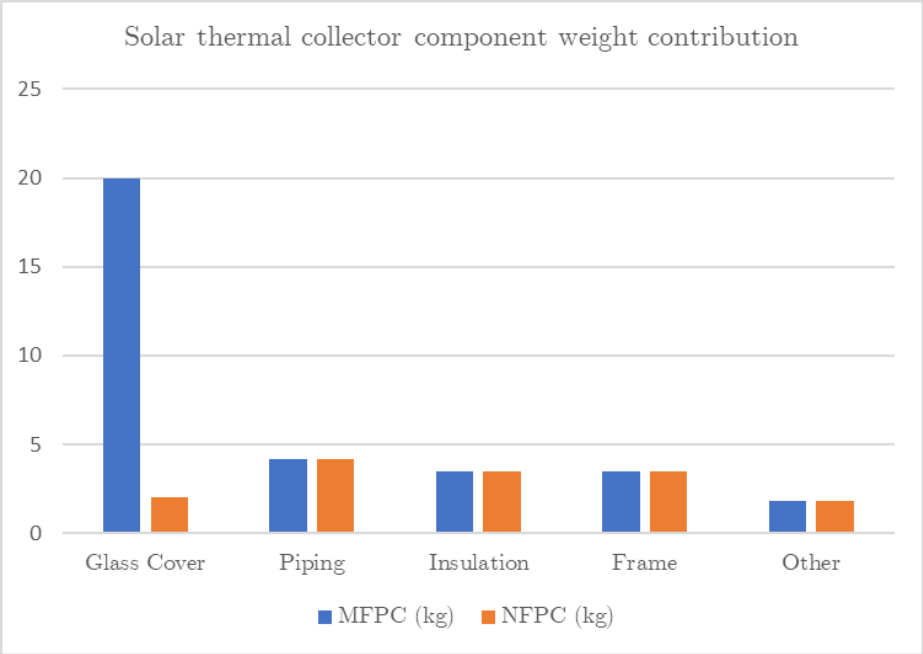

Figure 54. Component weight contribution to a MFPC and NFPC solar thermal collector

3.6.6 Simple Payback Period

The simple payback period of a solar thermal system in Ireland can range from 13 to 48.5 years depending on if the consumer availed of government grants and what type of immersion heater they have fitted [26]. For a household which installed a solar thermal

system using the grant and have an electric immersion heater the simple payback period was reduce to 10.81 years from 13.04 years by using the NFPC.

3.6.7 Net Present Value

The net present value (NPV) of the MFPC was found to be €674.55 and the NPV of the NFPC was found to be €1439.32. These values shows that both solar thermal systems are economically viable in Ireland at this time under the right conditions. However, the NFPC will provide 113% more value to the public given its higher efficiency. This should hopefully make solar thermal systems more attractive to homeowners in Ireland.

3.7 System Level Modelling in Other Climates

Following the promising results that the NFPC produced in an Irish climate, an analysis of other climates around the world was carried out. This was done to explore the possibilities of the NFPC in other climates. A list of countries was comprised based on their latitudes from 90° N to 90° S in 15° increments. The countries were also chosen based on the data available in the TMY Weather data in TRNSYS. This list is shown in Table 11 below. This international analysis demonstrates the efficiency and economic viability of the NFPC in all major climates across the global.

Table 11. Chosen countries and their latitude for an international system level modelling analysis of solar thermal collectors

Latitude	Country	Weather Data
90° N	North Pole	Not available
75° N	Canada	Edmonton
60° N	Norway	Bergen
45° N	France	Paris
30° N	Egypt	Cairo
15° N	Thailand	Bangkok
0°	Ecuador	Quito
15° S	Australia	Darwin
30° S	South Africa	Cape Town
45° S	Chile	Punta Arenas
60° S	South Orkney Islands	Not available
75° S	Antarctica	Not available
90° S	South Pole	Not available

Table 12 shows the simulation data of the MFPC and NFPC in the locations mentioned above in Table 11. This was done to analyse at a high level whether the NFPC would provide meaningful improvements to a solar thermal collector at various locations around the world. As can be seen from the results the NFPC performed better in all climate conditions at all latitudes. It consistently produced a higher internal temperature and a greater amount of useful energy.

Table 12. Average collector temperature and average useful energy gained by the NFPC and MFPC in various climates around the world

	NFPC	MFPC	NFPC	MFPC
Location	Avg T (C)	Avg T (C)	Avg Q_useful (kWh)	Avg Q_useful (kWh)
Canada	69.26	60.69	308.62	295.53
Norway	62.17	59.43	256.38	230.66
France	74.85	58.38	464.07	374.61
Egypt	67.15	61.67	372.04	368.96
Thailand	75.05	64.43	184.71	183.76
Ecuador	62.17	54.12	316.58	301.09
Australia	62.71	59.71	354.28	345.05
South Africa	52.5	48.24	241.67	227.68
Chile	31.12	26.84	43.86	15.99

3.8 Dual Glass TIM

The properties of a dual glass TIM structure were examined in the hopes of reducing the temperature of the TIM within the solar cavity. This was done as the melting point of polycarbonate was identified in Section 3.2, as ≈ 147°C. Whereas the temperature within the solar cavity were found to reach over 160°C at the point of the TIM barrier if left to stagnate without any hot water being drawn off by the DHWS. It was thought that enclosing the TIM with the ultra-thin glass both above and below, as shown in Figure 55, would reduce the temperature that the TIM was exposed to.

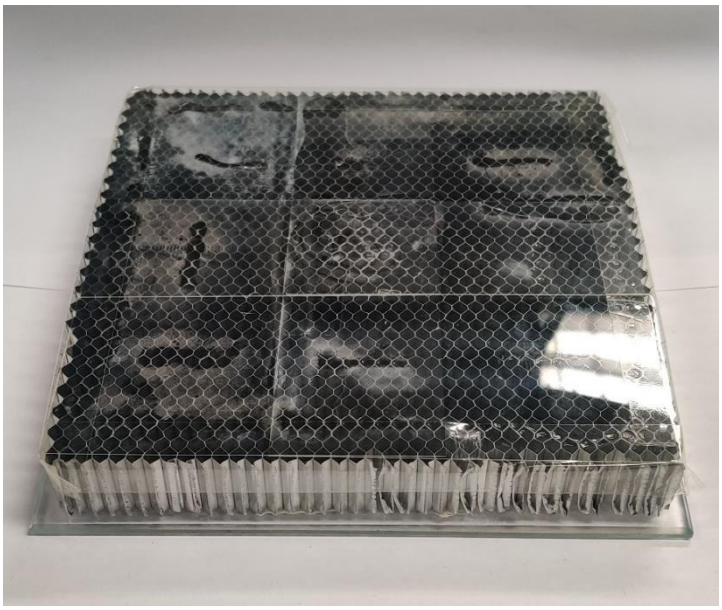

Figure 55. Dual Glass Transparent Insulating Material (TIM) structure used in testing

However, the opposite effect was found upon both simulation and experimentation. The temperature within the air cavity of the solar thermal panel and the temperature that the TIM was exposed to were both increased dramatically due to the presence of the second layer of glass. Figure 56, shows that in simulation at the point at which the TIM is exposed to the highest temperature, the temperature has increase to ≈ 190°C.

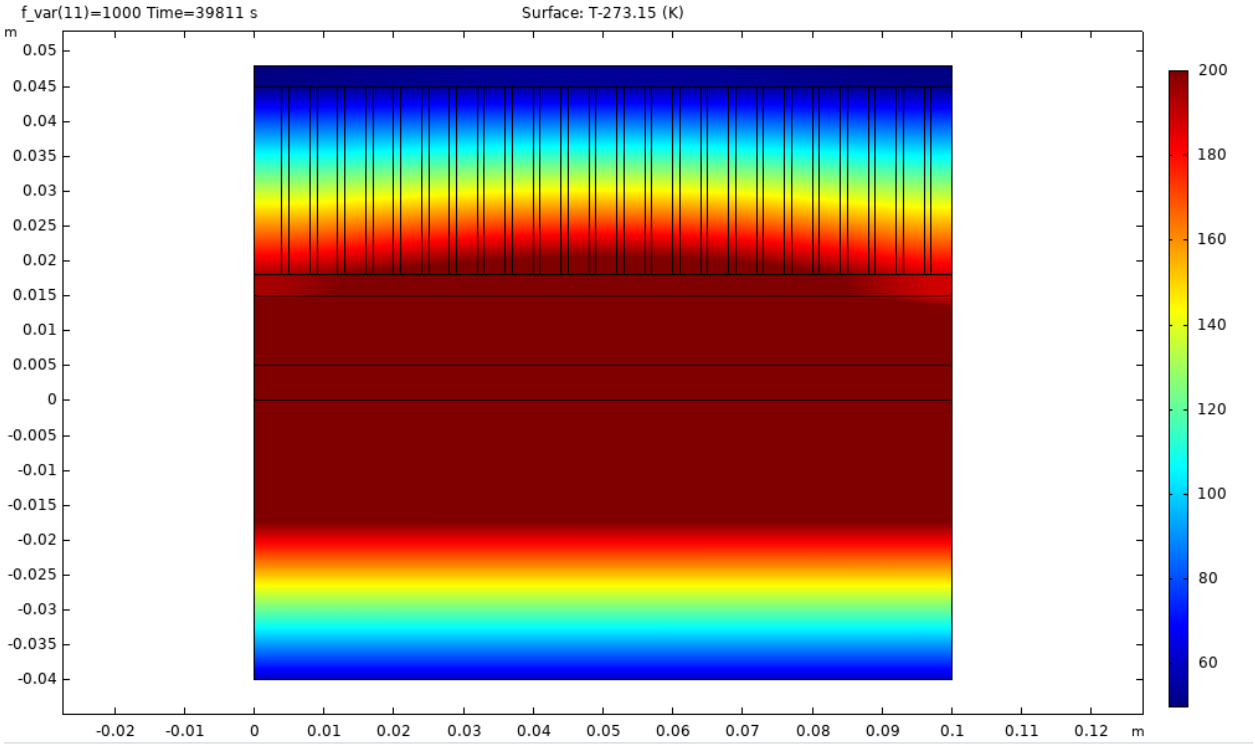

Figure 56. Finite Element Analysis (FEM) simulation of dual glass TIM structure within solar thermal cavity. Temperature scale units

While this didn't have the desired effect to reduce the temperature that the TIM was exposed to, it did show that the temperature and thus the efficiency of the solar thermal collector could be increased further using this method. The efficiency performance curve of the dual glass TIM solar collector is shown in Figure 57.

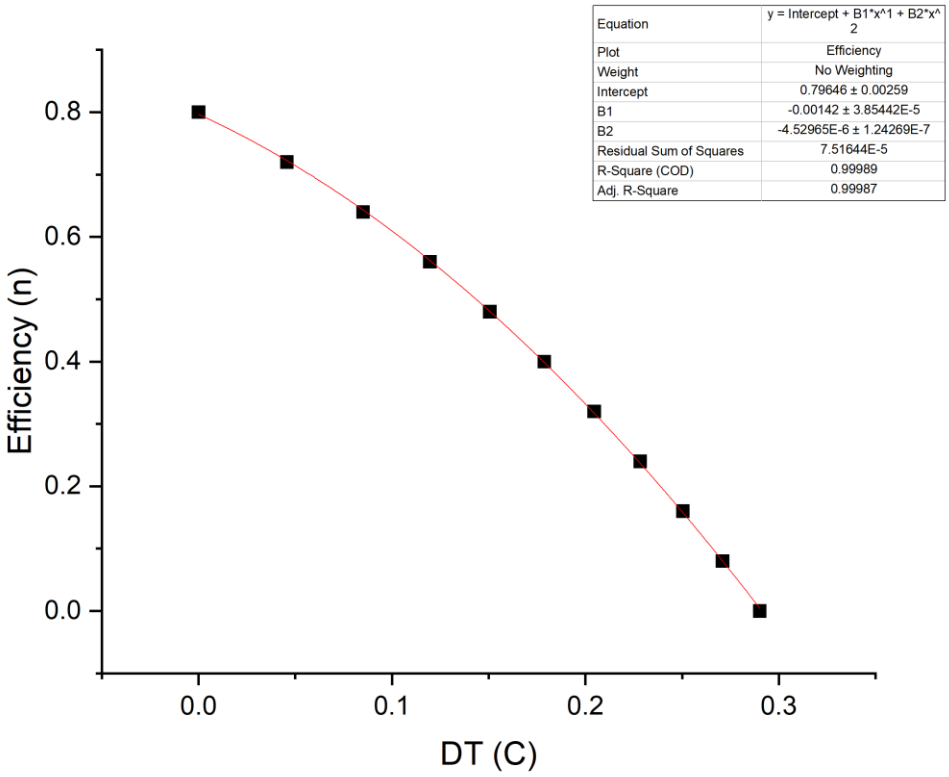

Figure 57. Efficiency performance curve of dual glass TIM solar thermal collector

A value of $a_1 = 1.42x10^{-3}$ W/(m^{2}K) and $a_2 = 4.52x10^{-6}$ W/(m^{2}K) were found for the dual glass system. This is compared to a value of $a_1 = 2.69x10^{-3}$ W/(m^{2}K) and $a_2 = 7.45x10^{-6}$ W/(m^{2}K) for the MFPC, and $a_1 = 1.56x10^{-3}$ W/(m^{2}K) and $a_2 = 6.52x10^{-6}$ W/(m^{2}K) for the NFPC. A notable efficiency increase is seen at the working temperature range of a solar thermal collector (40°C - 80°C) compared to both the MFPC and NFPC. The efficiency is also greater at higher temperatures; however, this does not mean as much in this application as it is outside the normal working range.

While this result shows that the dual glass isn't good for the intended application (to reduce the temperature that the polycarbonate TIM structure is opposed to), it does provide promise elsewhere. If a material with similar optical, structural, and economic properties to polycarbonate but with a higher melting point was discovered then this dual glass method

could be very effective as increasing the efficiency of solar thermal panels. Another, possibly easier solution, would be to incorporate a pressure valve into the solar thermal system. This type of temperature release valve is around used in other solar thermal systems. It is designed to open and release the heat within the solar cavity once a certain internal temperature is reached. This would mean that the dual glass would be a viable option and its efficiency benefits could be revolutionary in the solar thermal industry. However, this temperature release valve was unfortunately outside the scope of this thesis.

Outside of the solar thermal industry this dual glass technology could be very useful given its optical and thermal properties. It could be employed in industries such as greenhouses or windows. The thermal conductivity of the TIM structure was found to be 0.066 W/mK. This means it is more insulating than a double-glazed window (1 W/mK) and nearly as insulating as a triple glazed window (0.031W/mK). This means that this technology could provide similar thermal properties to a triple glazed window, however, at a much lower weight. A triple glazed window can weight up to 45 kg/m^2 [65], compared to just 2 kg/m^2 for the dual glass TIM structure. This would represent a very significant reduction

The optical properties of the dual glass TIM structure aren't suitable for regular windows that people look through, as it has a small field of view. However, it was shown throughout this study that an adequate amount of diffused light and radiation can pass through the structure. This makes the structure perfect for applications where thermal insulation and diffused radiation are sought-after such as in greenhouses, sky lights and privacy windows. This dual glass TIM structures display huge potential for applications in these industries which warrants further investigations.

4. Discussion

Throughout this study, various methods of increasing the efficiency of solar thermal collectors were examined.

A lab-scale solar thermal collector, with an adjustable cavity height was successfully designed to test the optimal internal cavity height of a solar thermal collector. Successful tests were carried out to show that the optimal cavity height was 1cm between absorber plate and glass cover on a flat surface. The U-value at 1cm was found to be 8.29 ± 0.68 W/m^2. Testing at the working angles of a solar cell in Ireland were performed afterwards to determine if the mounted angle of the solar cell affected the results. Once again the tests proved successful, with a 1cm cavity height proving to be optimal at all angles and having the lowest U-value of 8.17 ± 0.75 W/m^2 for this model solar collector. This optimum cavity height is lower than expected from numerical simulation. Despite this result being in contrary to previous literature and the standard cavity height used in the solar thermal industry, the result was verified by FEM simulations and lab-scale experiments. A smaller cavity height would be very beneficial to all parties as it would use less material, look more attractive, weigh less and cost less to produce and for the customer.

Following on from these successful experiments, **a novel hexadic structure was designed and produced.** The same experimentally setup was then used to test the hypothesis that convection suppression techniques can be used to increase the efficiency of solar thermal collectors. Tests were carried out similar to the initial testing, however, this time the hexadic structure was included within the solar cell cavity. Identical tests were conducted to the previous experiments, with somewhat similar yet even more promising results. The 1cm cavity gap was again verified to be the most efficient with a U-value of 6.958 ± 1.385 W/m^2. This result shows a 19.2% rise in the efficiency of the solar collector compared to the MFPC without a hexadic structure present in the cavity. As previously, these tests were carried out independently at the working angles of a solar cell in Ireland. The tests proved successful, with the 1cm cavity height proving to be optimal at all angles with an average U-value of 7.073 ± 0.142 W/m^2.

Given the successful efficiency increases shown by incorporating a hexadic structure within the solar collector, the next part of this study was to identify a material suitable for this purpose. Polycarbonate was chosen as a material which is widely produced, and which may have the properties required of a TIM in a solar thermal application. The optical, thermal

and UV properties of polycarbonate were analysed experimentally and through a literature review. The materials properties were found to be suitable for this application and thus an NFPC was produced using a polycarbonate TIM structure. The one concern with using polycarbonate was its melting point. The melting point was determined to be in the range of 146.69 – 148.97°C. While solar thermal collectors usually work in a lower temperature range, if the collector is left to stagnant without the hot water being used the temperature in the solar collector cavity could increase to over 190°C in the Irish climate which would cause the polycarbonate to melt. To solve this issue a release valve may be incorporated to decrease the temperature if it became too hot. This solution is already used in the solar industry so could be incorporated into the system. However, this solution was not examined due to time constraints. This result did spark a new idea to employ the same technology in a different industry. The transparent dual glass TIM structure showed extremely promising thermal insulation properties. It has a U-value almost in line with a triple-glazed window, however, it is 182% lighter than a triple-glazed window. This technology could be used to increase the efficiency of greenhouses or windows in houses where full transparency isn't the main objective.

From analysing the properties of polycarbonate, it was seen that the hexadic structure provided impressive structural support and flexibility to the solar thermal collector. This improved support could circumvent the use of the thick glass covers currently employed thus a thinner and lighter solution could be used.

A lab scale novel flat plate collector (NFPC) using a polycarbonate hexadic TIM structure and ultra-thin borosilicate glass was produced for further experimentation. Tests were carried out using FEA techniques on COMSOL Multiphysics simulations and physically on a lab-scale NFPC model. These tests showed that the NFPC outperformed a regular MFPC in all areas. The most important of these results being the performance efficiency curve where a 20.84% relative increase in efficiency was achieved. This efficiency increase came with no increase in cost for the manufacturer or the end consumer as it uses the natural insulating properties of stagnant air. This was a very important aspect of this research as the costs could not increase so that solar thermal can become more competitive in the eyes of consumers. As the regular glass cover was replaced with an ultra-thin glass cover the weight of the overall system was decreased dramatically by 18kg. It is difficult to quantify the exact reduction in costs due to the weight reduction however it should make the products easier to product, transport, and install.

Following the lab scale experiments and simulations, the NFPC was tested in a system level model. This model was designed on TRNSYS and replicated a standard domestic hot water system plus climate in Ireland. Essentially it provided an analysis of how the NFPC would perform in real world conditions. The results showed that it outperformed the current market standard in flat plate solar thermal collectors and brought the efficiency more in line with the more expensive and higher maintenance evacuated tube collectors.

The consistency of these measurements, within the range of experimental error, provided a promising outlook for the future development of a higher efficiency and more cost effective solar thermal system.

5. Conclusions

An analysis of the existing solar thermal industry was performed to identify possible areas of improvement. Top losses of heat through convection and conduction were found to be the largest contributor to heat loss in solar thermal collectors. Convection suppression techniques were identified as a possible way to reduce these losses and increase the efficiency of solar thermal technology to make it more attractive to consumers.

The performance of a market available flat plate solar thermal collector (MFPC) and a novel hexadic flat plate solar thermal collector (NFPC) was analysed for a year-round domestic hot water system in an Irish climate. The analysis consisted of FEM simulations, transient system simulations, lab-scale experimentation and real-world date collection.

The results obtained in this study show that for an annual incident solar insolation consistent with the Irish weather a total 1022.22 kWh of useful heat energy was collected by the $6m^2$ MFPC system. The NFPC collected 1237.36 kWh of useful heat energy under the same conditions. For 2465.62 kWh and 2409.37 kWh of additional auxiliary energy supplied to the MFPC and NFPC, their annual solar fractions were 28% and 32% respectively. The annual collector efficiencies were 40.93% and 49.46%, the NFPC showing a large relative efficiency increase of 20.84%. This is a dramatic increase over the current market leading solar thermal collector efficiencies. The inclusion of the hexadic TIM reduced the air circulation speed within the solar collector cavity by 79.16%, producing near stagnant air. An economic analysis showed that using the NFPC instead of a MFPC reduces the simple payback period by 2.23 years and can save an additional €337.50 for the consumer. The weight reduction of 18kg achieved by using the hexadic polymer structure could further reduce the costs of transport and installation. The net present value showed that both MFPC and NFPC were economically viable with an NPV of €674.55 and €1439.32 respectively.

This study demonstrates that a novel transparent insulating material configuration employed within the air cavity of a solar thermal collector can greatly increase the collector's efficiency. The cost of the solar panel does not increase with its inclusion and the weight of the panel is greatly reduced due to the TIM's structural integrity allowing thinner glass to be used. These results are quite promising as the energy performance analysis shows the NFPC compares favourably with the MFPC.

6. Further Research & Recommendations

This project provided insight into how the efficiency of solar thermal collectors could be increased through convection suppression methods. It also showed that if a TIM structure was found for this, the added structural support it would provide could reduce the need for a thick glass cover, hence reducing the overal weight significantly. In this time limited project it was not possible to verify these results on a full scale solar thermal panel. The next step would be to make full scale versions of the NFPC produced in this project and test the performance of the collector in a northern European climate. A test site has been constructed on the east coast of Ireland in County Louth. On this test site there are currently both a flat plate collector and an evacuated tube collector installed. Further research could be carried out at this location to verify this project's results in a working environment.

One of the main issues that arose in this research was the temperature within the solar cavity increasing above the melting point of polycarbonate. This meant that if the solar collector system was left to stagnant in a real world situation the polycarbonate would melt and the system would fail. Polycarbonate was chosen as most of its properties fit the requirements for this application. It is highly transparent, it is UV resistant, it is readily available in the market, it can be moulded into a hexadic channel form and it is relatively cheap. However, to make it a fully viable solution in the marketplace the issue of overheating would have to be addressed further. This could be done with a simple fix of adding a pressure release valve into the system. This is a common overheating fail safe in solar thermal systems and is already used in other system. The solution could also be found in a different material with all the same properties of polycarbonate but a higher melting point. This is an aspect of the research that the author greatly wanted to explore further, however, due to time constraints they could not.

Throughout the course of the project, a new avenue of research came to light with the discovery of the interesting properties of a dual-glass TIM structure. It was found that the system provided a U-value comparable with triple-glazed windows, however, it weighed ≈ 43 kg less. This technology could have huge implications of industries such as greenhouses and windows. Although the dual glass TIM structure isn't as transparent as a regular glass window, it still allows almost the same amount of light through via diffused light. For applications where transparency isn't the key factor such as a greenhouse or a skylight, this system could be a cheap way to increase the thermal insulation of a building. The research

team including the author of this thesis and supervisor have been communicating with Corning Inc. an international company which specialises in speciality glass creation regarding this discovery. This company focuses on producing ultra-thin and ultra-strong glass and are used in many applications such as in most mobile phones, laptops, and smartwatches. The plan was to use Corning glass to replace the regular glass cover in solar thermal collectors to produce the NFPC which would provide superior convection suppression while also reducing one of the largest cost factors in solar panel creation *i.e* the thick glass cover. It was also proposed to explore the dual-glass TIM system with the same company as the product could be mass produced easily and have a far-reaching impact. This is an idea that the author of this thesis believes has huge potential and would love to pursue at some future date.

Blank Page

References

[1] Christine W. Njiru, Sammy C. Letema, "Energy Poverty and Its Implication on Standard of Living in Kirinyaga, Kenya", Journal of Energy. (2018).

[2] FACT SHEET: COP26 - Children and climate change. UNICEF. Accessed 01/11/2021.

[3] Sustainable Energy Authority of Ireland, "Residential Statistics." https://www.seai.ie/data-and-insights/seai-statistics/key-statistics/residential/

[4] Sustainable Energy Authority Of Ireland, "Energy in Ireland 2020." (https://www.seai.ie/publications/Energy-in-Ireland-2020.pdf)

[5] Statistical Review of World Energy 2020, 69th edition, BP.

[6] World Commission on Environment and Development. *Our common future*. Oxford: Oxford University Press. (1987).

[7] An Introduction to Energy – World Energy Assessment: Energy and the Challenge of Sustainability. Hans-Holger Rogner and Anca Popescu.

[8] V.Smil, General energetics: Energy in the Biosphere and Civilization. John Wiley & Sons. (1991).

[9] Stickler, Greg. "Educational Brief - Solar Radiation and the Earth System". National Aeronautics and Space Administration.

[10] Glaser, Peter E. "Power from the sun: Its future." Science 162, no. 3856: 857-861. (1967).

[11] Ayompe, L., Duffy, A., McCormack, S., Conlon, M., Measured performance of a 1.72 kW rooftop grid-connected photovoltaic system in Ireland, Energy Conversion and Management, Vol 52, Issue 2, Pages 816-825. (2011).

[12] Climate Change: The Clean Disruption Continues, Institute of Climate Studies USA. (2017).

[13] Abdellah Shafieian, Mehdi Khiadani, Ataollah Nosrati, Thermal performance of an evacuated tube heat pipe solar water heating system in cold season, Applied Thermal Engineering, Vol 149, Pages 644-657. (2019).

[14] Benjamin Greening, Adisa Azapagic, Domestic solar thermal water heating: A sustainable option for the UK, Renewable Energy, Vol 63, Pages 23-36.

[15] Solarworld.ie, Product Range. Accessed 27/04/2022. http://www.solarworld.ie/

[16] Olczak, Piotr, Dominika Matuszewska, and Jadwiga Zabagło. "The Comparison of Solar Energy Gaining Effectiveness between Flat Plate Collectors and Evacuated Tube Collectors with Heat Pipe: Case Study." Energies 13, Vol. 7: 1829. (2020).

[17] Hottel, H., Woertz, B. Performance of flat-plate solar-heat collectors. ASME. (1942).
[18] Flat plate solar collectors. Ibrahim Dincer, Muhammad F. Ezzat, in Comprehensive Energy Systems. (2018).
[19] Kalogirou, S.A., Solar Energy Engineering, Elsevier. (2009).
[20] M. Nabag, M. Al-Radhawi, and M. Bettayeb, "Model reduction of flat-plate solar collector using time-space discretization," IEEE International Energy Conference and Exhibition, pp. 45–50. (2010).
[21] J. A. Duffie, W. A. Beckman, and N. Blair, Solar engineering of thermal processes, photovoltaics and wind. John Wiley & Sons. (2020).
[22] Tiwari RC, Kumar A, Gupta SK, Sootha GD. Thermal performance of flat-plate solar collectors manufactured in India. Energy Convers Manage; 31(4):309 -13. (1991).
[23] Dang A, Sharma JK. Performance of flat plate solar collectors in off-south orientation in India. Energy Convers Manage; 23(3):125-30. (1983).
[24] Amer EH, Nayak JK, Sharma GK. Transient method for testing flat-plate solar collectors. Energy Convers Manage; 39(7):549-58. (1998).
[25] Alvarez A, Cabeza O, Muñiz MC. Experimental and numerical investigation of a flat-plate solar collector. Energy; 35(9):3707-16. (2010).
[26] Ayompe LM, et al., Comparative field performance study of flat plate and heat pipe evacuated tube collectors (ETCs) for domestic water heating systems in a temperate climate, Energy. (2011).
[27] Zambolin E, Del Col D. Experimental analysis of thermal performance of flat plate and evacuated tube solar collectors in stationary standard and daily conditions. Solar Energy; 84(8):1382-96. (2010).
[28] Allen SR, Hammond GP, Harajli HA, McManus MC, Winnett AB. Integrated appraisal of a solar hot water system. Energy; 35(3):1351-62. (2010).
[29] K. Hollands, "Honeycomb devices in flat-plate solar collectors," Solar Energy, vol. 9, no. 3, pp. 159–164. (1965).
[30] Covert, T., Greenstone, M., Knittel, C.R. Will we ever stop using fossil fuels? SSRN Electron. (2016).
[31] Shafiee, S., Topal, E. When will fossil fuel reserves be diminished? Energy. (2009).
[32] Mekhilef, S., Saidur, R., Safari, A. A review on solar energy use in industries. Renew. Sustain. Energy. (2011).

[33] Kalogirou, S. The potential of solar industrial process heat applications. Appl. Energy. (2003).
[34] Zheng, H. Solar concentrating directly to drive desalination technologies. Solar Energy Desalination Technology, Elsevier. (2017).
[35] International Energy Agency, SHC. Solar Heat Worldwide. Global Market Developments and Trends in 2020.
[36] Solar Heat Europe. Solar Heat Markets in Europe, Trends and Market Statistics. (2019).
[37] V. B. Veinberg, Optics in equipment for the utilization of solar energy. Office of Technical Services, vol. 4471. (1959).
[38] K. Hollands and K. Iynkaran, "Proposal for a compound honeycomb collector," Solar Energy, vol. 34, no. 4, pp. 309 – 316. (1985).
[39] K. Hollands, K. Iynkaran, C. Ford, and W. Platzer, "Manufacture, solar transmission, and heat transfer characteristics of large-celled honeycomb transparent insulation," Solar Energy, vol. 49, no. 5, pp. 381 – 385. (1992).
[40] N.D. Kaushika, K. Sumathy, Solar transparent insulation materials: a review, Renewable and Sustainable Energy Reviews, Vol 7, Issue 4, Pages 317-351. (2003).
[41] Wong, Ing & Eames, P.C. & Perera, Srinath.A review of transparent insulation systems and the evaluation of payback period for building applications. Solar Energy. 81. 1058-1071. (2007).
[42] P. Pellette, M. Cobble, and P. Smith, "Honeycomb thermal trap," Solar Energy, vol. 12, no. 2, pp. 263–265. (1968).
[43] K. Marshall, R. Wedel, and R. Dammann, "Development of plastic honeycomb flat-plate solar collectors," STIN, vol. 77, p. 25640. (1976).
[44] J. G. Symons, "The solar transmittance of some convection suppression devices for solar energy applications: an experimental study," Journal of Solar Energy Engineering, vol. 104. (1982).
[45] W. J. Platzer, "Advances and problems of transparent insulation in the market professionalization and diversification," EuroSun, vol. 1.4-1. (1998).
[46] A. Abdullah, H. Abou-Ziyan, and A. Ghoneim, "Thermal performance of flat plate solar collector using various arrangements of compound honeycomb," Energy conversion and management, vol. 44, no. 19, pp. 3093–3112. (2003).

[47] A. Ghoneim, “Performance optimization of solar collector equipped with different arrangements of square-celled honeycomb,” International Journal of Thermal Sciences, vol. 44, no. 1, pp. 95 – 105. (2005).
[48] Israel Ministry of Foreign Affairs, “Israel’s sweetest solar energy” Accessed: 19.9.21, https://mfa.gov.il/MFA/InnovativeIsrael/Pages/Israel’s-sweetest-solar-energy.aspx
[49] Kizildag, D. *et al.* First test field performance of highly efficient flat plate solar collectors with transparent insulation and low-cost overheating protection. Solar Energy. (2022).
[50] A Petrov et al. Test bench flow straightener design investigation and optimization with computational fluid dynamics methods IOP Conf. Ser.: Mater. Sci. Eng. 492 012036. (2019).
[51] Hüsing, N., Schubert U. Aerogels - Airy materials: chemistry, structure, and properties Angew Chem Int Ed, 37. (1998).
[52] Zhao L. Harnessing Heat Beyond 200 °C from Unconcentrated Sunlight with Nonevacuated Transparent Aerogels. ACS Nano. (2019).
[53] Lumira® aerogel product specifications datasheet. https://www.buyaerogel.com. Accessed 10/05/2022.
[54] Woignier, T.; Primera, J.; Alaoui, A.; Etienne, P.; Despestis, F.; Calas-Etienne, S. Mechanical Properties and Brittle Behavior of Silica Aerogels. Gels, 1, 256-275. (2015).
[55] Getling, A. V. Bénard–Rayleigh Convection: Structures and Dynamics. World Scientific. (1998).
[56] S. Eve, J. Mohr, Study of the surface modification of the PMMA by UV-radiation. Proc. Eng. 1(1), 237–240. (2009).
[57] T. Sharma, S. Aggarwal, A. Sharma, S. Kumar, V.K. Mittal, P.C. Kalsi, V.K. Manchanda, Modification of optical properties of polycarbonate by gamma irradiation. Radiat. Eff. Defects Solids. 163(2), 161–167. (2008).
[58] W.A. MacDonald, M.K. Looney, D. MacKerron, R. Eveson, R. Adam, K. Hashimoto, K. Rakos, Latest advances in substrates for flexible electronics. J. Soc. Inf. Disp. 15(12), 1075. (2007).
[59] A. Factor, M.L. Chu, The role of oxygen in the photo-ageing of bisphenol-A polycarbonate. Polym. Degrad. Stab. 2(3), 203–223. (1980).

[60] Yazdan Mehr, M.; van Driel, W.D.; Jansen, K.M.B.; Deeben, P.; Boutelje, M.; Zhang, G.Q. Photodegradation of bisphenol A polycarbonate under blue light radiation and its effect on optical properties. Optical Materials, 35(3), 504–508. (2013).

[61] Carroccio, Sabrina; Puglisi, Concetto; Montaudo, Giorgio "Mechanisms of Thermal Oxidation of Poly(bisphenol A carbonate)". Macromolecules. 35 (11): 4297–4305. (2002).

[62] H. Buchberg, I. Catton, and D. Edwards, "Natural convection in enclosed spaces—a review of application to solar energy collection." (1976).

[63] N. Nahar and M. P. Gupta, "Studies on gap spacing between absorber and cover glazing in flat plate solar collectors," International journal of energy research, vol. 13, no. 6, pp. 727–732. (1989).

[64] Paxton, S. Economic and Thermal Loss Analysis of Flat Plate Solar Thermal Collectors. Trinity College Dublin. (2020).

[65] Glazing Centre. The Weight of Double and Triple Glass Units 2021. https://glazingcentre.co.uk/the-weight-of-double-and-triple-glass-units/ Accessed on 30/05/2022.

[66] J. A. Duffie, W. A. Beckman, N. Blair. Solar Engineering of Thermal Processes, Photovoltaics and Wind 5th Edn. Elsevier. (2020).

[67] Norton, B. Anatomy of a solar collector: Developments in Materials, Components and Efficiency Improvements in Solar Thermal Collector Systems. Refocus, Elsevier. (2006).

[68] BOROFLOAT ® 33 technical data sheet. https://www.schott.com/en-ie/products/borofloat-p1000314/downloads. Accessed 18/04/2022

[69] Glass in building — Determination of light transmittance, solar direct transmittance, total solar energy transmittance, ultraviolet transmittance and related glazing factors, ISO 9050:2003.

[70] Plastics — Determination of thermal conductivity and thermal diffusivity — Part 2: Transient plane heat source (hot disc) method, ISO 22007-2:2015.

[71] A. Factor, ''Mechanisms of Thermal and Photodegradations of Bisphenol A Polycarbonate,'' in Polymer Durability, vol. 249, no. Scheme I, pp. 59–76 (1996)

[72] Joule Navitas 2m solar specification data sheet. https://www.joule.ie/on-roof-2m-2-5m-solar-thermal-system/. Accessed 21/04/2022.

[74] D.C. Wilcox, Turbulence Modeling for CFD, 2nd ed., DCW Industries. (1998).

[75] Mandate to CEN and CENELEC for the elaboration and adoption of measurement standards for household appliances: water-heaters, hot water storage appliances and water heating systems. European Commission. (2002).

[76] Kalogirou S. Solar Energy Engineering: Processes and Systems 2nd Edn. Elsevier. (2013).

[77] Sustainable Energy Authority of Ireland, "Prices". Accessed 25/04/2022. https://www.seai.ie/data-and-insights/seai-statistics/key-statistics/prices/

[78] Kalogirou S. Thermal performance, economic and environmental lifecycle analysis of thermosiphon solar water heaters. Solar Energy. (2009).

[79] Masters GM. Renewable and efficient electric power systems, 2nd Edn. Wiley and Sons. (2013).

[80] Sustainable Energy Authority Of Ireland, Best practice for solar photovoltaics (PV) https://www.seai.ie/publications/Best_Practice_Guide_for_PV.pdf. Accessed on 13/05/2022.

[81] Kalogirou, S. Solar Energy Engineering (Second Edition). (2014).

[82] ISO 4892 – 3: 2016. Plastics — Methods of exposure to laboratory light sources — Part 3: Fluorescent UV lamps. Accessed on 11/05/2022

[83] Radiation. A Review of Human Carcinogens, IARC Monographs on the Evaluation of Carcinogenic Risks to Humans, No. 100D.

[84] Getling, A. V. Bénard–Rayleigh Convection: Structures and Dynamics. World Scientific. (1998). ISBN 978-981-02-2657-2.